Synthesis, electrochemical, kinetic and thermodynamic studies of new ruthenocene-containing betadiketonato rhodium(I) complexes with biomedical applications

A dissertation submitted in accordance with the requirements for the degree

Magister Scientiae

In the

Department of Chemistry

Faculty of Science

At the

University of the Free State

By

Kingsley Christian Kemp

Supervisor

Prof. J.C. Swarts

Co-Supervisor

Dr. J. Conradie

May 2004

I dedicate this thesis to Huwald Bösenberg
Grandfather and friend.

The autumn has gone,
The winter has come,
But the tree lives on
Through all the extremes.
Years of knowledge,
Gained in every spring,
Much to be learnt,
From the past.

The memories live on,
As the oak grows and grows,
A place to remember,
And to sit in the shade.
Knowledge passed on,
To contemplate life,
Rules to live by,
A remembrance of the past.

ACKNOWLEDGEMENTS

I would like to thank my supervisor, Prof. J.C. Swarts, as well as my co-supervisor, Dr. J. Conradie, for the support, guidance and time they devoted to my studies.

I would like to thank my family for the support over these past years. I would also like to thank all my friends and colleagues that were there to give a helping hand when necessary.

Finally thanks to all the people who put up with my moods and sometimes irrational decision making. Thanks for the support and the understanding.
They are: Prof. J.C. Swarts, Dr. J. Conradie, Heinrich (Pottie) Potgieter, Christiaan (Loop en Val) van Vuuren, Johan (Jay) Pieterse, Margeaux (Little L) Kemp, Elizabeth (Lizette) Erasmus, Meyrick Kemp (a big thank you), Ingrid Kemp, Jaco (Neef) Brand, Deon Visser, Ernst Langer, Ina du Plessis, Morgan and Gemma Kemp and Phillip Fullaway (thanks mate).

Kingsley Christian Kemp
May 2004

CONTENTS

CONTENTS

CONTENTS

CONTENTS

LIST OF ABBREVIATIONS

$\nu_{C=O}$	carbonyl stretching frequency
χ_R	group electronegativity
[Rh(brcm)(cod)]	rhodium 1-ruthenocenyl-3-phenylpropan-1,3-dionato 1,8-cyclooctadiene
[Rh(drcm)(cod)]	rhodium 1,3-diruthenocenylpropan-1,3-dionato 1,8-cyclooctadiene
[Rh(rca)(cod)]	rhodium 1-ruthenocenylbutan-1,3-dionato 1,8-cyclooctadiene
[Rh(rcfcm)(cod)]	rhodium 1-ruthenocenyl-3-ferrocenylpropan-1,3-dionato 1,8-cyclooctadiene
[Rh(rctfa)(cod)]	rhodium 1-ruthenocenyl-4,4,4-trifluorobutan-1,3-dionato 1,8-cyclooctadiene
$[Rh_2(cod)_2Cl_2]$	di-μ-chloro-*bis*[(1,2,5,6-η)1,5-cyclooctadiene]rhodium
ArN_2^+	aryl or alkyl diazonium salt
BA	benzylacetone
brcm	1-ruthenocenyl-3-phenylpropan-1,3-dionato
Bu_3P	tributyl phosphine
cod	1,8-cyclooctadiene
CoLo	an intrinsically multi-drug resistant human colon adeno carcenoma cell line
COR	a sensitive human lung large cell carcinoma
DBM	dibenzoylmethane
DCM	dichloromethane
DMF	dimethylformamide
drcm	1,3-diruthenocenylpropane-1,3-dionato
$E^{o/}$	formal reduction potential
E_p	peak oxidation potential
Fc	ferrocene
Hacac	acetylacetone
Hbfcm	1-ferrocenyl-3-phenyl-1,3-propanedione
Hbrcm	1-ruthenocenyl-3-phenylpropan-1,3-dione, benzoylruthenocenoylmethane
HCONMePh	N-methylformanilide
Hdfcm	1,3-diferrocenyl-1,3-propanedione
Hdrcm	1,3-diruthenocenylpropane-1,3-dione, diruthenocenoylmethane
HeLa	a sensitive human cervix epithelial carcinoma cell line
HFAA	hexafluoroacetylacetone
Hfca	1-ferrocenyl-1,3-butanedione

ABBREVIATIONS

Hfctca	1-ferrocenyl-4,4,4-trichloro-1,3-butanedione
$Hg(Oac)_2$	mercury acetate
HMPT	hexamethylphosphoric triamide
Hrca	1-ruthenocenylbutan-1,3-dione, ruthenocenoylacetone
Hrcfcm	1-ruthenocenyl-3-ferrocenylpropan-1,3-dione, ruthenocenoylferrocenoylmethane
Hrctfa	1-ruthenocenyl-4,4,4-trifluorobutane-1,3-dione, ruthenocenoyltrifluoroacetone
K-*t*-OC_4H_9	potassium *tertiary*-butoxide
LiBu	n-butyl lithium
$LiN(^{i}pr)_2$	lithium diisopropylamide
MeI	methyliodide
$pK_a^{/}$	acid dissociation constant
Rc	ruthenocene
rca	1-ruthenocenylbutan-1,3-dionato
rcfcm	1-ruthenocenyl-3-ferrocenylpropan-1,3-dionato
rctfa	1-ruthenocenyl-4,4,4-trifluorobutane-1,3-dionato
$RhCl_3$	rhodium trichloride
SCE	saturated calomel electrode
$TBA[B(C_6F_5)_4]$	tetrabutylammonium tetrakispentafluorophenylborate
$TBAClO_4$	tetrabutylammonium perchlorate
TBAHFP	tetrabutylammonium hexafluorophosphate
TBATFPB	tetrabutylammonium tetrakis[3,5-bis(trifluoromethyl)phenyl]borate
TBATTFPB	tetrabutylammonium tetrakis[3,5-bis(trifluoromethyl)phenyl]borate
TFAA	trifluoroacetylacetone
TFBA	trifluorobenzylacetone
THF	tetrahydrofuran

1. INTRODUCTION AND GOALS

β-Diketones have a wide range of uses ranging from metal extraction by chelation[1,2], to biomedical applications such as use in antibacterial antibiotics[3], to being used as a ligand in metal complexes for catalysis.

The most commonly used catalytic metals are platinum, rhodium, iridium and palladium. Rhodium compounds in particular have been used as catalysts in the Monsanto process where alcohols are converted to carboxylic acids[4,5]. Rhodium (I) complexes of β-diketonates have also been used in the hydrogenation of unhindered alkenes at low temperatures[6]. The reaction mechanism of catalytic processes often involves oxidative addition to the metal by a suitable substrate, migration and insertion of a suitable ligand between metal and coordinated product followed by reductive elimination of the final product[7]. The electronic effect that different substituents have on the oxidative addition reactions is substantial. It has, for example, been shown that electron donating groups accelerate the rate of oxidative addition while electron withdrawing groups retard the rate of oxidative addition.

The group electronegativity of the R groups in complexes of type [Rh(RCOCHCOR$^{/}$)(cod)] has also been shown to have an effect on the rate of β-diketonato substitution with 1,10-phenanthroline[8]. In contrast to oxidative addition, electron donating groups were found to decelerate the kinetics of substitution. This study aims to determine the electronic influence ruthenocene-containing β-diketones have on the rate of substitution from complexes of the type [Rh(RCOCHCOR$^{/}$)(cod)] by 1,10-phenanthroline where R = ruthenocenyl. However no ruthenocene containing β-diketones have ever been synthesised. Thus, this study will also include a synthetic component to establish new ruthenocene chemistry.

With the above background the following goals of this study were identified:

1. Synthesis and characterization of the new β-diketones containing a ruthenocenyl (Rc) moiety;
2. Complexation of these ruthenocene-containing β-diketones with rhodium(I) to obtain complexes of the type [Rh(RcCOCHCOR)(cod)] with R=CF_3, CH_3, Ph (phenyl), Rc (ruthenocenyl) and Fc (ferrocenyl);

3. Determination of the rates of conversion between the enol and keto isomers of the new ruthenocene-containing β-diketones by means of NMR spectroscopy;
4. Determination of the group electronegativity of the ruthenocenyl group by utilization of spectroscopic (IR, $\nu_{C=O}$ values), thermodynamic (pKa') and electrochemical ($E_{pa\ Ru}$) measurements;
5. Determination of the mechanism of substitution of the β-diketonato ligand in [Rh(β-diketonato)(cod)] with 1,10-phenantroline by means of a stopped flow kinetic study. Rate constants will be related to Rc and R group electronegativities to quantify the electronic effect these groups have on substitution kinetics.

2. LITERATURE SURVEY

2.1. SYNTHESIS

With reference to goal 1, the synthesis of new β-diketones containing a ruthenocenyl moiety was desired. A discussion of the general synthesis of the precursors used in the synthesis of β-diketones as well as a discussion of the general chemistry of ruthenocene derivatives is presented.

2.1.1. GENERAL CHEMISTRY OF RUTHENOCENE

The general organic chemistry of ruthenocene pertaining to this study is shown in Schemes 2.1. and 2.2.

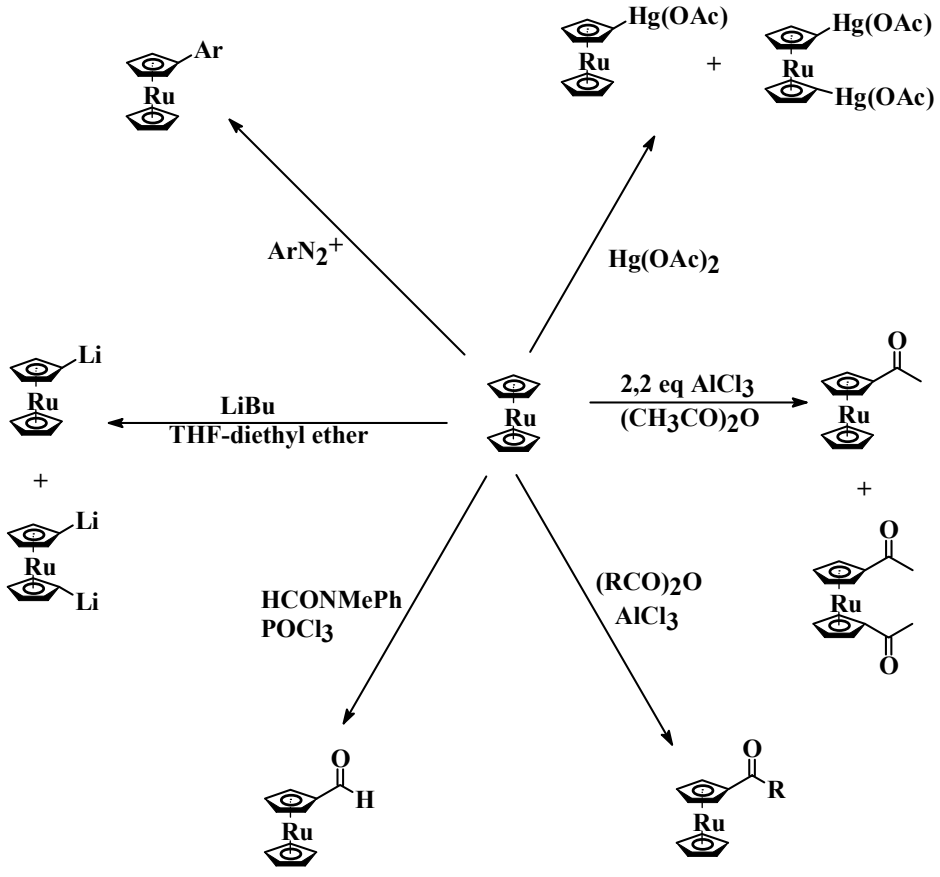

Scheme 2.1. Synthesis of a variety of ruthenocene precursors. (LiBu = n-butyllithium, $Hg(OAc)_2$ = mercury acetate, ArN_2^+ = aryl or alkyl diazonium salt)

The chemistry prevalent to monosubtstution or disubstitution for ruthenocene to give 1 and 1/ substituted products is shown in scheme 2.1. The monolithiated and dilithiated ruthenocene can be obtained by reacting ruthenocene with n-butyllithium[1,2]. The monoacetylated and diacetylated products can be obtained by reacting ruthenocene with the appropriate anhydride in the presence of aluminum trichloride[1,2]. It is important to note that the pattern of 1,1/-diacylation in the di-substituted products occurs due to the deactivation of the cyclopentadienyl rings after the first acylation on the 1 position by the electron withdrawing deactivating aroyl groups. The second substitution must therefore occur on the 1/ position. The mercurated products were obtained by reacting ruthenocene with mercury acetate in a methanol-ether solution[1,2]. These mercurated products can be separated and then lithiated to obtain the pure monolithiated or dilithiated products as shown in Scheme 2.2. The ruthenocene aldehyde is obtained by reacting ruthenocene with N-methylformanilide in the presence of phosphorus oxychloride[3,1]. The aryl or alkyl-substituted ruthenocene derivatives are obtained by reacting ruthenocene with the appropriate diazonium salt[4,1].

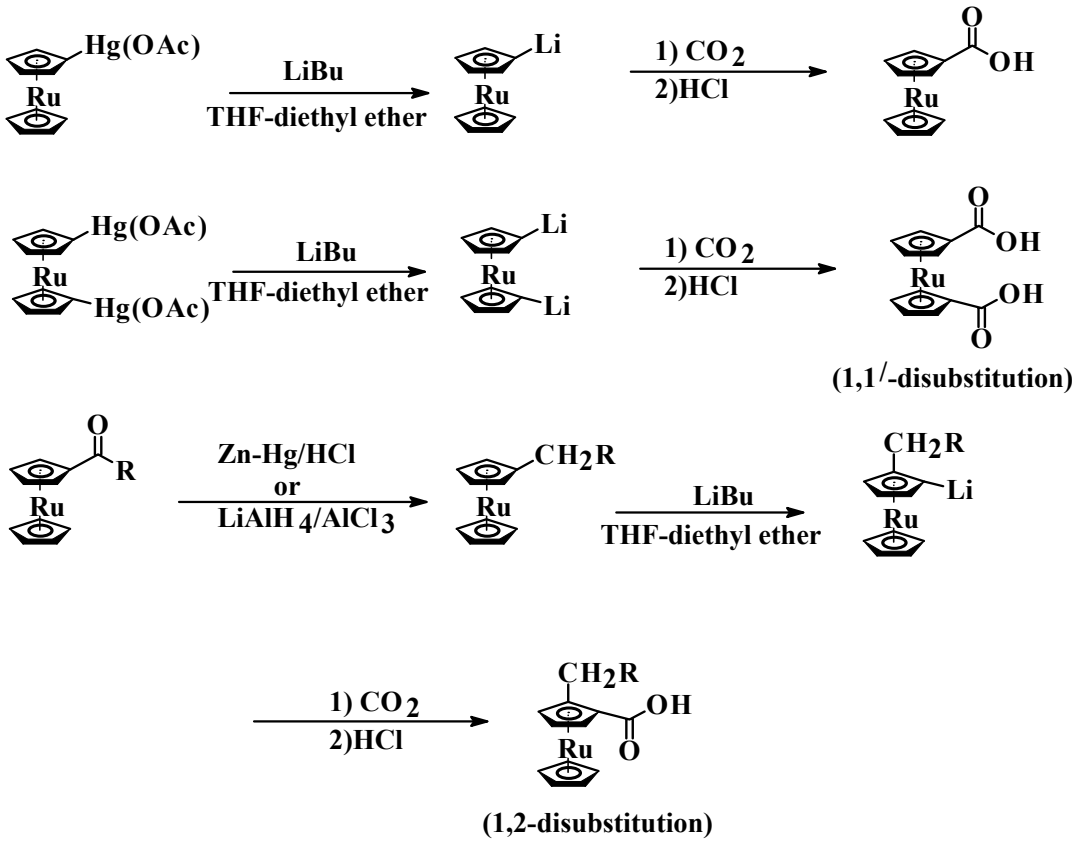

Scheme 2.2. Formation of various substituted ruthenocenes from precursors in Scheme 2.1. (LiBu = n-butyllithium, $LiAlH_4$ = lithium aluminium hydride)

Lithiated ruthenocenes can be converted to the carboxylic acids by reacting them with carbon dioxide followed by hydrochloric acid[1,2,4], as shown in Scheme 2.2. The carboxylated ruthenocenes can be reduced to the corresponding aliphatic chain by reacting them with lithium aluminium hydride in the presence of aluminium trichloride[1,4]. These can then be converted to the lithiated product by reacting them with n-butyllithium[1]. We see in this case that the pattern of substitution is 1,2 rather than 1,1/ which is due to the activation of the substituted cyclopentadienyl ring by the electron-donating aliphatic group.

2.1.2. SYNTHESIS OF METALLOCENE CARBOXYLIC ACIDS

The synthesis of β-diketones utilising a Claisen condensation reaction implies the availability of a metallocene ester and/or an acetyl metallocene. Apart from the lithiation route to obtain ruthenocenic acid shown in Scheme 2.2., the synthesis of metallocene carboxylic acids has been mainly documented for ferrocene. Three different methods for the synthesis of ferrocenecarboxylic acid are shown in Scheme 2.3.

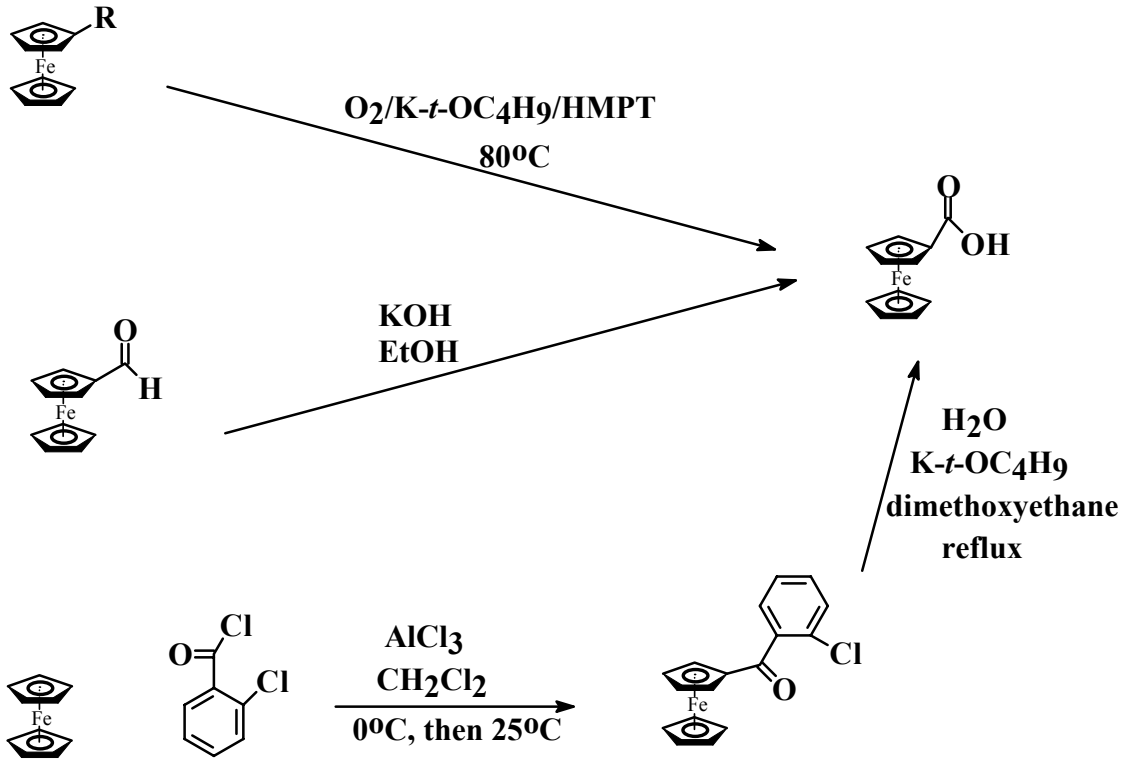

Scheme 2.3. Synthesis of ferrocenecarboxylic acid via three pathways. (K-*t*-OC_4H_9 = Potassium *tertiary*-butoxide, HMPT = hexamethylphosphoric triamide)

The synthesis of ferrocenecarboxylic acid was conducted by Schmitt and Özman[5], they found that the carboxylic acid could be obtained from aliphatic substituted ferrocenes. The yields for these reactions vary from 25-86%, with the type of substituent [R= CH_2OH, CHO, $COCH_3$, $CH_2N(CH_3)_2$] when the substituted ferrocene was reacted with potassium *tert*-butoxide in hexamethylphosphoric triamide (HMPT)[5]. An alternative synthesis of ferrocenecarboxylic acid consists of reacting ferrocene aldehyde in the presence of potassium hydroxide in ethanol[6]. The most commonly used synthesis to obtain ferrocenecarboxylic acid is the method described in the Organic Synthesis series[7]. Here ferrocene is first reacted with 2-chlorobenzoylchloride to yield 2-chlorobenzoylferrocene. This product is then reacted with potassium *tert*-butoxide in the presence of water to yield the desired carboxylic acid. The yield for this reaction is 74-83%. This method was adapted during the course of this study to obtain the ruthenocenoic acid.

2.1.3. SYNTHESIS OF ACETYL METALLOCENES

Friedel-Craft's acetylation reactions have mostly been performed on group VIII metallocenes. These reactions are shown in Scheme 2.4.

It was found by Graham and co-workers that the most effective way to acetylate ferrocene is to use 85% meta-phosphoric acid as the Lewis acid in the reaction[8]. The yield for this reaction after chromatographic separation was 71%. In this reaction there is only monoacetylation because of the weak Lewis acid, H_3PO_4 used. However, phosphoric acid cannot be used to acetylate the less reactive ruthenocene. The Lewis acid needed is aluminium trichloride because the reactivity of the metallocene decreases down group VIII for their respective metallocenes. In this case, however, diacetylation as well as monoacetylation is observed because of a stronger Lewis acid. The overall yield for this reaction is 67% and the products are separated by means of column chromatography. An effective way to acetylate osmocene has been described by Rausch and co-workers. In this acetylation reaction one has to use acetyl chloride [2]. The yield for this reaction was reported to be 89%. With acetyl chloride only monoacetylation occurs for osmocene. For ruthenocene and ferrocene monoacetylation and diacetylation is possible. An excess reagent ensures diacetylation but monoacetylation requires careful stoichiometric control.

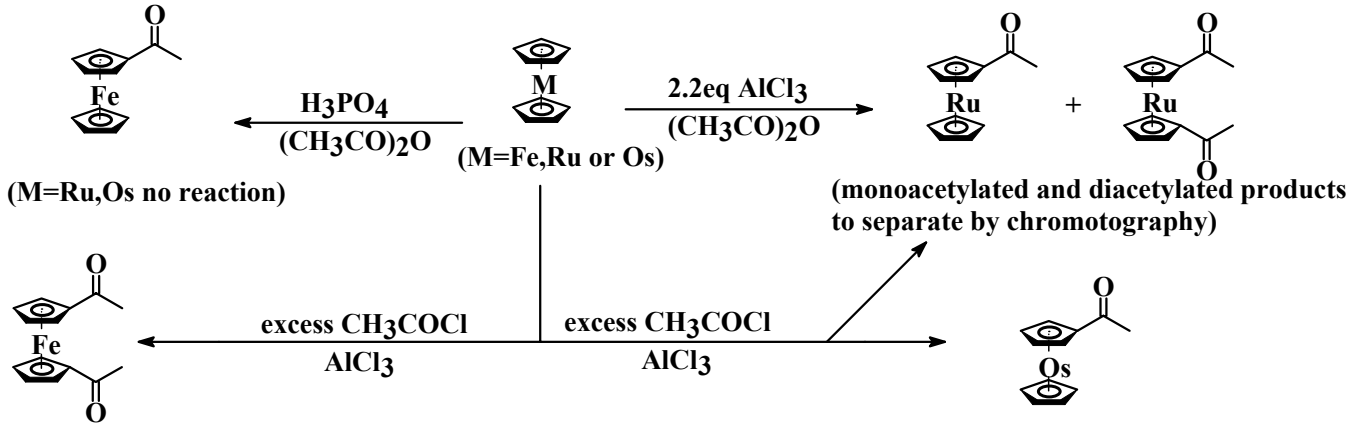

Scheme 2.4. Acetylation reactions for the group VIII metallocenes require more drastic conditions for M =Os than M = Ru while M =Fe requires the mildest conditions.

2.1.4. SYNTHESIS OF METALLOCENE ESTERS

Normally esters are obtained by reacting a carboxylic acid with an alcohol in the presence of a catalytic amount of a mineral acid such as H_2SO_4 or HCl. There does however exist alternative routes. It has been reported that the cobaltocene ester can be obtained by reduction of cobaltocene to the cobaltocenium anion and then reacting this with carbon dioxide in a dimethylformamide/methyl iodide solution[9].

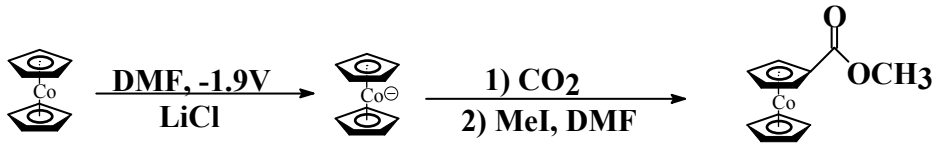

Scheme 2.5. Synthesis of the cobaltocene methyl ester

Diazomethane based esterification is also widespread and this method has been used for the synthesis of the methyl ester of 2-methylruthenocenoic acid.[10].

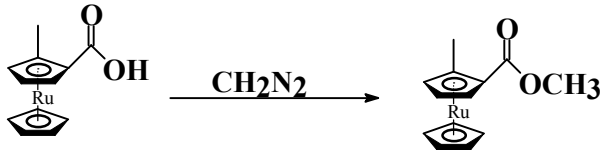

Scheme 2.6. Synthesis of a methyl-ruthenocene ester.

2.1.5. SYNTHESIS OF β-DIKETONES

Most often β-diketones are synthesised by Claisen condensation. This method is discussed in section 2.1.6. pertaining to the synthesis of metallocene containing β-diketones. There are, however, alternative routes one can follow.

An alternative route to prepare β-diketones has been shown by Suzuki and co-workers. In their method they heat an α,β-epoxy ketone at 80-140°C in toluene with small amounts of $(Ph_3P)_4Pd$ and 1,2-bis(diphenylphosphino)ethane. The β-diketone forms by a pinacol rearrangement[11,12]. The reaction of 2-methyl-3,4-epoxy-5-hexanone under the above conditions yields 80% 2-methyl-3,5-hexanedione. The reaction is shown in Scheme 2.7.

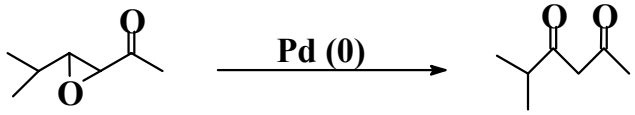

Scheme 2.7. Synthesis of 2-methyl-3,5-hexanedione according to the method of Suzuki

The method adopted by Roth and co-workers was to convert a thioester containing a β keto group in the alkyl postion. The β-diketone is formed by treatment with a tertiary phosphine under basic conditions[13]. A yield of 72% was obtained for the reaction where butyl butanethioate was converted to octane-3,5-dione. This reaction is shown in Scheme 2.8.

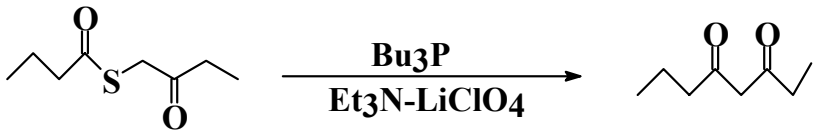

Scheme 2.8. Synthesis of octa-3,5-dione by the method of Roth

A number of novel β-diketones have been synthesized like the 4-pivaloyl –3-methyl-1-phenyl-5-pyrazolone complex by Umetani and co-workers[14]. This synthesis was carried out by the condensation reaction of 3-methyl-1-phenyl-5-pyrazalone with pivaloyl chloride in the presence of calcium hydroxide. The yield for this reaction is 19% and is shown in Scheme 2.9.

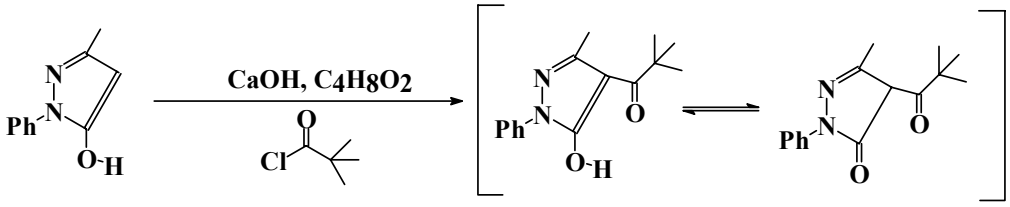

Scheme 2.9. Synthesis of 4-pivaloyl –3-methyl-1-phenyl-5-pyrazolone according to the method of Umetani

The method of synthesis for β-diketones as demonstrated by Cravero and co-workers involves acid-catalyzed condensation[15]. The compound *para*-NO_2-benzoylacetone was obtained by adding a mixture of *para*-NO_2-acetophenone and acetic anhydride to an acetic acid-BF_3 complex at 0°C for 30 minutes and then at 25°C for 24 hours. The reaction is shown in Scheme 2.10.

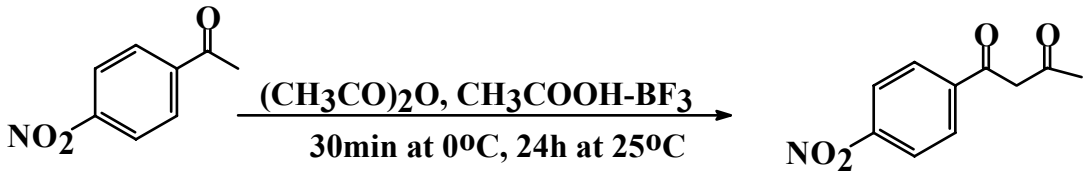

Scheme 2.10. Synthesis of para-NO_2-benzoylacetone according to the method of Cravero

With the advent of enzyme catalyzed reactions Gunslus and co-workers described the microbial degradation of (1R)-(+)-camphor by Corynebacterium T1. They found degradation to the symmetrical β-diketone 2,6-diketocamphane from the optically pure camphor.[16,17]. This enzymatic degradation is shown in Scheme 2.11.

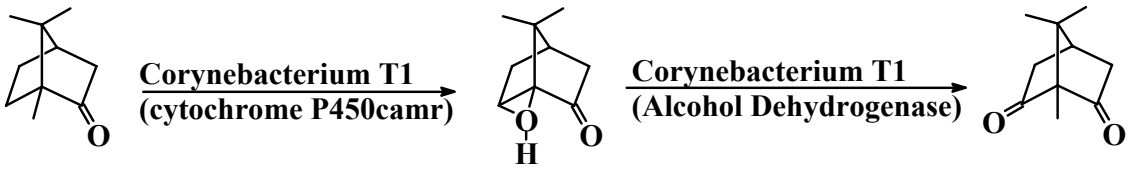

Scheme 2.11. Synthesis of 2,6-diketocamphane according to the method of Gunslus

2.1.6. SYNTHESIS OF METALLOCENE β-DIKETONES

The synthesis of metallocene-containing β-diketones has been achieved by Claisen condensation between acetylferrocene and the appropriate methyl or ethyl esters in the presence of a strong base. The methods adopted are shown in Schemes 2.12. and 2.13.

An effective method to obtain ferrocene-containing β-diketones was to use potassium amide as the strong base in a mixture of liquid ammonia and ether as shown by Hauser and co-workers[18] in Scheme 2.12. Yields of 65% for 1-ferrocenylbutane-1,3-dione (R=CH_3) and 63% for 1-ferrocenyl-3-phenylpropane-1,3-dione (R=C_6H_5) were achieved. Weinmayr demonstrated that the synthesis of the ferrocene-containing β-diketones could be achieved by using the base sodium methoxide[19] as shown in Scheme 2.12. With the use of this base a yield of 29% was achieved for 1-ferrocenylbutane-1,3-dione (R=CH_3) while 1-ferrocenyl-4,4,4-trifluorobutan-1,3-dione (R=CF_3) was obtained in 80% yield. The base sodium methoxide is a stronger base than sodium hydroxide but is still weaker than potassium amide and this explains the lower yield of 1-ferrocenyl-butane-1,3-dione in the method adapted by Weimayer compared to that of Hauser. Cullen and co-workers demonstrated the use of the hindered base lithium diisopropylamide[20] in the synthesis of 1-ferrocenylbutane-1,3-dione. This method has since been adopted by Du Plessis and co-workers to synthesize a variety of ferrocene-containing β-diketones[21].

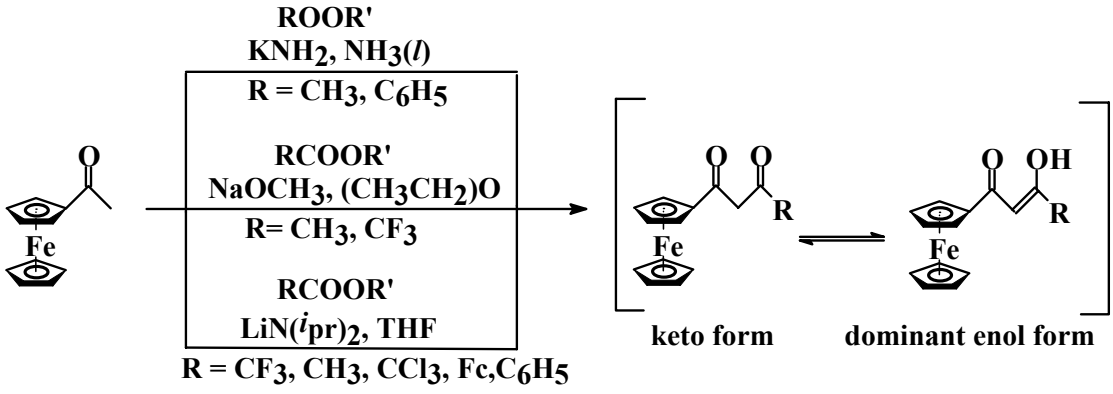

Scheme 2.12. Synthesis of ferrocene-containing β-diketones by Claisen condensation with the use of three different bases. (LiN(^{I}pr)$_2$ = lithium diisopropylamide, R$^{/}$ = methyl or ethyl)

In the work by Hauser it was shown that Claisen condensation between bisacetylferrocene and an appropriate ester could be obtained with potassium amide in liquid ammonia[22,23] as shown in Scheme 2.13. The yields were 72% for 1,1/-bis(1-butan-1,3-dione)ferrocene (R=CH_3) and 1,1/-bis[1-(3-phenyl)propane-1,3-dione]ferrocene (R=C_6H_5) was isolated in a 46% yield.

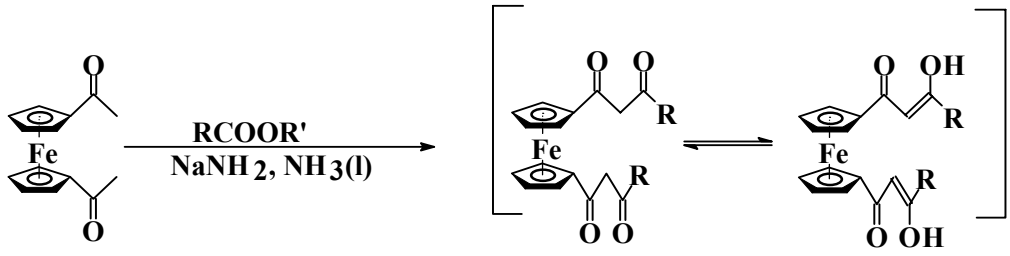

Scheme 2.13. Synthesis of ferrocene-containing bis-β-diketones . R = CH_3 or C_6H_5, R/ = CH_3 or C_2H_5

2.1.7. SYNTHESIS USING GRIGNARD REAGENTS

During the course of this study it was necessary to synthesise new electrolytes for electrochemical applications and in these syntheses it was necessary to use Grignard reagents[24]. Grignard reagents have been used in a variety of synthesis reactions, namely to form alkanes, carboxylic acids, alchols and ketones, as well as their use in solid-phase synthesis.

2.1.7.1. PREPARATION OF GRIGNARD REAGENTS

It was noted by Baker & co-workers that for some halides the Grignard reagents were unable to form unless activated magnesium was used. The activated magnesium was reacted with the halide and the Grignard reagent that formed was generally in excess of 90%. For the reaction in Scheme 2.14. the formation of the Grignard reagent was 100%[25].

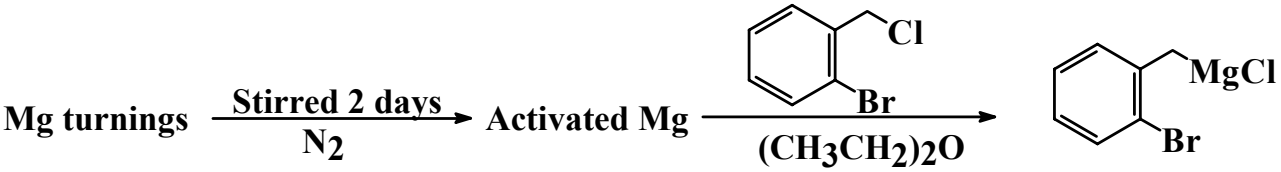

Scheme 2.14. Formation of a Grignard reagent according to the method of Baker

It was found by Knochel & co-workers that the conversion of the iodonaphthalene to its Grignard reagent proceeds with a 90% conversion when the reagents are reacted with *i*PrMgBr or $i Pr_2Mg$ in THF[26]. This is shown in Scheme 2.15.

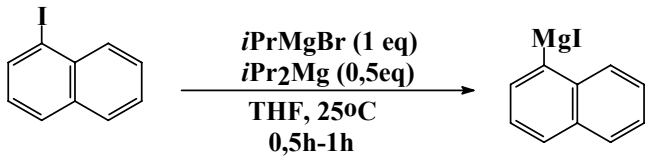

Scheme2.15. Formation of a Grignard reagent according to the method of Knochel

Grignard reagents have traditionally been prepared in ether solvents. However, Ashby & Reed found that Grignard reagents could be formed in hydrocarbon solvents using a tertiary amine as a complexing agent[27]. For these formation reactions in benzene the general yield was above 80%. In Scheme 2.16. the formation of the iodoethane Grignard reagent in a yield of 97% is shown.

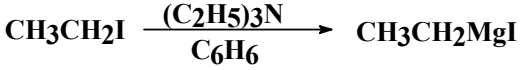

Scheme 2.16. Formation of a Grignard reagent in benzene according to Ashby & Reed

In recent years the [Mg(anthracene)$(thf)_3$] complex has been used in the synthesis of Grignard reagents where one has non-activated phenyl ring compounds, as well as when there are ether groups in the compound[28]. The yields for these reactions are usually above 90%. A typical reaction of this type is shown in Scheme 2.17.

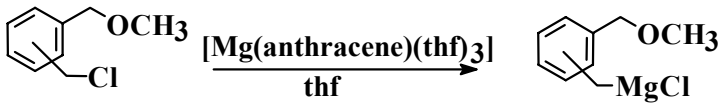

Scheme 2.17. Formation of a Grignard benzylic compound following the method of Gallagher

2.1.7.2. STABILIZING GRIGNARD REAGENTS

Grignard reagents are fickle reagents as they react with both water and oxygen, hence they are prepared in an anhydrous nitrogen atmosphere. As these reagents cannot be stored, they are used generally directly after formation[29]. There are, however, ways to stabilize Grignard reagents for later use. Grignard reagents generally are unreactive at low temperatures towards many

functional groups. They can be kept *in-situ* with less chance of negative side-reactions at lower temperatures[26].

Boudin & co-workers demonstrated that Grignard reagents could be stabilized in a powder form when a Grignard reagent in solution was chelated with a tertiary amine[30]. The stabilized Grignard reagent in Scheme 2.18. forms with a 72% yield when ethane bromide is first reacted with magnesium and then with TDA-1 ($[N(CH_2CH_3OCH_2CH_2OCH_3)_3]$).

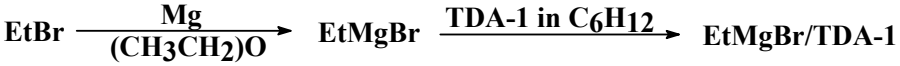

Scheme 2.18. Formation of a solid stabilized Grignard reagent

2.1.7.3. REACTION OF GRIGNARD REAGENTS WITH BORON COMPOUNDS

In this study we desired the formation of sodium borate salts from which the various electrolytes could be obtained. It was shown by Nishida that the sodium tetrakis[3,5-bis(trifluoromethyl)-phenyl]borate could be obtained by reacting the Grignard reagent 3,5-bis(trifluoromethyl)phenyl-magnesium iodide with an ethereal solution of boron trifluoride[31].

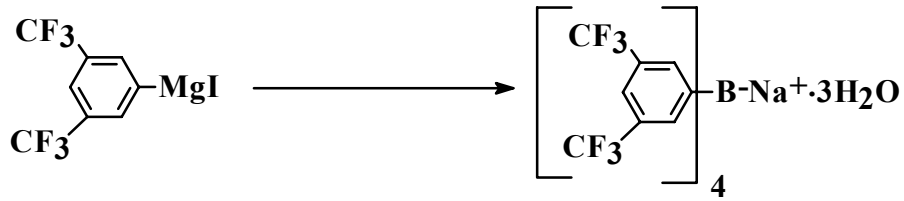

Scheme 2.19. Formation of sodium tetrakis[3,5-bis(trifluoromethyl)-phenyl]borate

2.2. MEDICINAL PROPERTIES OF METAL COMPLEXES

2.2.1. ANTI-CANCER PROPERTIES

2.2.1.1. CISPLATIN, THE FLAGSHIP MOLECULE

Cisplatin (see Figure 2.1.) has been actively used in the treatment of cancer since the chance discovery in 1965 by Rosenberg, Van Camp and Krigas of its activity in inhibiting bacterial growth[32]. Since then there have been various studies on the effectiveness of cisplatin against different cancers, its cytotoxicity, its distribution in the body, the mechanism by which it destructs cancer cells and dose concentration[32,33].

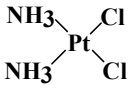

Figure 2.1. Structure of Cisplatin

Although cisplatin has been used against cancer, it does have many side effects. For instance, it causes the formation of lung adenomas. Also repeating cell lines develop resistance to the drug. Fortunately, cisplatin can still be used effectively with other drugs in a synergistic manner and so much so that cisplatin is still used today[34]. Some of the side-effects of cisplatin have been countered by the simultaneous use of other drugs[35]. The resistance of some cancer cell lines has been addressed by using other platinum coordination compounds that are similar in structure to cisplatin[36,37], such as carboplatin. However, even these new generation platinum drugs have severe side-effects, and hence the search for new cancer drugs is a world-wide priority.

2.2.1.2. THE USE OF RHODIUM AND RUTHENIUM DRUGS IN CANCER THERAPY

Various metals other than platinum have been used in the treatment of cancer. Some of the first ruthenium and rhodium complexes that compared to cisplatin in effectivity were discussed by Giraldi & co-workers[38]. This [(acetylanato)(cycloocta-1,5-diene)rhodium] complex showed less histiological damage than cisplatin. The complex acetylacetonate-1,5-cyclooctadiene rhodium (I) shown in Figure 2.2. is analogous to the ruthenocene compounds synthesised in this study.

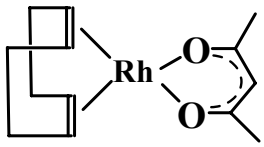

Figure 2.2. Structure of acetylacetonate-1,5-cyclooctadiene rhodium (I)

The ferrocene-containing β-diketone in Figure 2.3., an analogue of the complex in Figure 2.2., has been tested against HeLa (a sensitive human cervix epithelial carcinoma cell line), CoLo (an intrinsically multi-drug resistant human colon adeno carcinoma cell line) and COR (a sensitive human lung large cell carcinoma cell line) cancer lines. These complexes were found in some cases to be twice as effective in killing cancer cells than cisplatin. It was also shown they can differentiate between cancer cells and healthy cells in a ratio 8:1.[39].

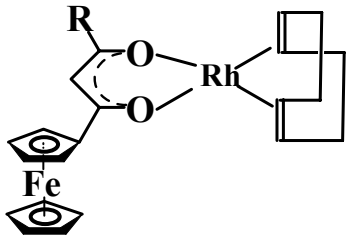

Figure 2.3. Structure of the ferrocene-containing β-diketone complexes analogous to that of Figure 2.2. R = CF_3, CH_3, CCl_3, C_6H_5

Future studies of the new ruthenocene analogues developed during the course of this study may show that the ruthenocene centre may induce further beneficial effects in the treatment of cancer with these types of complexes.

There have been various other rhodium- and ruthenium-containing complexes used in the fight against cancer. However, more recently there have been some interesting developments in organometallics with ruthenium as the metal center. New antineoplastic ruthenium compounds have been developed[40] and it has been shown that some ruthenium compounds prevent cytotoxicity which has been induced by other chemotherapeutic drugs[41,42].

2.2.1.3. RUTHENOCENE COMPOUNDS IN CANCER THERAPY

The radiopharmaceutical acetyl-(^{103}Ru)-ruthenocene has been used in the investigation of the affinity of acetylruthenocene for the adrenal glands of mice. This labelled compound was prepared by heating acetyl ferrocene with 103-ruthenium trichloride. It was shown that the compound has an affinity for the regions of the adrenal gland where adrogen and glucocorticoid syntheses occur[43]. A study was then carried out to show the effect of hormones on the localization of acetylruthenocene. It was found that if the hormones can be controlled, the target of the acetyl ruthenocene can also be controlled *in vivo* [44].

2.2.1.4. FERROCENE COMPOUNDS IN CANCER THERAPY

Ferrocene derivatives have been linked to water-soluble polymers, so that the dose-limiting factors in chemotherapy in terms of poor solubility can be overcome. It was also found that for the water-soluble polymeric drug fewer drug units were needed for the same effectiveness than when the drug was administered in monomeric form[45]. This is shown in Figure 2.4.

It was shown in this study that both the size of the spacer between the ferrocene drug from the polymer backbone as well as the formal reduction potential of the ferrocenyl group play an important role in drug activity. Longer spacers and lower ferrocenyl formal reduction potentials both enhance the anticancer activity.

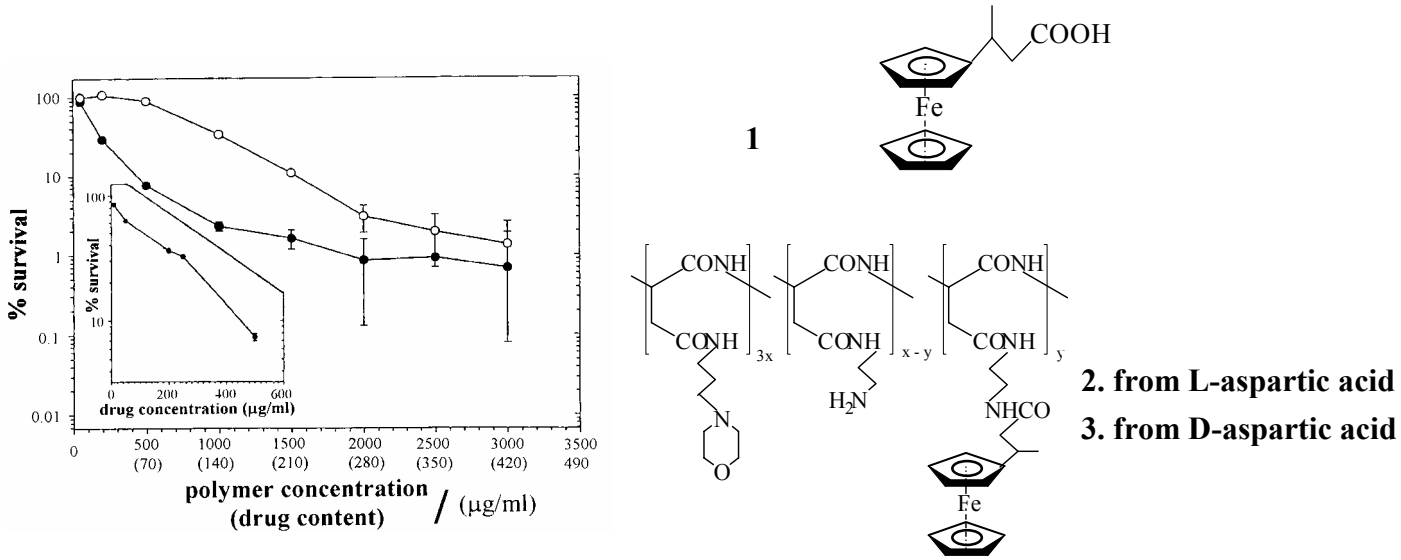

Figure 2.4. % Survival of murine EMT-6-cells after 24 hours of incubation with ferrocene derivatives 1 (inset), 2 (○) and 3 (•). (J.C. Swarts, D.M. Swarts, D.D. Maree, E.W. Neuse, C. La Madeleine and J.E. Van Lier, *Anticancer Res.*, 2000, 20, **1)**

2.2.2. ANTI-MALARIAL PROPERTIES

Chloroquine and sulfadoxine pyrimethamine are the most effective drugs in the fight against malaria. Due to increased resistance of malaria strains to these drugs, some novel organometallic anti-malarial drugs have been synthesised. It was found that by co-ordination of ruthenium and rhodium to chloroquine, these new complexes where highly active against chloroquine-resistant malaria strains[46]. It was also shown that in *in vivo* tests against *Plasmodium berghei* there is no associated toxicity of the drug.

The gold complex $[Au(PPh_3)(chloroquinone)]PF_6$ has also been synthesised for the enhancement of anti-malarial action against chloroquine-resistant strains[47].

With increased resistance of *Plasmodium falciparum* towards the anti-malarial drug chloroquine, it was found that by introducing a ferrocene moiety to this compound the anti-malarial activity of this drug could be increased. It was also found that the amine and urea analogues of ferrochloroquine had a better activity in the death of the resistant strains of malaria as well as the sensitive strains of malaria[48,49]. The compounds tested are shown below in Figure 2.5.

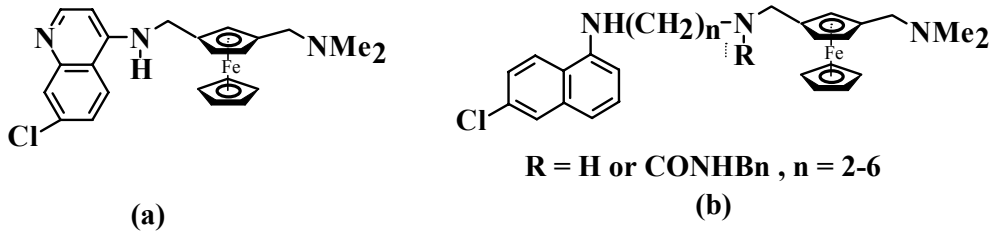

(a) **(b)**

Figure 2.5. Structures of (a) ferrochloroquine and (2) its new analogues.

It was shown in this study that there is good activity of the compounds where there is a 3-carbon methylene spacer which yields an activity 3 times that of chloroquine. It was also found that the easier the oxidation of the compound the lower the antimalarial activity. This follows the opposite trend that was observed for anticancer therapy.

Studies by Beagley and co-workers on the ruthenocene analogues of the aforementioned drugs, showed that the activity of the ferrocene and ruthenocene compounds were comparable[50].

2.3. ELECTROCHEMISTRY

An interested reader can find detailed treatments of the cyclic voltammetry technique elsewhere[51-54].

2.3.1. NEW ELECTROCHEMICAL TECHNIQUES

Experiments have been conducted by Tsionsky and co-workers to analyze the effect of a lipid monolayer on electron transfer between a liquid/liquid interface. They found that the lipid monolayer resulted in a decreased rate of interfacial electron transfer between the aqueous redox species and the oxidized form of zinc porphyrin in benzene[55]. The redox systems they used in the aqueous phase were $Ru(CN)_6^{3/4-}$, $Mo(CN)_8^{3/4-}$, $Fe(CN)_6^{3/4-}$, $Fe^{3/2+}$, $V^{3/2+}$, or Co(III)/(II) sepulchrate. The anion used was ClO_4^- and it could readily cross the interface to maintain electro-neutrality. They showed that these charge transfer processes at the lipid monolayer are relevant to those at biological membranes. The process between these two layers is shown below in Figure 2.6.

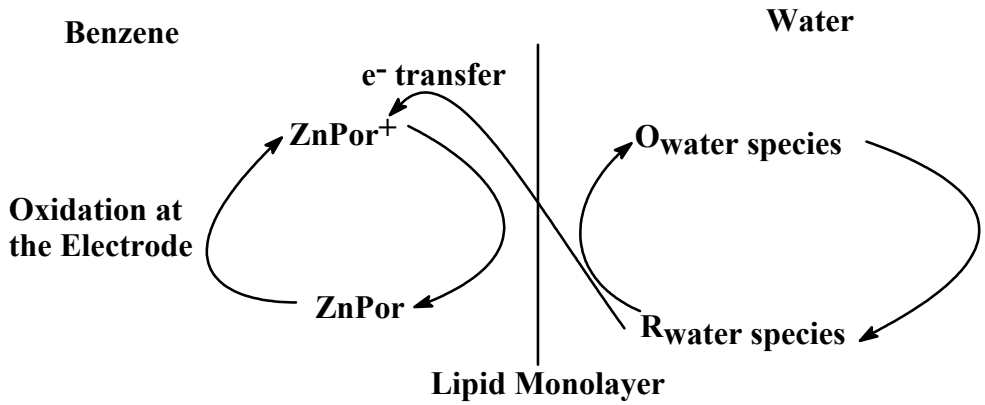

Figure 2.6. Mimicking of a biological membrane. O = oxidised aqueous species, R = reduced aqueous species and Por = porphyrin (from M. Tsionsky, A.J. Bard and M.V. Mirkin, *J. Am. Chem. Soc*., 1997, 119, 10785)

Wu has showed that by modifying the edge plane pyrolytic graphite electrode surface one is able to obtain a cyclic voltammogram of some albumin-heme hybrids in aqueous solution. In comparison, when the electrode surface was not modified, one was unable to observe the reduction and oxidation processes[56]. Electrode modification was achieved by immobilizing the sample under study on the electrode surface and thus forming a thin film for analysis.

Van Staveren and co-workers have shown that by electrochemical analysis at variable temperatures one is able to detect different conformations of the complex under study in solution [57]. They found in their study of the complex [Mo(His-N_ε-$C_2H_4CO_2Me$)(η-allyl)$(CO)_2$] there are two different conformers of the complex in both the reduced and oxidized forms.

Another method where temperature has been used in electrochemical analysis is that by Cosmo and co-workers[58]. The work conducted involved studying the highly reduced porphyrins and the only way they could stabilize the reduced porphyrins was to conduct the electrochemical analysis at –20ºC. At this temperature they were able to study the different reduction steps of the porphyrin.

2.3.2. ELECTROCHEMISTRY OF RUTHENOCENE

Traditionally the view has been that the oxidation of ruthenocene proceeds by a $2e^-$ irreversible process[59]. This result was observed by using tetrabutylammonium perchlorate as supporting electrolyte. However, this electrolyte has weak coordinating properties.

It was later shown that a $1e^-$ reversible electrochemical process occurs when the electrochemistry is performed utilising a noncoordinating electrolyte in a noncoordinating solvent[60]. The electrolyte was tetrabutylammonium tetrakis[3,5-bis(trifluoromethyl)phenyl]borate (TBA^+TFPB^-). A reduction potential of 1.03V was obtained for ruthenocene *versus* an aqueous AgCl/Ag (1.0M KCl) reference electrode. The CV is shown in Figure 2.7.

A quasi-reversible $1e^-$ oxidation of ruthenocene in Lewis acid-base molten salts was also demonstrated[61]. In their analysis the solvent was a mixture of 0.8:1 $AlCl_3$: 1-butylpyridinium chloride, into which the ruthenocene was dissolved. This CV is shown in Figure 2.8.

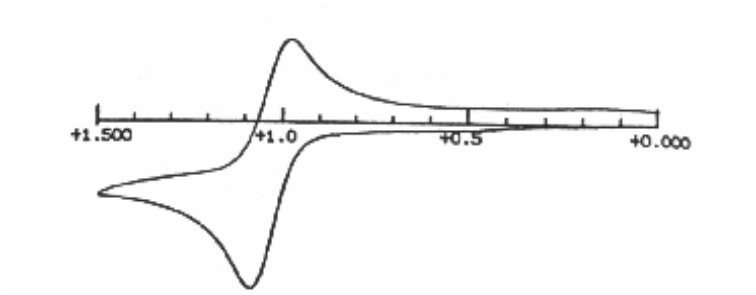

Figure 2.7. The $1e^-$ reversible electrochemistry of ruthenocene (0.5mM), in 0.1M TBA^+TFPB^- in dichloromethane. Scan Rate = 100mV/s. (from M.G. Hill, W.M. Lamanna and K.R. Mann, *Inorg. Chem*., 1991, 30, 4687)

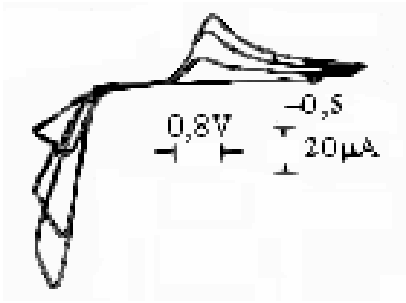

Figure 2.8. The quasi-reversible 1e$^-$ oxidation of ruthenocene (22.2mM) in Lewis acid-base molten salts. (from R.J. Gale and R. Job, *Inorg. Chem*., 1981, 20, 42)

In ruthenocene-substituted derivatives there is a deviation from the known electrochemistry of the parent metallocene compound. It has been recently shown by Jacob and co-workers that the electrochemistry of a newly synthesised novel ruthenocene surfactant is irreversible[62]. In this study it was demonstrated that there are two oxidation peaks at 740mV and 910mV for the compound dodecyl-dimethyl(methylruthenocenyl)-ammonium bromide in an 0.1M NaCl aqueous solution. It was further noted that even at very high scan rates there was no observable reduction peak.

Sato and co-workers found irreversible electrochemistry for binuclear ruthenocene compounds[63]. They showed that for the compound 1,4-bis(ruthenocenyl)benzene the two oxidation potentials were 0.42V and 0.56V *versus* the ferrocene/ferrocenium couple, the reduction peak occurred at 0.28V. The CV of the binuclear compound is shown in Figure 2.9.

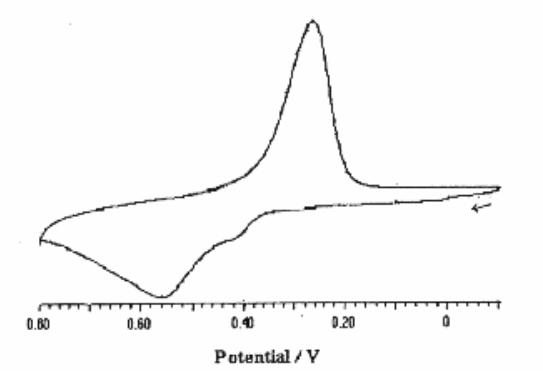

Figure 2.9. Irreversible electrochemistry of 1,4-bis(ruthenocenyl)benzene in dichloromethane utilising a glassy carbon electrode. Scan rate 0.1 V s^{-1}. Supporting electrolyte $TBAClO_4$ (from M. Sato, G. Maruyama, A. Tanemura, *J. Org. Chem*., 2002, 655, 23)

2.3.3. DEVELOPMENTS IN SOLVENTS AND ELECTROLYTES

Recent developments in the development of new supporting electrolytes and the use of nontraditional solvents have increased options in electrochemical studies. It has been demonstrated by Ohrenberg and Geiger that using the noncoordinating solvent α-α-α-trifluorotoluene (or (trifluoromethyl)benzene) and the electrolyte tetrabutylammonium tetrakispentafluorophenylborate (TBA[$B(C_6F_5)_4$]) reversible electrochemistry could be obtained for nickelocene [64]. In their analysis they found that the Ni (II) /Ni (III) and Ni (III) / Ni (IV) couples yielded i_{pa}/i_{pc} ratios of 1 and ΔE_p values of 75mV and $E^{o/}$ values of –0.42V and 1.10V *vs* Fc/Fc^+ respectively. The analysis of the cobaltocene Co (III) /Co (II) couple also yielded reversible electrochemistry with $E^{0/} = -1.35V$, while the Co (II) /Co (I) couple was observed at –2.48V but due to solvent destruction this couple does not exhibit an i_{pa}/i_{pc} ratio of exactly 1. The CV of the reversible electrochemistry of cobaltocene and nickelocene is shown in Figure 2.10.

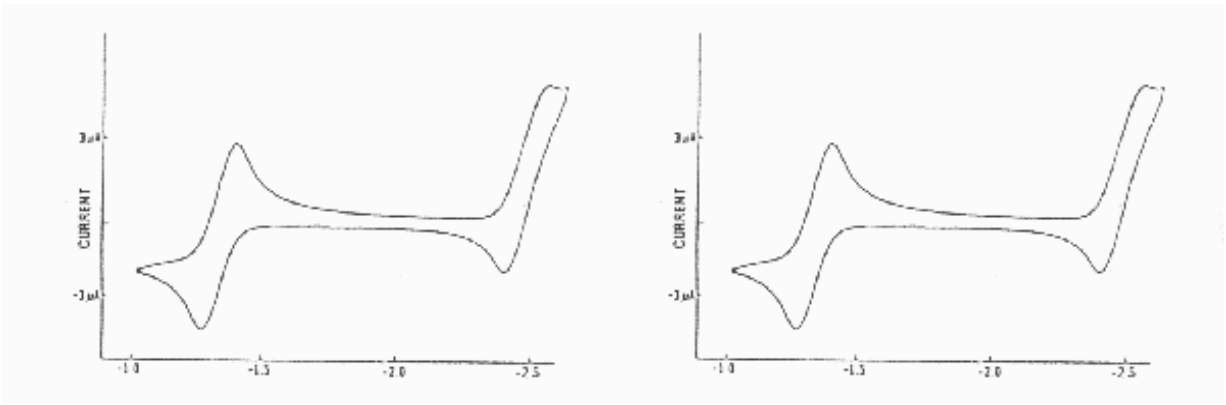

Figure 2.10.The reversible electrochemistry of cobaltocene (left) (1 mM) and nickelocene (right) (5 mM) in α-α-α-trifluorotoluene utilising a glassy carbon electrode. Supporting electrolyte TBA[$B(C_6F_5)_4$] (0.1 M). Scan rate 0.1 V s^{-1}. (from C. Ohrenberg and W.E. Geiger, *Inorg. Chem*., 2000, 39, 2948)

LeSeur and Geiger showed that the use of the non-coordinating supporting electrolyte tetrabutylammonium tetrakis(pentafluorophenyl)borate improves electrochemistry compared to electrochemistry incorporating the weak coordinating electrolyte tertrabutylammonium hexafluorophosphate [65]. It was shown that with the use of this electrolyte electrochemistry could be conducted in solvents of low dielectric strength, for

example, in *t*-butyl methyl ether. It was also shown that the peak separation between two very close oxidation peaks can be better analyzed with the use of this electrolyte. This can be seen in Figure 2.11. where the CV of the triferrocenyl compound $[Fe(\eta\text{-}C_5H_4)_2]_3$ $(SiMe_2)_2$ is shown.

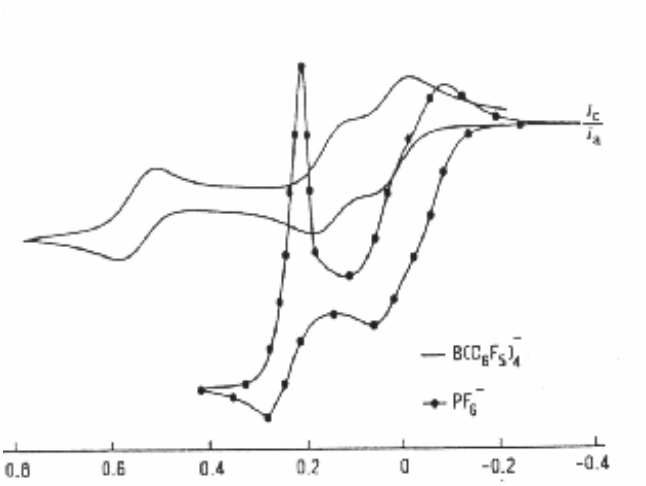

Figure 2.11. Electrochemistry of $[Fe(\eta\text{-}C_5H_4)_2]_3$ $(SiMe_2)_2$ (1.0 mM) with the electrolyte ─ $[NBu_4]$ $[B(C_6F_5)_4]$ and the electrolyte ─● $[NBu_4][PF_6]$ versus Ag/AgCl reference electrode. Solvent dichloromethane. Scan rate 0.2 V s^{-1}. (from R.J. le Suer and W.E. Geiger, *Angew. Chem*., Int. Ed. Engl., 2000, 39, 248)

In the work by Pospišil and co-workers cyclic voltammetry was possible with the use of the supporting electrolyte dodecamethylcarba-*closo*-dodecaborate in benzene. It was demonstrated that there was an increased electrical conductivity in these solutions[66]. From their analysis they obtained a ΔE_p value of 59 mV for the ferrocene/ferrocenium couple, which is closer to the ideal than has been previously reported.

2.4. KINETICS

In this study the kinetics of the isomerization of the β-diketones was studied as well as the substitution kinetics relating to β-diketone substitution in [Rh(β-diketanato)(cod)] complexes with 1,10-phenantroline.

2.4.1 ISOMERIZATION KINETICS

A detailed treatment of the isomerization kinetics understudy can be found in the literature[67].

The equilibrium between the keto and enol isomers of a β-diketone is well known. It is possible to follow the rate of keto- to enol-conversion (and *vice versa*) kinetically, provided the rate of conversion from the one form to the other is slow.

In the work of Cravero the tautomeric equilibrium between the two enol isomers of the benzoylacetones where studied with the use of ^{13}C NMR[68]. It was found that with electron-withdrawing para groups the equilibrium shifts towards the keto form. The equilibria studied are illustrated in Scheme 2.20.

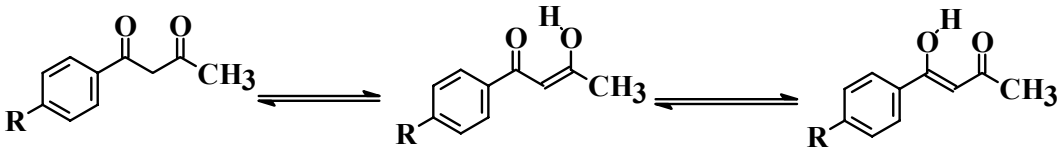

Scheme 2.20 Types of keto-enol equilibria studied by Cravero

Blokzijl and co-workers showed that solvents affect the keto-enol equilibrium[69]. They showed in their studies that the keto-enol equilibrium of pentane-2,4-dione was affected by the alcohol:water ratio. More alcohol in solution favoured the enol isomer.

Iglesias and Ojea-Cao demonstrated that the equilibrium between the keto and enol forms of benzoylacetone could be shifted towards the enol form by adding β-cyclodextrin and sodium dodecyl sulfate[70]. The results suggest that the enol form protrudes deeper into the β-cyclodextrin cavity, whereas in the keto form only the phenyl ring is enclosed in the β-cyclodextrin cavity.

In the study by Du Plessis and co-workers the rate of conversion between the two tautomers of the ferrocene-containing β-diketones were studied using ^{1}H NMR. They found that the dominant enol isomer in solution had the OH on the carbon furthest from the ferrocenyl moiety[71]. The equilibria studied are shown in Scheme 2.21.

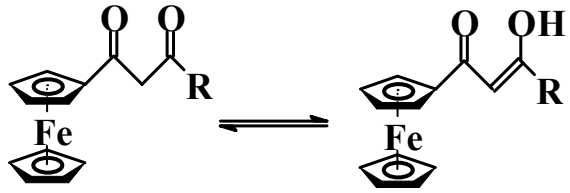

Scheme 2.21. The keto-enol tautomerizations studied by Du Plessis. (R = CF_3, CCl_3, CH_3, C_6H_5 and ferrocenyl.)

They showed that the equilibrium constant was not affected much by varying the β-diketone concentration. In temperature studies they showed that by increasing the temperature from 20°C to 60°C the percentage keto isomer at equilibrium increased for R = ferrocene, CH_3, C_6H_5 and CCl_3, while it decreased for R= CF_3. An important observation in their study was that by leaving the β-diketone in the solid state for a minimum of two months, all the β-diketone was converted to the enol form.

2.4.2. SUBSTITUTION KINETICS

For the interested reader a detailed study of substitution kinetics and activation parameters can be found elsewhere[71-76].

It was shown by Leipoldt and co-workers that the substitution of carbonyl ligands in β-diketonatocarbonylrhodium(I) complexes by cyclooctadiene occurs through an associative mechanism[78]. They further showed that the reactivity of the β-diketone complexes is of the order BA<DBM<<TFAA<TFBA<<HFAA (BA = benzoylacetone, DBM = dibenzoylmethane, TFAA = 1,1,1,-trifluoro-2,4-pentadione, TFBA = 1,1,1,-trifluoro-4-phenyl-2,4-pentanedione, HFAA = 1,1,1,-trifluoro-5,5,5-trifluoro-2,4-pentanedione). This reveals that an increase in electron affinity of the R groups in the β-diketone has an effect on the kinetics. The reaction and rate law from this study was:

$$[Rh(\beta\text{-diketone})(CO_2)] + cod \longrightarrow [Rh(\beta\text{-diketone})(cod)] + 2CO$$

$$\frac{d[Rh(\beta\text{-diketone})(cod)]}{dt} = (k_s + k_2[cod])[Rh(\beta\text{-diketone})(CO)_2] = k_{obs}[Rh(\beta\text{-diketone})(CO_2)]$$

where $k_{obs} = k_s + k_2[cod]$

Potgieter studied the substitution of the β-diketonato ligand in β-diketonato(1,5-cyclooctadiene)rhodium(I) complexes by benzoyl-1,1,1-trifluoroacetone[79] (β-diketonato = acac, BA, DBM TFAA and HFAA). It was found that the rate of the reaction depends on which bond between the leaving β-diketone group and the rhodium atom will be cleaved first. It was further shown that in some cases the rate is influenced by which bond between the incoming β-diketone and the rhodium atom forms first. Thus it was demonstrated that the rate was influenced by the rate-determining step which is either the cleavage of the β-diketone rhodium bond or the formation of the rhodium β-diketone bond. Due to the large negative ΔS_y^* it was deduced that the reaction proceeds *via* an associative mechanism. The proposed mechanism for the reactions studied is:

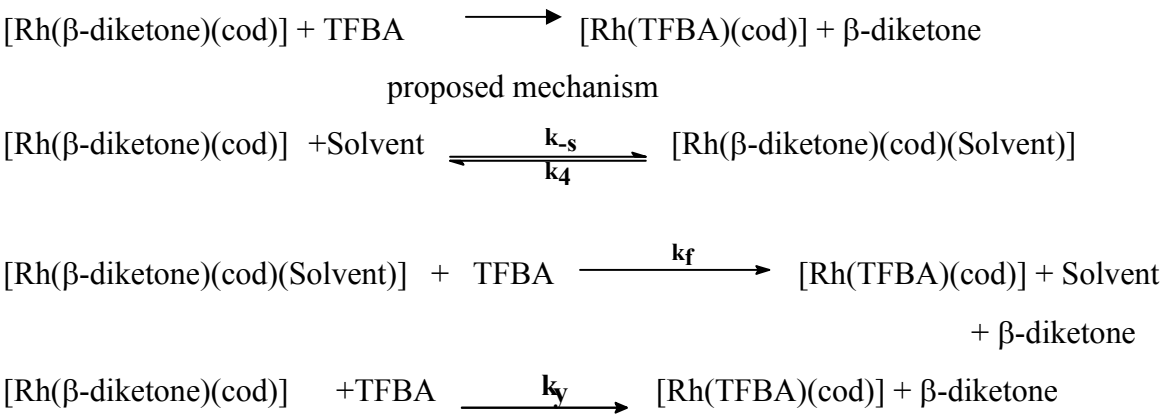

The kinetics for the substitution of the cyclooctadiene ligand in β-diketonato(1,5-cycloocta diene)rhodium(I) complexes (with the β-diketones: acac, BA, DBM, TFAA, TFBA and HFAA) by triphenylphosphite was studied by Leipoldt and co-workers [80]. It was demonstrated that there was no solvent pathway for this substitution. They showed that displacement of the cod ligand by the solvent would be more difficult than the displacement by the monodentate triphenylphosphite ligand. This was observed in the plot of observed rate constants versus triphenylphosphite concentration where a zero intercept for the substitution reaction at the different temperatures was obtained. This plot is shown in Figure 2.12.

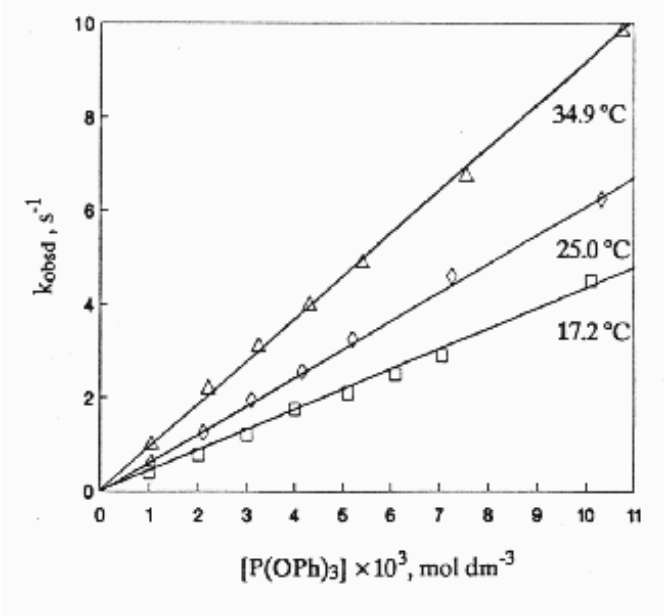

Figure 2.12. Plot of k_{obs} versus $[P(OPh)_3]$ at various temperatures for the substitution of the cyclooctadiene ligand in [Rh(TFAA)(cod)] (0.1 mM) by triphenylphosphite (from J.G. Leipoldt, G.J. Lamprecht and E.C. Steynberg, *J. Organomet. Chem*., 1990, 397**, 239)**

In a study by Leipoldt and co-workers on the substitution kinetics between β-diketonato-1,5-cyclooctadienerhodium(I) (β-diketones: acac, BA, DBM, TFAA, TFBA, HFAA) complexes and 1,10phenantroline, they found that the substitution proceeds by an associative mechanism[81,82,83]. From the graphs of k_{obs} versus [Phen] they were able to conclude that the reactions did not proceed through a solvent pathway due to the zero intercepts. They showed further that with different R groups of the β-diketones the value of the rate constant increased when the electronegativity of the R group increases, and that the more basic the β-diketone, the slower the rate of the reaction.

Work was also conducted by Vosloo and co-workers on ferrocene-containing β-diketonato complexes of the type [Rh(FcCOCHCOR)(cod)] with R=CF_3,CCl_3,CH_3,C_6H_5 and Fc=ferrocenyl where the β-diketonato ligand is replaced by 1,10-phenanthroline. They found an associative substitution mechanism, in addition a solvent pathway mechanism was followed that was most pronounced for the $FcCOCH_2COC_6H_5$ complex[84]. The plots of rate constants versus 1,10-phenanthroline concentration can be seen in Figure 2.13. An associative mechanism was assigned, due to the large negative activation energies. In contrast to other work with β-diketone containing rhodium(I) complexes the substitution process is only affected significantly by β-

diketanato pK_a provided $pK_a < 10$. When the $pK_a > 11$, the substitution process was almost independent of β-diketanato pK_a. This is shown in Figure 2.14. [81]. They concluded that this was due to the very strong Rh-O bonds that the ferrocenyl group induces. They were then further able to determine that the rate-determining step in the substitution mechanism was the breaking of the Rh-O bond rather than the formation of the Rh-N bond.

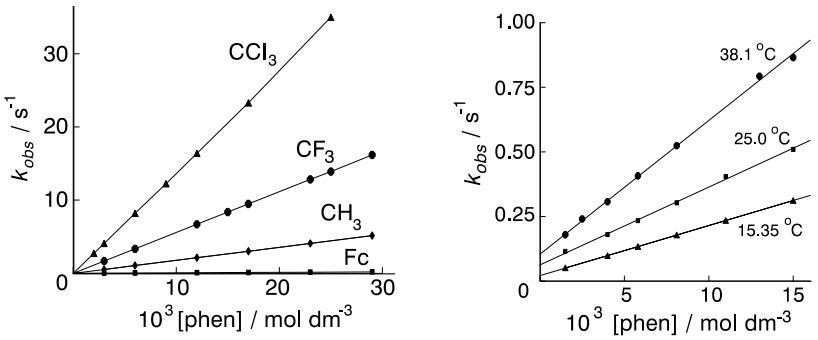

Figure 2.13. Plots of the pseudo-first order rate constants versus [phenanthroline] for the non-solvent pathway (left) and solvent pathway (right for R = C_6H_5) for the β-diketonato substitution from [Rh(FcCOCHCOR)(cod)] with 1,10-phenanthroline, R = CCl_3, CF_3, CH_3, Fc or C_6H_5. (from T.G. Vosloo, W.C. du Plessis and J.C. Swarts, *Inorg. Chim. Acta*, 2002, 331**, 188)**

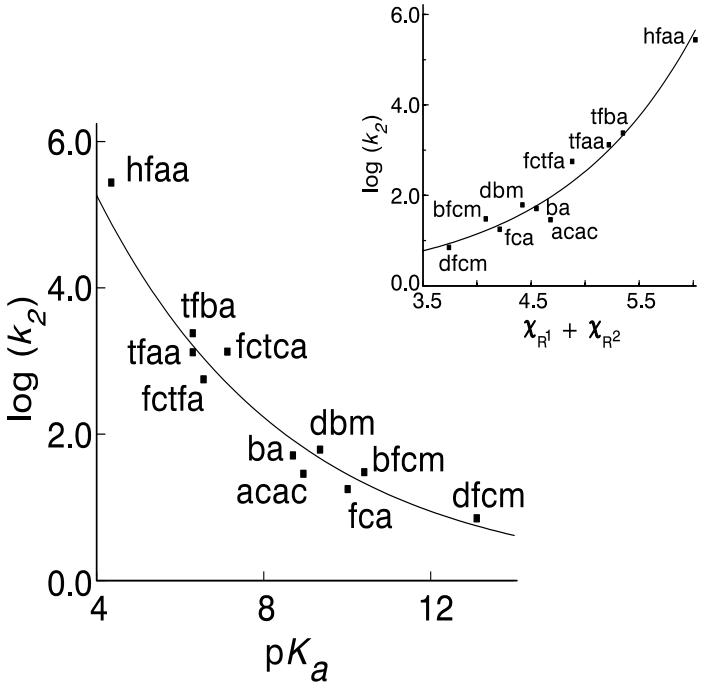

Figure 2.14. Plot of log k_2 versus acid dissociation constant values for the free β-diketones for the substitution of RCOCHCOR$^{/}$ in complexes of the type [Rh(RCOCHCOR$^{/}$] with 1,10-phenanthroline. Insert: plot of accumulative electronegativities of R groups on β-diketone versus log k_2. (from T.G. Vosloo, W.C. du Plessis and J.C. Swarts, *Inorg. Chim. Acta*, 2002, 331, 188)

2.5. ACID DISSOCIATION CONSTANTS

The acid dissociation constant is the equilibrium constant for the ionization of a weak acid, and this can be shown by looking at the following equation.[85]

$HA(aq) + H_2O(l) \rightleftharpoons H_3O^+(aq) + A^-(aq)$

From the equation the equilibrium constant is

$$K_c = \frac{[H_3O^+][A^-]}{[HA][H_2O]}$$ which rewritten gives

$$K_a = K_c[H_2O] = \frac{[H^+][A^-]}{[HA]}$$

note $pK_a = -\log K_a$.

For the ferrocene-containing β-diketones synthesized by Du Plessis, $pK_a^/$ refers to the process shown in Scheme 2.22.

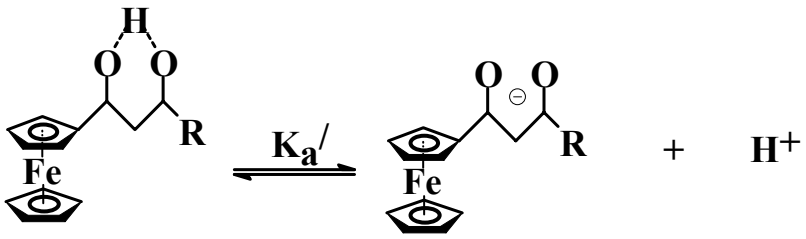

Scheme 2.22. A schematic defining the acid dissociation constant equilibrium for metallocene-containing β-diketones

In the work done by Du Plessis and co-workers they referred to the $pK_a^/$ and not pK_a since there was no attempt to partition between the separate pK_a values for the enol and keto tautomers[21].

The two most common methods used in the determination of pK_a values are the spectroscopic monitoring of an acid base titration and the conductometric method. The conductometric method involves conductometric measurements of diluted solutions so as to obtain a value for the limiting conductance as well as to obtain a value for the equivalent conductance, and from this data it is possible to determine the pK_a.

The absorbance method was adapted by Du Plessis and co-workers in their study of ferrocene β-diketones[21,86]. The $pK_a^{/}$ values for the ferrocene-containing β-diketones $FcCOCH_2COR$ (R = Cl_3, CH_3, C_6H_5 , Fc) were obtained by inserting the pH data into the following equation utilizing the fitting program MINSQ[87].

$$A_T = \frac{A_{HA}10^{-pH} + A_A 10^{-pKa^{/}}}{10^{-pH} + 10^{-pKa^{/}}}$$

For the ferrocene β-diketone with R = CF_3, however, two pK_a values were observed. The second pK_a value was proposed to be due to the attachment of a hydroxide group to the β-diketone at the carbonyl group to which the CF_3 group was attached. This reaction that was proposed to occur is shown in Scheme 2.23. Similar situations were proven by crystallographic studies[88,89,90]. For the CF_3 β-diketone, the equation needed to determine the $pK_a^{/}$ by inserting the pH data utilizing the fitting program MINSQ is.

$$A_t = \frac{A_{HA}(10^{-pH})^2 + A_A(10^{-pKa^{/}})(10^{-pH}) + A_F(10^{-pKa^{/}})(10^{-pKa2^{/}})}{(10^{-pH})^2 + (10^{-pH})(10^{-pKa^{/}}) + (10^{-pKa^{/}})(10^{-pKa2^{/}})}$$

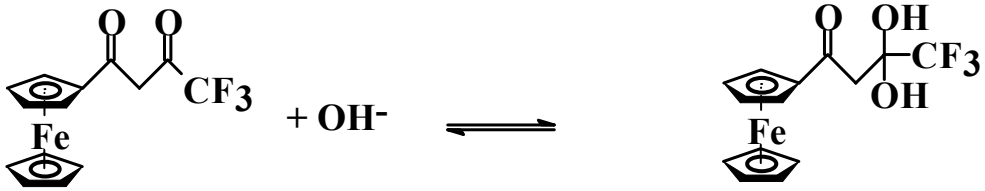

Scheme 2.23. The reversible hydroxylation that occurs between the compound 1-ferrocenyl-4,4,4-trifluorobutane-1,3-dione and the incoming hydroxide ion.

Fuoss and Kraus have used the conductivity method of determining acid dissociation constants. The conductivity method is especially useful at low pH but not at high pH values[91,92]. In their study method they applied the general equation

$$K_a = \frac{\Lambda_c}{\Lambda_o} = \frac{\alpha^2 c}{1-\alpha}$$ (α is the degree of ionization, Λ_c is the equivalent conductance and Λ_o is the limiting conductance). From this equation, the pK_a value obtained was refined further by applying activity coefficient corrections.

In work done by Ballinger and Long they showed that by using conductometric methods, they where able to determine the pK_a values for substituted methanols[93,94]. They where able to

determine acid dissociation constant values up to a pK_a =15.5 for propan-1-ol, and an extrapolated value of 15.9 for ethanol. Here, the method applied did not require refining but merely the determination of the conductance of dilute solutions to obtain the limiting conductance as well as the equivalent conductance. The pK_a data obtained for the range of substituted methanols as studied by Ballinger is given in Table 2.1.

During the course of this study the author made exclusive use of the spectoscopic method for determining the $pK_a^{/}$s of a series of new ruthenocene containing β-diketones.

Table 2.1. Substituent effects on the acid dissociation constants for substituted methanols (RCH_2OH) as studied by Ballinger

R group	pK_a
CH≡C-	13.55
CH_2Cl-	14.31
CH_3OCH_2-	14.8
$HOCH_2$-	15.1
H-	15.5
CH_2=CH-	15.5
CH_3-(extrapolated)	15.9

2.6. ELECTRONEGATIVITIES

Electronegativity (χ) is an emperical measure of the ability of an atom in a molecule to attract bonding electrons to itself[95,96]. These values vary with the oxidation states of the atom, the amount of outer lying energy levels, the atom bonded to the atom of which we want to determine the electronegativity, bond distance between the atoms and various other factors. The values thus obtained are only useful as a semiquantitative notion. Group electronegativities (χ_R) refer to the combined electronegativity of not only one atom but also a specific side group. If we consider the group electronegativity for the CF_3 group in the ester $CH_3CH_2COOCF3$, then the group electronegativity will be 3.01 on the Gordy scale.

There are four different scales for expressing χ. They are the Pauling χ_P; Allerd & Rochow χ_{A+R}; Allen χ_{spec} and Gordy χ_G scales.

The Pauling χ_P scale[95,96] is defined by the observation that the energy of the bond A-B is generally larger than the mean of the A-A and B-B bond energies. Pauling suggested that the energy enhancement could be used as a measure of the differences in χ between A and B. The expression used to determine the electronegativity differences between the atoms in the bond is defined as

$\chi_A - \chi_B = 0.102\Delta_{AB}^{1/2}$

This expression relates the difference in χ between atoms A and B to the difference in bond dissociation energies (D) of AB and the arithmetic mean of A_2 and B_2 with the values for the bond dissociation energies customarily given in kJ mol^{-1}. The equation describing the difference in bond dissociation energies is shown below.

$\Delta_{AB} = D(A\text{-}B) - \frac{1}{2}[D(A\text{-}A) + D(B\text{-}B)]$

Values obtained for χ *via* the Pauling method are shown in comparison with the other methods in Table 2.2.

The method of Allerd and Rochow [96,95] has the advantage of being applied more easily to a larger number of elements. Their rationale in determining the electronegativity is that an atom will attract electron density in a chemical bond according to Coulomb's law, which is shown below.

$$Force = \frac{(Z^* e)(e)}{4\pi\ r^2\ \in_0}$$

Here Z^* is the effective nuclear charge, e is the charge of the electron, and r is the mean radius of the electron. Then χ_{A+R} can be given by the following equation

$$\chi_{A+R} = 0.359\frac{Z^*}{r^2} + 0.744$$

The numerical constants in the above equation were chosen to bring the range of the values for χ_{A+R} into accord with the electronegativity values of Pauling. Values obtained for χ *via* the Allerd and Rochow method are shown in comparison with the other methods in Table 2.2.

The more recent method of Allen[95] to determine χ has been developed for nontransitional elements. The spectroscopic electronegativity χ_{spec} can be calculated by applying the equation.

$$\chi_{spec} = \frac{m \in_p + n \in_s}{m+n}$$

where m and n are the number of p and s electrons respectively, and $\in_p$ and $\in_s$ are the average one-electron ionization enthalpies of an atom. Precise values of $\in_p$ and $\in_s$ can be determined using high-resolution spectroscopic data. This method is satisfactory since the tendency of an atom to attract electrons to itself should be related to the average one-electron valence shell ionization enthalpy of that atom. Values obtained for χ via the Allen method are shown in comparison with the other methods in Table 2.2.

The method of calculating χ according to the Gordy scale[96] suggests that χ values for atoms on the Gordy scale may be related to the number of valence electrons n and the covalent radius r (in Å). The equation used in this determination is as follows:

$$\chi_G = 0.31\frac{(n+1)}{r} + 0.50$$

This arises from the interpretation of χ as the potential due to the *effective* nuclear charge Z^*, at the covalent boundry, employing

$Z^* = n - 0.5(n-1) = 0.5\,(n+1)$

The above equation assumes all electrons in closed shells below the valence shell exert a full screening effect, while the screening constant for one valence shell electron on another is 0.5. Values obtained for χ via the Gordy method are shown in comparison with the other methods in Table 2.2.

Table 2.2. Comparison of the group electronegativity values, χ, determined by the Pauling (χ_P), Allerd and Rochow (χ_{A+R}), Allen (χ_{spec}) and Gordy (χ_G) methods.

Atom	χ_P	χ_{A+R}	χ_{spec}	χ_G
H	2.20	2.20	2.30	2.17
F	3.98	4.10	4.19	3.94
Cl	3.16	2.83	2.87	3.00
Br	2.96	2.74	2.69	2.68
Li	0.98	0.97	0.91	0.96
Na	0.93	1.01	0.87	0.90

Kagarise has shown that the group electronegativity χ_R in an ester (with ester type R-$COOCH_3$) could be related to the infrared carbonyl stretching frequency of the ester[97]. For example in this study it was assumed that the χ of the –O-CH_3 group is constant and has the value of $\chi_{\text{-O-CH3}}$ = 1.81. The data obtained from this study is summarized in Table 2.3.

Table 2.3. IR carbonyl stretching frequencies in esters of the type R-$COOCH_3$ and the χ_R values obtained according to the method of Kagarise

R	ν(C=O) cm^{-1}	χ_R
H	1717	2.13
CH_3	1738	2.35
CH_2Br	1740	2.44
CH_2Cl	1748	2.48
$CHCl_2$	1755	2.62
CCl_3	1768	2.76

In a study by Du Plessis and co-workers [21]on ferrocene-containing β-diketones, they were able to determine the χ_R of the ferrocenyl group. This was achieved by plotting a graph of known IR ester carbonyl stretching frequencies *versus* known χ_R. They were then able to obtain χ_{Fc} by extrapolation of this plot by inserting the IR carbonyl stretching frequency of the ester Fc-CO-OCH_3. The data thus obtained gave a χ_{Fc} = 1.87 and χ_{CF3} = 3.0 [96,98]. It was further shown in their study that the formal reduction potentials ($E^{o/}$) of the ferrocene-containing β-diketone compounds are linearly related to χ_R[88].

3. RESULTS AND DISCUSSION

3.1. INTRODUCTION

The compounds 1-ruthenocenyl-4,4,4,-trifluorobutan-1,3-dione (ruthenocenoyltrifluoroacetone, Hrctfa, pKa^1=7.36 ± 0.03), 1-ruthenocenyl-3-phenylpropan-1,3-dione (benzoylruthenocenoylmethane, Hbrcm, pKa^1=11.31 ± 0.04), 1-ruthenocenyl-3-ferrocenylpropan-1,3-dione (ruthenocenoylferrocenoylmethane, Hrcfcm; pKa^1 >13), 1-ruthenocenylbutan-1,3-dione (ruthenocenoylacetone, Hrca, pKa^1=10.22 ± 0.01) and 1,3-diruthenocenylpropane-1,3-dione (diruthenocenoylmethane, Hdrcm, pKa^1 >13) were prepared by Claisen condensation of acetylruthenocene and the appropriate ester under the influence of lithium diisopropylamide.

[Rh(β-diketonato)(cod)] complexes were obtained by treating the appropriate β-diketone with $[Rh_2(cod)_2Cl_2]$.

Peak anodic potentials (E_{pa} values *vs* Ag/Ag^+) of the ruthenocene(Rc)-containing β-diketones and the [Rh(β-diketonato)(cod)] complexes in acetonitrile are reported for the ruthenium as well as rhodium centers. Formal reduction potentials ($E^{o/}$ values *vs* Ag/Ag^+) are reported for the iron center in the Rc-containing β-diketone Hrcfcm and the complex [Rh(rcfcm)(cod)].

Kinetics results for the conversion of the β-diketones from the enol- to the keto-isomer and *vice versa* are described. Kinetics results for the substitution of the RcCOCHCOR-moiety from the [Rh(RcCOCHCOR)(cod)] with 1,10-phenantroline are also presented.

Manipulation of the electron density on the metal center was achieved by changing the R group on the Rc-containing β-diketone. The effect that the R group electronegativity has on electrochemistry, substitution kinetics and isomerization kinetics was studied.

3.2. SYNTHETIC ASPECTS

3.2.1. β-DIKETONES

Five new ruthenocenyl-containing β-diketones (Hrctfa, Hrca, Hbrcm, Hrcfcm and Hdrcm) were prepared in this study according to Scheme 3.1. by Claisen condensation of acetylruthenocene with the appropriate ester RCOOMe or RCOOEt (R = Rc, Fc, C_6H_5 for methyl esters; R = CH_3, CF_3 for ethyl esters) , under the influence of the hindered base lithium diisopropylamide (LiDPA). R = trifluoromethyl for Hrctfa, methyl for Hrca, phenyl for Hbrcm, ferrocenyl for Hrcfcm and ruthenocenyl for Hdrcm.

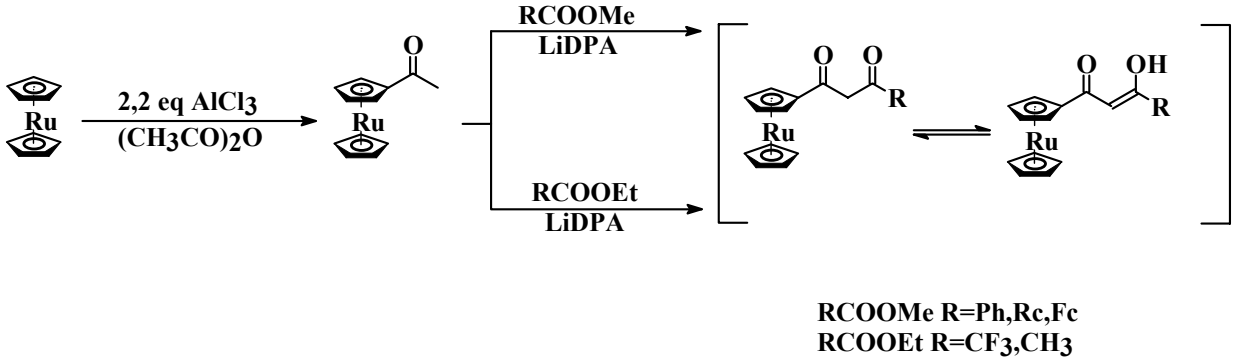

Scheme 3.1. Reaction scheme for the preparation of the new ruthenocenyl-containing β-diketones Hrctfa (R =CF_3), Hrca (R =CH_3), Hbrcm (R=C_6H_5), Hrcfcm (R=Fc) and Hdrcm (R=Rc).

Acetylruthenocene was prepared by Friedel Crafts acetylation with acetic anhydride and aluminum trichloride according to a known method[1] giving a 61 % yield. Important factors in this reaction are, the correct number of equivalents of aluminium trichloride in relation to the ruthenocene, as well as the purity of the aluminium trichloride. The synthesis of the

β-diketones according to the method of Scheme 3.1. gave varied yields: Hrctfa (83 %), Hrca (27 %), Hbrcm (41 %), Hrcfcm (34 %) and Hdrcm (28 %)

The high yield for the synthesis of Hrctfa, can be explained on the assumption that the liberated ethoxide base during the reaction is able to catalyze β-diketonato formation which does not occur in the synthesis of the other β-diketones. The triflate ester is also more susceptible to attack from the *in situ* generated $RcCOCH_2^-$ group as the trifluoromethyl electron-withdrawing group generates a more positive charge on the carbonyl carbon of the ester. Hrca synthesis failed if the ethyl acetate used was not freshly purified and dried. This is due to the acetic acid, formed by decomposition of ethyl acetate and moisture destroying the $RcCOCH_2^-$ reactive species as well as the unreacted LiDPA base. With the synthesis of Hdrcm it was found that the yield increases from 13 % to 28 % when the ester is added in the solid form by way of a Schlenk apparatus. The Rc-containing β-diketones were purified by column chromatography.

3.2.2. COMPLEXATION REACTIONS OF β-DIKETONES WITH RHODIUM

The rhodium-dimer $[RhCl_2(cod)_2]$ was synthesized by the reaction of $RhCl_3$ with cyclooctadiene in yields of 62 %[2] according to Scheme 3.2.(a). The rhodium β-diketone complexes of type [Rh(RcCOCHCOR)(cod)] were obtained by the complexation reaction of the ruthenocene-containing β-diketones with $[Rh_2Cl_2(cod)_2]$ in dry dimethylformamide according to the Scheme 3.2.(b). The yields for these reactions were [Rh(rctfa)(cod)] (45.47 %), [Rh(rca)(cod)] (49.18 %), [Rh(brcm)(cod)] (42.88 %), [Rh(rcfcm)(cod)] (18.27 %) and [Rh(drcm)(cod)] (51,26 %).

All products except [Rh(rca)(cod)] were separated from the reagents by means of column chromatography. The complex [Rh(rca)(cod)] could not be separated effectively by means of

column chromatography from the rhodium dimer. On Kieselgel TLC plates the compound [Rh(rca)(cod)] can be separated from the reactants but on a column it does not separate effectively. The reason TLC plates were not used to separate the product [Rh(rca)(cod)] from the reactants was due to the large amounts of product that needed separating and as such it became impractical. The only way to obtain a pure [Rh(rca)(cod)] product was to work stoichiometrically and then to leave the reaction to stir for at least two hours, followed by crystallisation.

The complexation reactions have very slow formation kinetics for all the β-diketones and the reaction mixtures were stirred for up to an hour to allow complex formation to proceed to completion. However in the formation of the complex [Rh(rcfcm)(cod)], the complex is extremely susceptible to acid. In the reaction vessel the complex starts decomposing due to the HCl liberated in the reaction by the breaking of the Cl bridges of the Rh-dimer. It is thus necessary to filter the reaction solution through alumina after only 5 minutes of stirring. The other compounds synthesized were not as susceptible to acid induced decomposition as the [Rh(rcfcm)(cod)] complex.

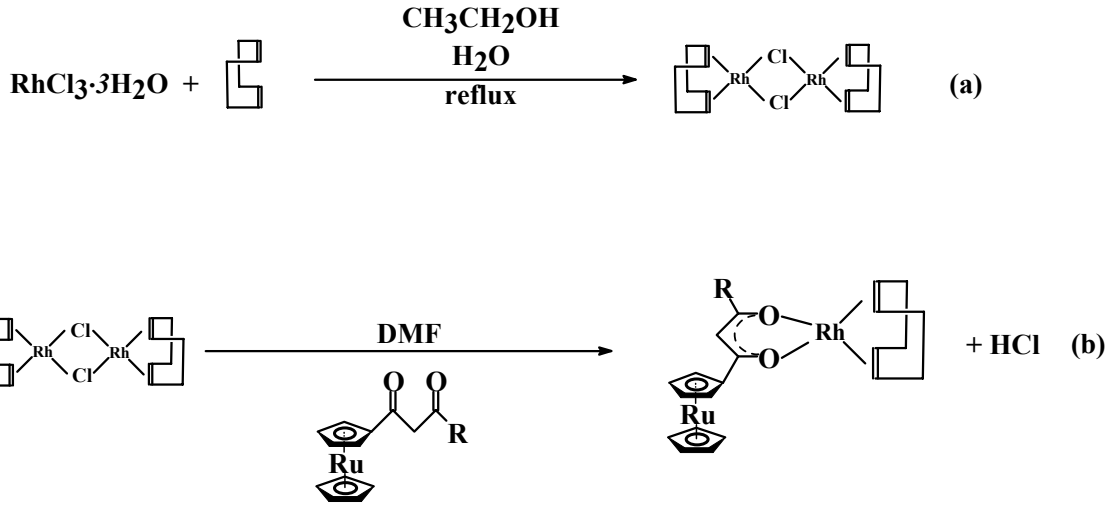

Scheme 3.2. Reaction scheme showing (a) the preperation of the Rh-dimer [$Rh_2Cl2(cod)_2$] and (b) the complexation reaction of the Rc containing β-diketones with the Rh-dimer [$Rh_2Cl_2(cod)_2$] to give complexes of the type [Rh(RcCOCHCOR)(cod)] with R = CF_3, CH_3, C_6H_5, Fc and Rc.

3.3. DETERMINATION OF THE GROUP ELECTRONEGATIVITY (χ_R) FOR THE RUTHENOCENYL GROUP

The group electronegativity (χ_{Rc}) for the ruthenocenyl group was obtained by inserting the value of the carbonyl stretching frequency for the methyl ruthenocenate ester into a plot of known carbonyl stretching frequencies versus Gordy scale group electronegativities for a range of methyl esters. The data used in the construction of this plot is given in Table 3.1. The plot with the inserted value for the ruthenocenyl group is shown in Figure 3.1.

From the plot in Figure 3.1. a value of $\chi_{Rc} = 1.94$ was calculated for the group electronegativity of the ruthenocenyl group according to the Gordy scale. From the data it can be seen that the ruthenocenyl group is a strong electron-donating group. The group electronegativities fit the general decreasing trend in the following order:
(largest χ_R) CF_3 >>CH_3>C_6H_5>Rc>Fc (smallest χ_R) , where the largest group electronegativity has the most electron withdrawing properties.

Table 3.1. IR carbonyl stretching frequencies of the methyl ester type $RCOOCH_3$ and group electronegativities, χ_R, of different R groups.

R	ν (C=O)/ cm^{-1}	χ_R
CF_3 [3]	1785	3.01
CH_3 [3]	1736	2.34
C_6H_5 [4]	1725	2.21
H [3]	1717	2.13
Rc [this study]	1708	1.99
Fc [4]	1700	1.87

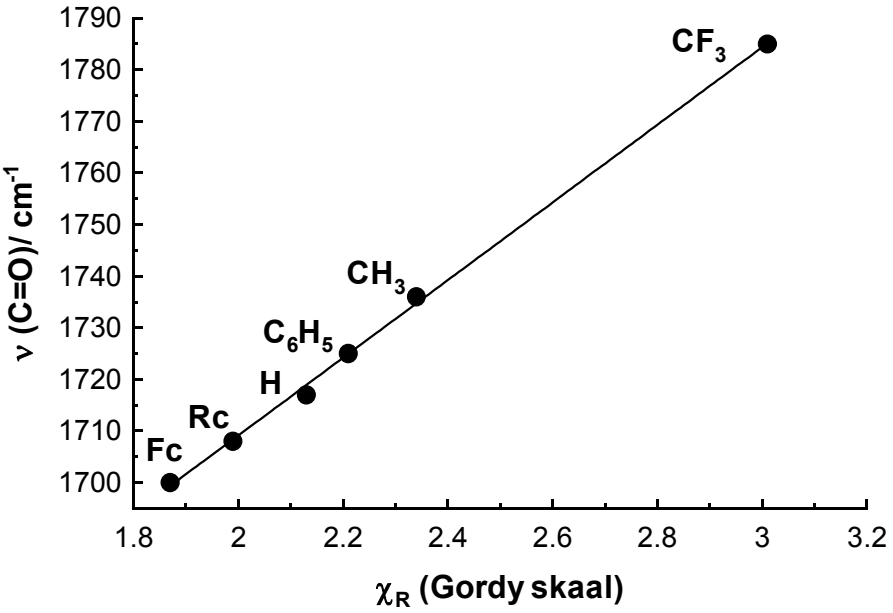

Figure 3.1. Plot of known carbonyl stretching frequencies versus Gordy scale group electronegativities, χ_R for a range of methyl esters (with R the side group when methyl ester has the structure CH_3OCOR). Inserted into this plot is the carbonyl stretching frequency for methyl ruthenocenate to obtain χ_{Rc} for the ruthenocenyl group (designated as Rc).

3.4. pK$_a$/ DETERMINATIONS

The reaction that takes place during the pK$_a$/ determinations of β-diketones is given in scheme 3.3.

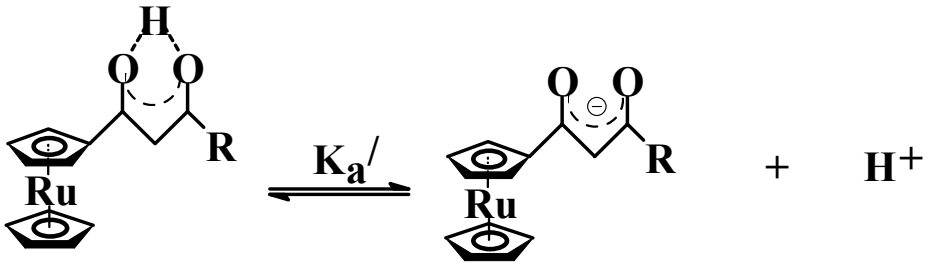

Scheme 3.3. The reaction that takes place in the determination of the pK$_a$/ showing the acid and the conjugated basic form of the β-diketone

$pK_a^{/}$ DETERMINATION

We refer in this study to the "apparent" pK_a or $pK_a^{/}$ rather than pure thermodynamic pK_a values because we do not distinguish between the experimentally observed $pK_a^{/}$ obtained, and the separate pK_a values for the keto- and enol-tautomers of the β-diketone. The newly determined $pK_a^{/}$ values for the β-diketones are given in Table 3.2. These values are obtained by applying a least squares fit of UV absorption *versus* pH data obtained from the acid (or base) titration of the β-diketone to Equation 3.1.[5]. See Figure 3.2. and Figure 3.3.

$$A_T = \frac{A_{HA}10^{-pH} + A_A 10^{-pKa^{/}}}{10^{-pH} + 10^{-pKa^{/}}} \qquad \text{Equation 3.1.}$$

In Equation 3.1., A_T = total absorption, A_{HA} = absorption of the protonated (acid) β-diketone and A_A = absorption of the deprotonated (basic) β-diketone.

Table 3.2. $Pk_a^{/}$ values (determined at λ_{exp}) and molar extinction coefficients ε (at λ_{max}) of the new ruthenocenyl containing β-diketones Hrctfa, Hrca and in 10% CH_3CN / water mixture at 25°C

Compound	$Pk_a^{/}$	λ_{exp} / nm	ε/ $dm^3mol^{-1}cm^{-1}$	β-diketone λ_{max}	β-diketonato λ_{max}
Hrctfa	7.36(3)	315	5960	260	315
Hrca	10.22(1)	319	16890	258	318
Hbrcm	11.31(4)	365	13610	333	347
Hrcfcm	>13		5840	259	331

The general instability of β-diketones towards strong aqueous alkali media, which lead to cleavage at the methine position[6], as well as the inaccuracy of pH measurements above 13 made it impossible to determine the $pK_a^{/}$ of the β-diketones Hrcfcm and Hdrcm by the spectroscopic as

well as potentiometric method[7]. All $pK_a^{/}$ values were determined in solvent mixtures containing 10%, acetonitrile 90% water with ionic strength maintained at 0.100 mol dm^{-3} [$NaClO_4$] with β-diketone concentration 0.2 mmol dm^{-3} at 25°C. A 10% acetonitrile solvent system was used since the β-diketones were insoluble in pure water.

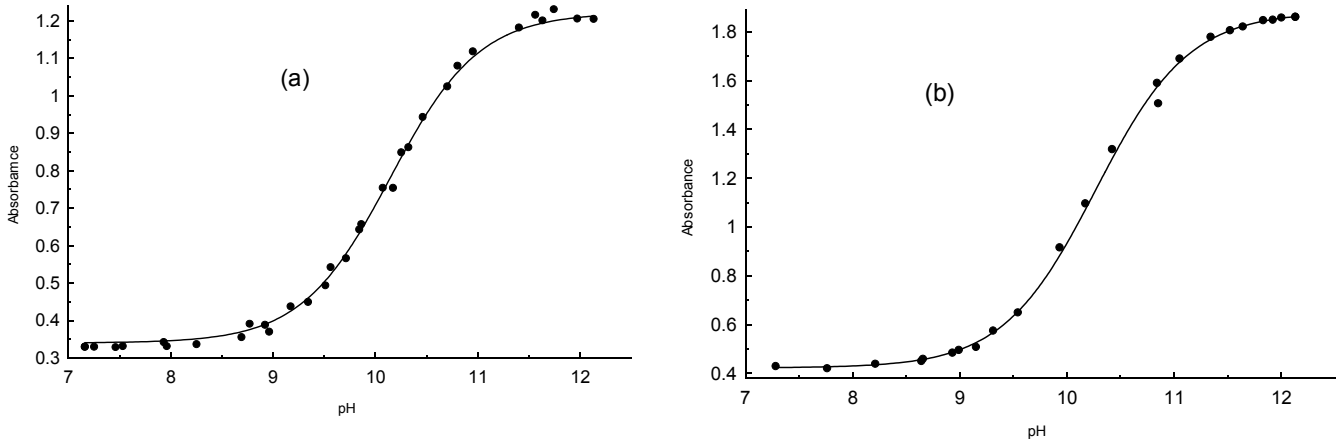

Figure 3.2. The change in absorbance of Hrca as a function of pH at 319nm and 25.0°C, I = 0.100 mol dm^{-3} $NaClO_4$ in (a) water containing 10% CH_3CN ($pK_a^{/}$ = 10.15(1)) and (b) water containing 25% CH_3CN ($pK_a^{/}$ = 10.22(4)). The solid lines are least squares fits of the data according to Equation 3.1.

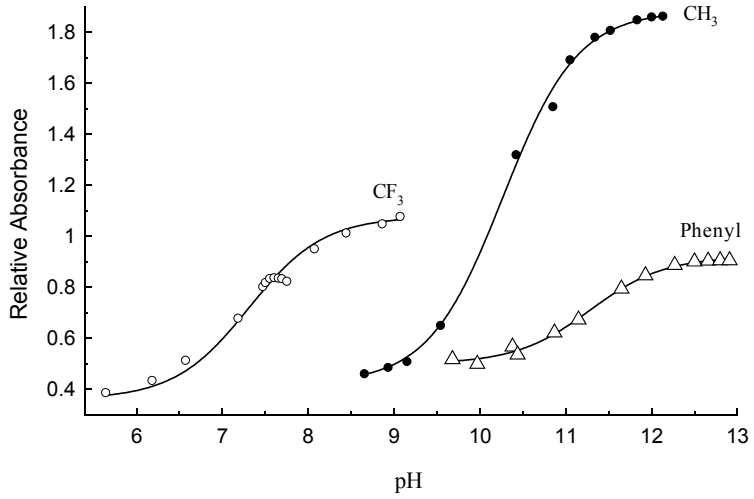

Figure 3.3. Absorbance/ pH profiles used for the $pK_a^{/}$ determination of Hrctfa (labeled CF_3), Hrca (CH_3) and Hbrcm (phenyl). 25.0°C, I = 0.100 mol dm^{-3} $NaClO_4$ in water containing 10% CH_3CN.

The wavelength utilized for the spectroscopic $pK_a^{/}$ determination was decided upon from the electronic spectra of the deprotonated and protonated forms of the β-diketones given in Figure 3.4.

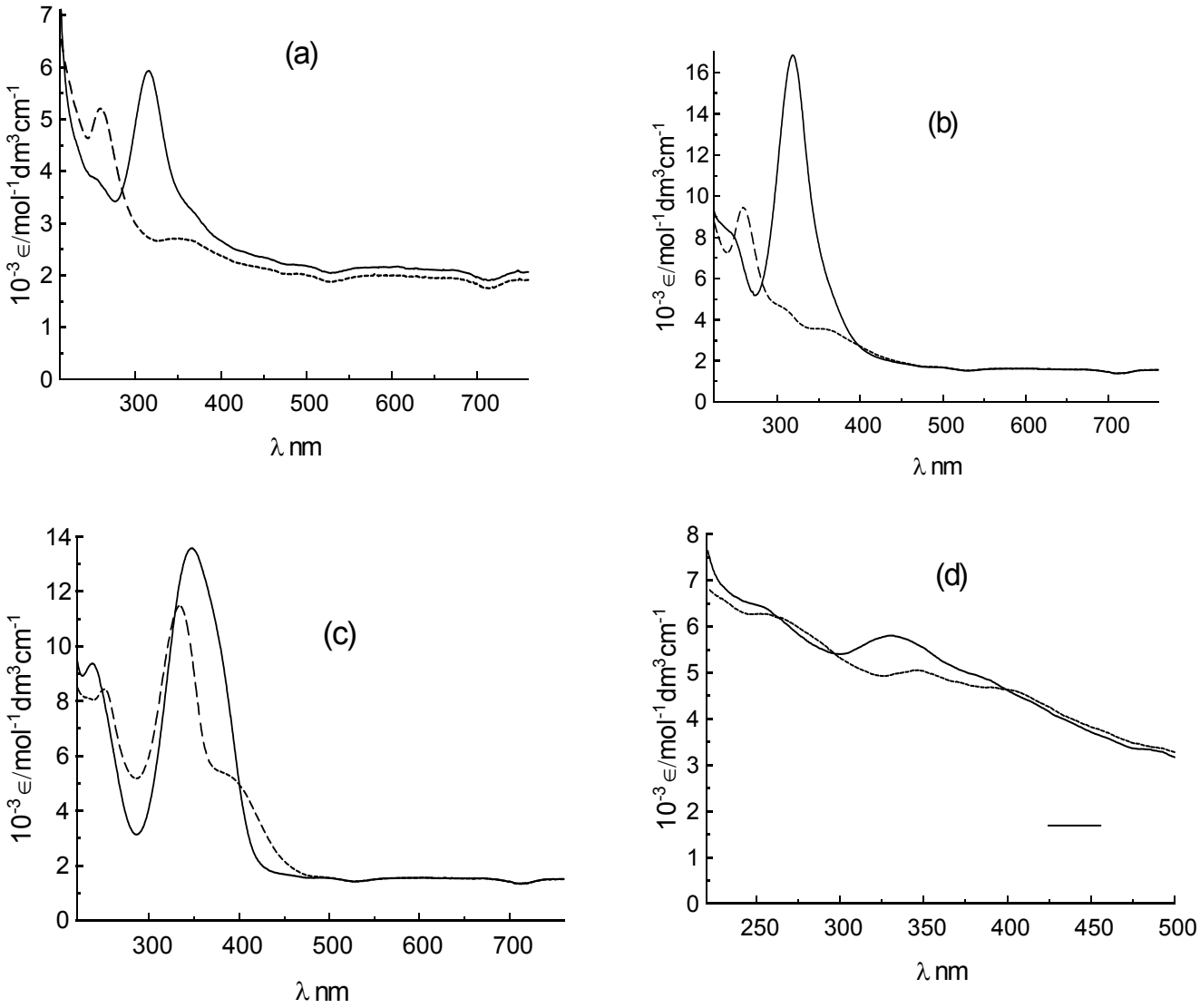

Figure 3.4. Electronic spectra of protonated (-------) and deprotonated (____) β-diketones in 10 % CH_3CN / H_2O (a) Hrctfa, (b) Hrca and (c) Hbrcm. For spectrum (d) Hrcfcm, the solid line is at pH = 13, but we are not convinced that this line represents the spectrum of $(rcfcm)^-$ as much larger differences were expected. Decomposition of $(rcfcm)^-$ is suspected.

It can be seen in spectrum (d) that even at a high pH of 13 the basic form of the Hrcfcm compound does not give a large difference in absorbance. In stronger basic solutions, decomposition (cleavage at the methine position) begins to take place. It was concluded that the $pK_a^{/}$ value of Hrcfcm lies above 13, but cannot be determined spectrophotometrically by following a pH titration of the compound. The same held true for the compound Hdrcm.

In changing the composition of acetonitrile in the solutions from 10% to 25%, an increase of the $pK_a^{/}$ of +0.05 pH units for the respective β-diketones were obtained. For example, for the Hrca compound, the $pK_a^{/}$ is 10.15(1) when there is 10% CH_3CN and the $pK_a^{/}$ is 10.22(4) when there is 25% CH_3CN, see Figure 3.3. This is an even smaller increase than obtained for acetylacetone, For acetylacetone the change from 0% CH_3CN ($pK_a^{/}$ = 8.878(5))[8] to 10% CH_3CN ($pK_a^{/}$ = 8.932(4)) to 25% CH_3CN ($pK_a^{/}$ = 9.292(5)) leads to an increase in pK_a of 0.414 pH units between the 0% and the 25% acetonitrile composition.

In the compound Hrctfa, complexation of a hydroxide anion to the carbonyl group closest to the trifluoromethyl group according to Scheme 3.4. is suspected. This complexation reaction also occurs during the titration of the ferrocene anologue[4]. It is presumed this occurs, because at the midpoint of the $pK_a^{/}$ titration for this compound there is a drop in pH as you add base. A crystal structure of the basic form of the β-diketone would prove this assumption.

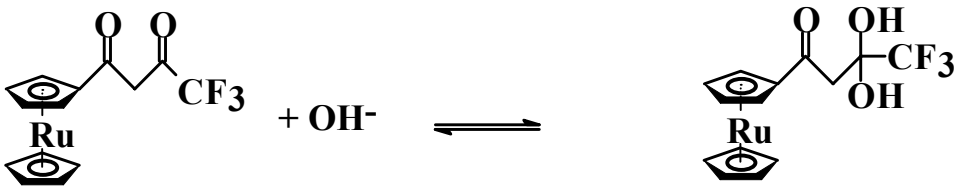

Scheme 3.4. The possible hydroxide complexation reaction that occurs between Hrctfa and an incoming hydroxide anion.

3.5. ISOMERIZATION KINETICS BETWEEN THE KETO- AND ENOL-TAUTOMERS OF THE β-DIKETONES

The isomerization kinetics between the keto- and enol-isomers of the β-diketones was followed spectroscopically. The equilibrium that was studied is shown in Scheme 3.5. Note that only one enol-isomer, RcCOCHC(OH)R, is shown. Although the enol-isomer RcC(OH)CHCOR must surely also exist, in analogy with the ferrocene-containing β-diketones[4], the dominant enol-isomer is considered to be RcCOCHC(OH)R.

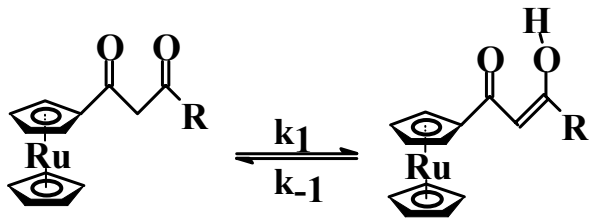

Scheme 3.5. The equilibrium between the keto- and enol-isomer of the ruthenocene-containing β-diketones that was studied kinetically. R= CF_3, CH_3, C_6H_5, Fc and Rc. k_1 = forward rate constant, k_{-1} = reverse rate constant, $K_c = \frac{k_1}{k_{-1}}$ = equilibrium constant.

The kinetic conversion was followed from both the keto- and enol-isomer sides of the equilibrium. In Figure 3.5. the NMR plots for the β-diketone Hbrcm is shown in the initial enol form and at time infinity for the equilibrium position.

The percentage keto-isomer at any given time during the course of the conversion from keto- to enol-isomer or *vice versa*, can be calculated using Equation 3.2.

% keto isomer = (I of keto signal)/[(I of keto signal) + (I of enol signal)] X 100 Equation 3.2.

In Equation 3.2. I = integral value of the NMR signal.

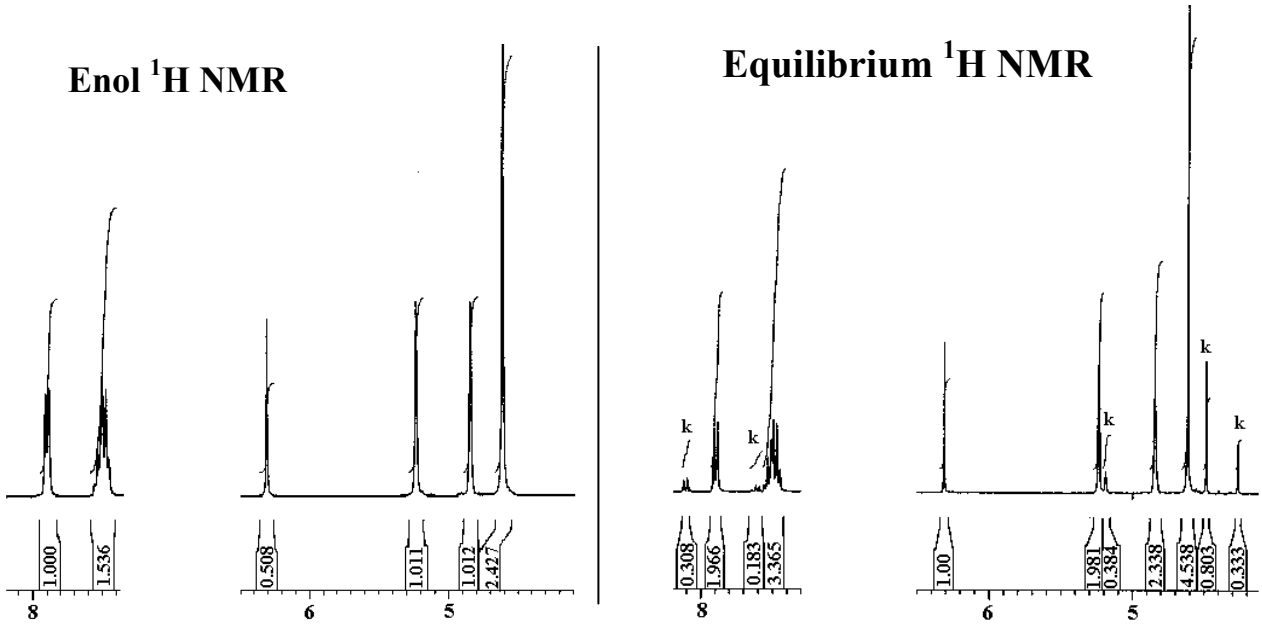

Figure 3.5. Spectrum on left: ^{1}H NMR of Hbrcm in enol-form at 293K in $CDCl_3$. Spectrum on the right: ^{1}H NMR of Hbrcm at equilibrium at 293K in $CDCl_3$. The keto content is 14.24 % and its signals are designated by k. Assignments: δ_H (300MHz; $CDCl_3$) enol-isomer, 4.59 (5H; s; C_5H_5), 5.20 (2H; t; C_5H_4), 6.28 (1H; s; COCHCOH), 7.46 (3H; C_6H_5), 7.85 (2H; C_6H_5) keto-isomer, 4.48 (5H; s; C_5H_5), 5.18 (2H; t; C_5H_4), 4.25 (2H;s;$COCH_2CO$), 7.60 (3H; C_6H_5), and 8.1 (2H; C_6H_5).

Once the percentage keto-isomer has been calculated, the equilibrium constant can be calculated from Equation 3.3.

K_c = (% enol isomer)/(% keto isomer) = $\frac{k_1}{k_{-1}}$ Equation 3.3.

An alternative way to find K_c is to recognize that K_c can be found directly from the integral values of the ^{1}H NMR spectra. Utilizing the integral values of the C_5H_5 signal of the C_5H_5 group in Figure 3.5., $K_c = \frac{4.538}{0.803} = 5.65$

From the K_c values that have been calculated for % keto-isomer or % enol-isomer utilizing Equation 3.3 we are able to draw plots of change in percentage of one of the isomers versus time. A plot of the change in percentage keto-isomer over time for the β-diketone Hrctfa is shown in Figure 3.6. From this plot one is able to determine the observed first order rate constant k_{obs} for the reaction by application of Equation 3.4.

$$\ln[\frac{C_0 - C_\infty}{C_t - C_\infty}] = k_{obs}t \; ; \; k_{obs} = k_1 + k_{-1} \qquad \text{Equation 3.4.}^{9}$$

C_o = initial concentration, C_t = concentration at time (t)

Insert in Figure 3.6. plot drawn to determine the first order rate constant.

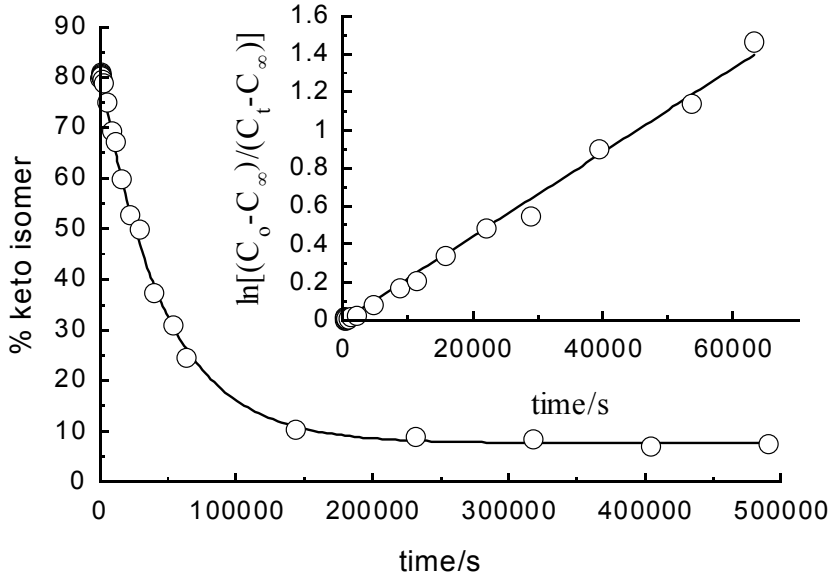

Figure 3.6. Time trace showing the conversion from keto- to enol-isomer for Hrctfa, at 293K in $CDCl_3$. Insert: a kinetic plot of data for this process that leads to the first order rate constant k_1.

The plots of the change in percentage keto-isomer versus time for the β-diketones Hrca, Hrcfcm, Hdrcm and Hbrcm are shown in Figure 3.7.

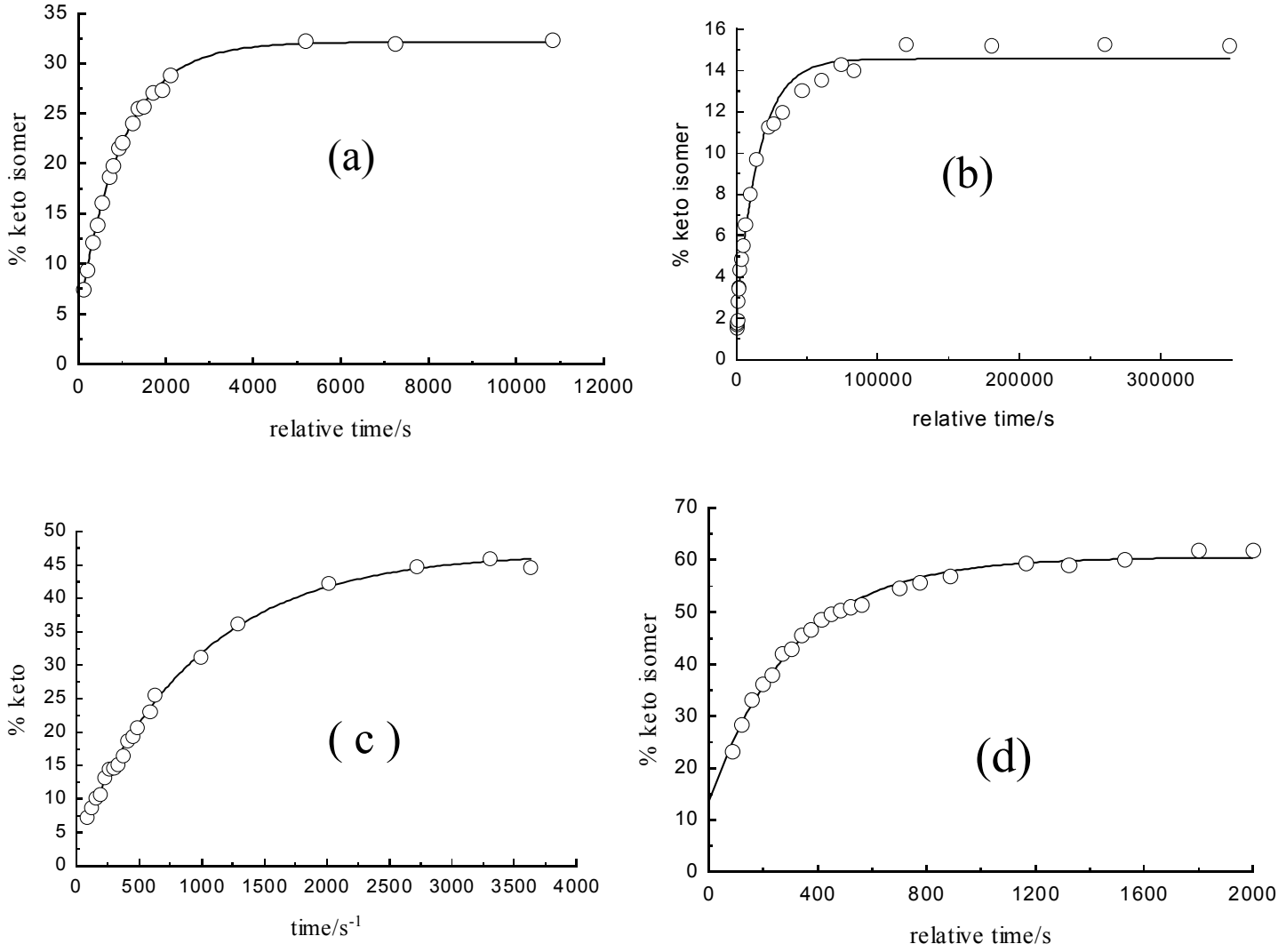

Figure 3.7. Time trace showing the conversion from the enol- to the keto-isomer for (a) Hrca, (b) Hbrcm (c) Hrcfcm and (d) Hdrcm, at 293K in $CDCl_3$.

By solving simultaneously the Equations $k_{obs} = k_1 + k_{-1}$ (Equation 3.4.) and $K_c = \frac{k_1}{k_{-1}}$ (Equation 3.3.), we were able to separate the rate constants k_1 and k_{-1}. The kinetic data obtained for the respective β-diketones is summarized in Table 3.3.

Table 3.3. Equilibrium constants K_C for the keto $\rightleftharpoons$ enol equilibrium of ruthenocene-containing β-diketones $RcCOCH_2COR$. The observed first order rate constant, k_{obs}, first order rate constant for the keto to enol half reaction, k_1 and first order rate constant for the enol to keto half reaction, k_{-1}, are also listed.

Compound	χ_R	$10^{-5}k_{obs}$ (s^{-1})	10^{-5} k_1 (s^{-1})	10^{-6} k_{-1} (s^{-1})	% enol at equil.	K_c in $CDCl_3$ at 293K	ΔG (kJ mol^{-1})
Hrctfa R = CF_3	3.01	2.17 (5)	2.01	1.63	92.5	12.3	-30.5
Hrca R = CH_3	2.34	98 (2)	68.3	297	68.5	2.2	-5.5
Hbrcm R = C_6H_5	2.21	6.3 (5)	5.36	9.4	85.0	5.7	-14.1
Hrcfcm R = Fc	1.87	107 (3)	50.7	563	47.0	0.9	-2.2
Hdrcm R = Rc	1.99	310 (10)	127.6	18240	39.43	0.7	-1.7

The Gibb's free energy for the keto $\rightleftharpoons$ enol isomerization processes can be obtained by application of Equation 3.5.

$$\Delta G = -RT\ln K_C \qquad \text{Equation 3.5.}$$

As K_c increases for the different β-diketones (Table 3.3), the value of ΔG becomes negative. The kinetic rate constant of k_1 and k_{-1} gives a perspective on why more negative ΔG values

favour the enol formation in the equilibrium shown in Scheme 3.5. More negative ΔG values result in k_1 becoming larger in comparison with k_{-1} in the ratio $K_c = \frac{k_1}{k_{-1}}$.

3.6. SUBSTITUTION KINETICS

The substitution reaction of the β-diketonato from [Rhodium(β-diketonato)(cod)] complexes by 1,10-phenanthroline is shown in Scheme 3.6.

The product $[Rh(phen)(cod)]^+$ shown in Scheme 3.6. was identified by comparing the UV spectrum of a sample of this reaction product with a spectrum of an authentic sample of $[Rh(phen)(cod)]^+$. This complex shows UV peak maxima at λ_{max} at 228nm and 277nm. In contrast the [Rh(β-diketonato)(cod)] complex shows UV peak maxima at other wave lengths. For example [Rh(cod)(rca)] shows UV maxima at λ_{max} 320nm and 384nm.

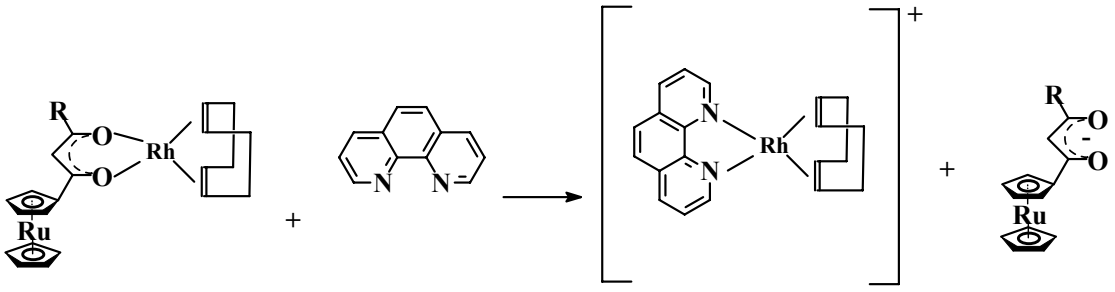

Scheme 3.6. The reaction between the [Rh (β-diketonato)(cod)] complexes and 1,10-phenanthroline. Kinetics of this reaction was studied by stopped flow techniques.

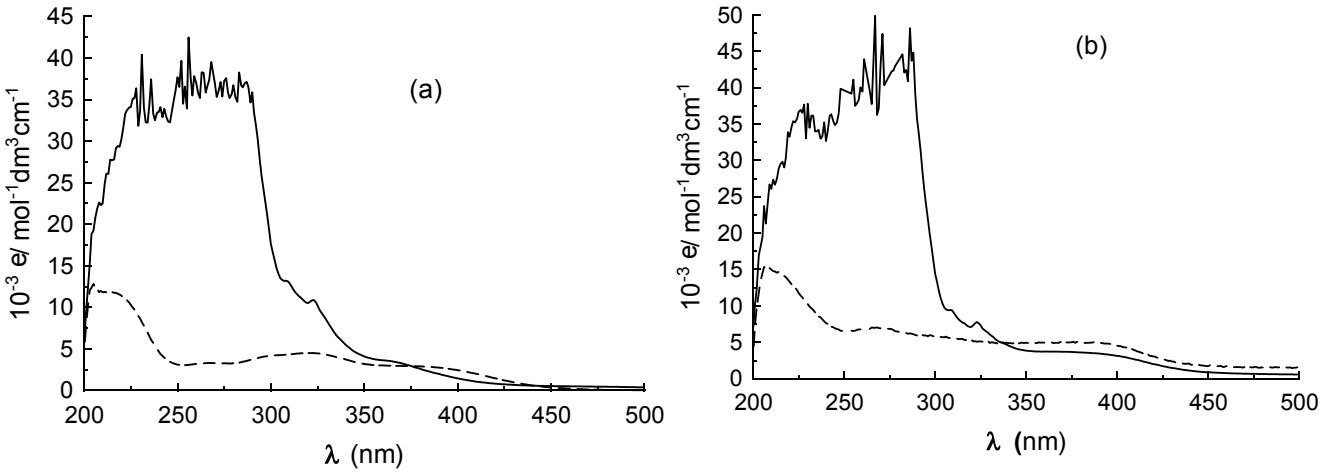

Figure 3.8. UV Spectra of (a): [Rh(rca)(cod)] (- - - -) and [Rh(phen)(cod)]$^+$ (_____) (b) [Rh(drcm)(cod)] (- - - -) and [Rh(phen)(cod)]$^+$ (_____) in methanol at 25°C

Figure 3.8. shows spectra of the complexes overlayed on the spectra of the product formed in the reaction. From these spectra the wavelengths where the reaction was followed kinetically was determined. The Beer-Lambert law held for all complexes at the wavelengths at which the kinetics where performed, Figure 3.9., demonstrates this for [Rh(rca)(cod)] and [Rh(drcm)(cod)].

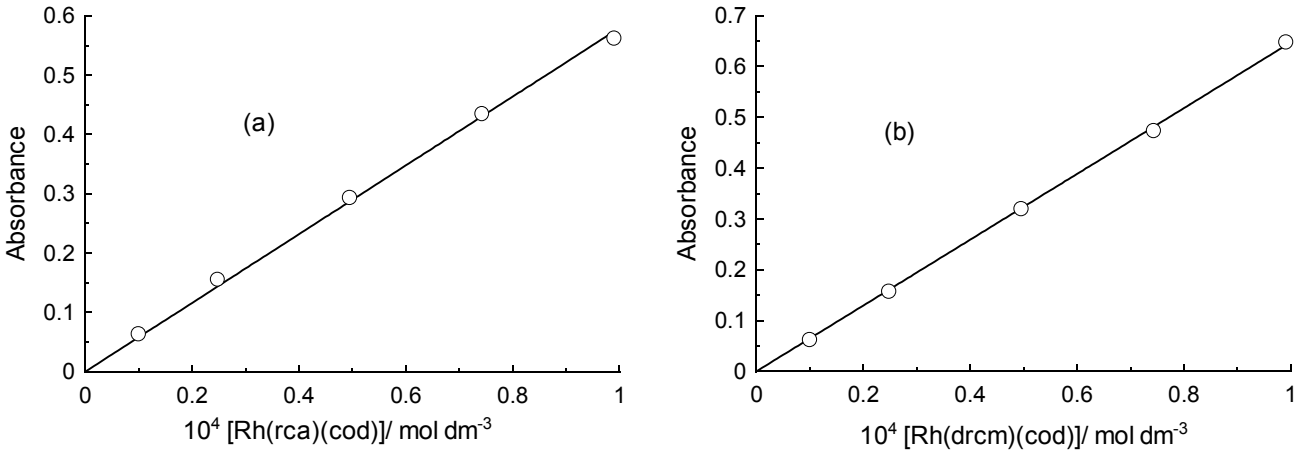

Figure 3.9. Graph of absorbance versus concentration for (a) [Rh(rca)(cod)] at 364 nm and (b) [Rh(drcm)(cod)] at 388 nm

Reactions were studied under pseudo first-order conditions with [1,10-phenanthroline] = (10-100)[Rh(β-diketonato)(cod)]. When a plot of lnC versus time is drawn there is a linear correlation (C is a quantity directly proportional to concentration of [Rh(β-diketonato)(cod)]). The stoppedflow apparatus used in the study uses "volt" as measurement quantity that is directly proportional to C. See Figure 3.10.

The k_{obs} values were obtained using the data analysis program that carries the same name which was supplied with the 8X.18MV stopped flow system that was used in this study. Figure 3.10. illustrates the least squares fitting of the raw data giving k_{obs} from the relationship $\ln (V-V_\infty) = (V_0 - V_\infty)e^{-kobs\ t}$.

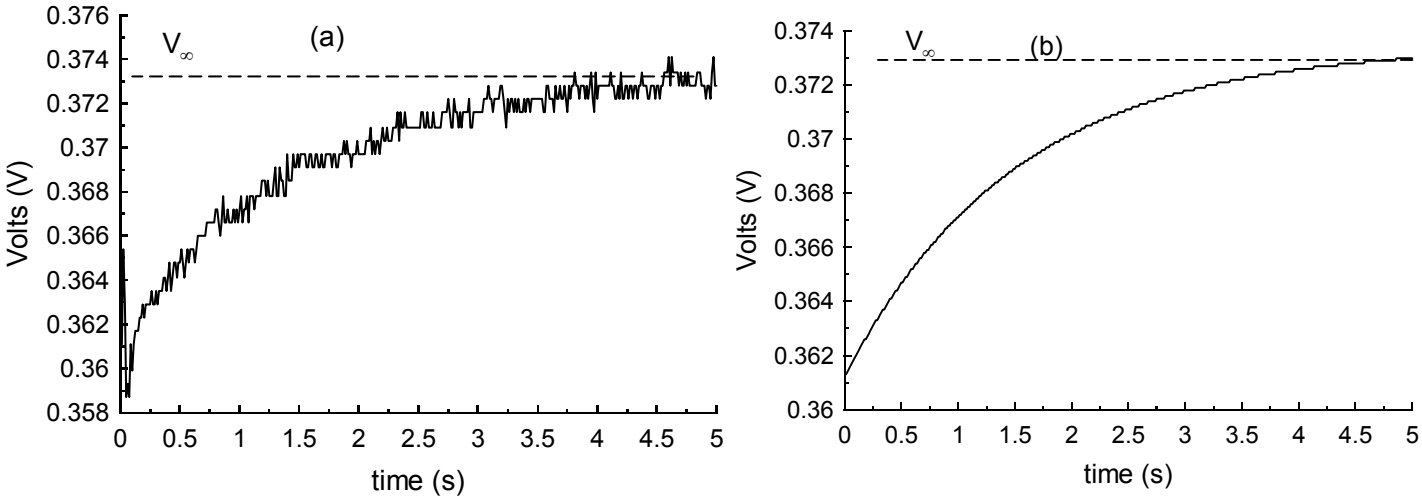

Figure 3.10. An example of graphs of (a) raw data and (b) smoothed data from which the k_{obs} values where determined by the fitting program of the 8X.18MV applied photophysics stopped flow system. The data shown in the graphs is for the substitution reaction between [Rh(rca)(cod)] and 1,10-phenanthroline

Figure 3.11. indicates that the substitution reaction is a first order reaction for the Rhodium complex. The slope of the linear relationship between the observed rate constant (k_{obs}) and concentration of 1,10-phenanthroline shown in Figure 3.11. gave the second order rate constant

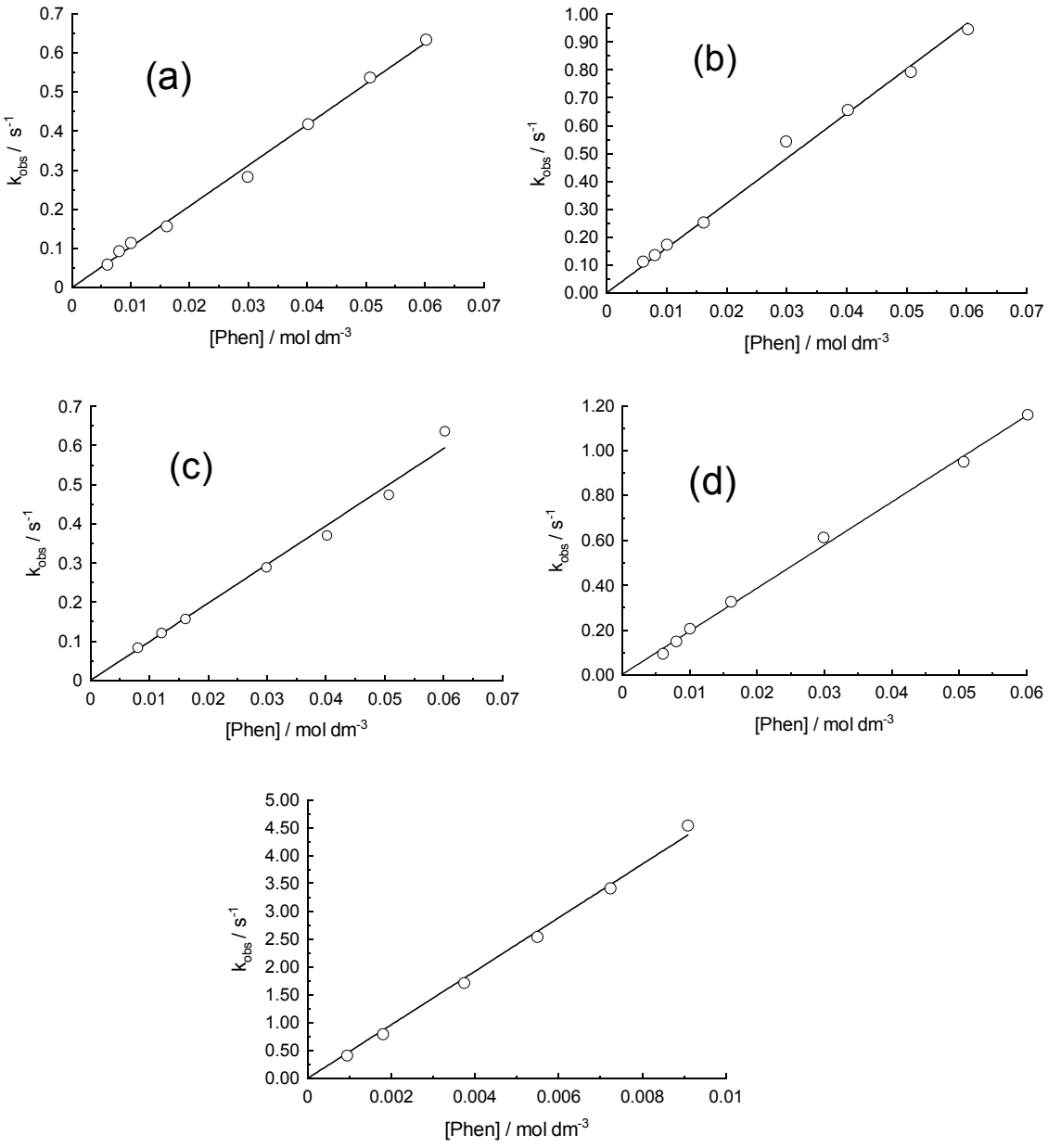

Figure 3.11. Graphs of pseudo first order rate constants (k_{obs}) versus [1,10-phenanthroline], designated [Phen], at 25°C for the complexes (a) [Rh(drcm)(cod)] , (b) [Rh(rca)(cod)], (c) [Rh(rcfcm)(cod)], (d) [Rh(brcm)(cod)] and (e) [Rh(rctfa)(cod)]. From the slopes of these plots the second order rate constant (k_2) can be obtained.

k_2 for the investigated substitution reactions, Table 3.4. For the complexes studied plots of k_{obs} *versus* varying concentration gave within experimental error a zero intercept. A case deserving special mention is the [Rh(brcm)(cod)] complex. Several previous studies showed that Rh complexes having a phenyl group in a β-diketonato ligand show a non-zero intercept in the plot k_{obs} versus [1,10-phenanthroline]. Thus the complex [Rh(PhCOCHCOCH$_3$)(cod)] had a y-intercept of 0.17 s^{-1}. The complex [Rh(FcCOCHCOPh)(cod)] had a y-intercept of 0.06(1) s^{-1} [10]. For the complex [Rh(brcm)(cod)] a y-intercept of 0.004 s^{-1} was found, implying the rate constant associated with a solvent participating step, k_s is very small compared to the rate constant associated with the non solvent route k_2 = 19.2(3) dm^3 mol^{-1} s^{-1}. Therefore, the solvent pathway does not contribute observably to substitution reactions for all the complexes studied in this research program.

The rate law for square-planar substitution reactions with an incoming 1,10-phenanthroline can be written as in Equation 3.6.

$$\text{Rate} = \{k_s + k_2[\text{phen}]\}[\text{Rh(RcCOCHCOR)(cod)}] \quad \text{Equation 3.6.}$$

$$= k_{obs}[\text{Rh(RcCOCHCOR)(cod)}] \quad \text{Equation 3.7.}$$

Here

$$k_{obs} = k_s + k_2[\text{phen}] \quad \text{Equation 3.8.}$$

$$= k_2[\text{phen}] \text{ because } k_s \approx 0 \quad \text{Equation 3.9.}$$

In the above equations, k_s = the rate constant for the solvent pathway, k_2 = the second order rate constant, k_{obs} = the pseudo first order rate constant when [1,10-phenanthroline] >>[[Rh(cod)(β-diketonato)]]. From Equation 3.9., the second order rate constant k_2, can be obtained from a plot of varying phenanthroline concentrations versus observed rate constants. These plots can be seen in Figure 3.11.

Activation parameters ΔH^* and ΔS^* for the studied substitutions can be obtained from a fit of k_2 and temperature data (temperature measured in kelvin) according to the Eyring Equation 3.10.

$$\ln\frac{k_2}{T} = -\frac{\Delta H^*}{RT} + \frac{\Delta S^*}{R} + \ln\frac{R}{Nh} \qquad \text{Equation 3.10}$$

k_2 = the experimentally determined second order rate constant, ΔH^* = the activation enthalpy, ΔS^* = the activation entropy, N = Avagrado's constant, h = Planck's constant, R = universal gas constant.

The slope of the graph $\ln\frac{k_2}{T} vs \frac{1}{T}$ gives $-\frac{\Delta H^*}{R}$ and ΔS^* can be determined from the intercept with the y-axis = $\frac{\Delta S^*}{R} + \ln\frac{R}{Nh}$.

Eyring plots of the experimental data over a temperature range of 15°C to 35°C are shown in Figure 3.12.

The Gibbs free energy of activation could be calculated at 25°C for the respective substitution reactions from Equation 3.11.

$\Delta G^* = \Delta H^* - T\Delta S^*$ Equation 3.11.

The activation parameters, the second order rate constant for the substitution reactions between the [Rh(β-diketonato)(cod)] complexes and 1,10-phenanthroline as well as the wavelenghts at which the various substitution reactions were followed, are tabulated in Table 3.4. From the data the following deductions could be made about the mechanism as well as the relative reactivities of the R groups of the new ruthenocene containing β-diketones.

The entropy values that were obtained from the temperature study were large negative for all the substitution reactions between the [Rh(β-diketonato)(cod)] complexes and 1,10-phenanthroline . These large negative entropy values obtained are indicative of an associative mechanism. The values obtained for the Gibbs free energy are all in the same range for the substitution reaction. Additional proof to ascertain the associative nature of the mechanism for these substitution

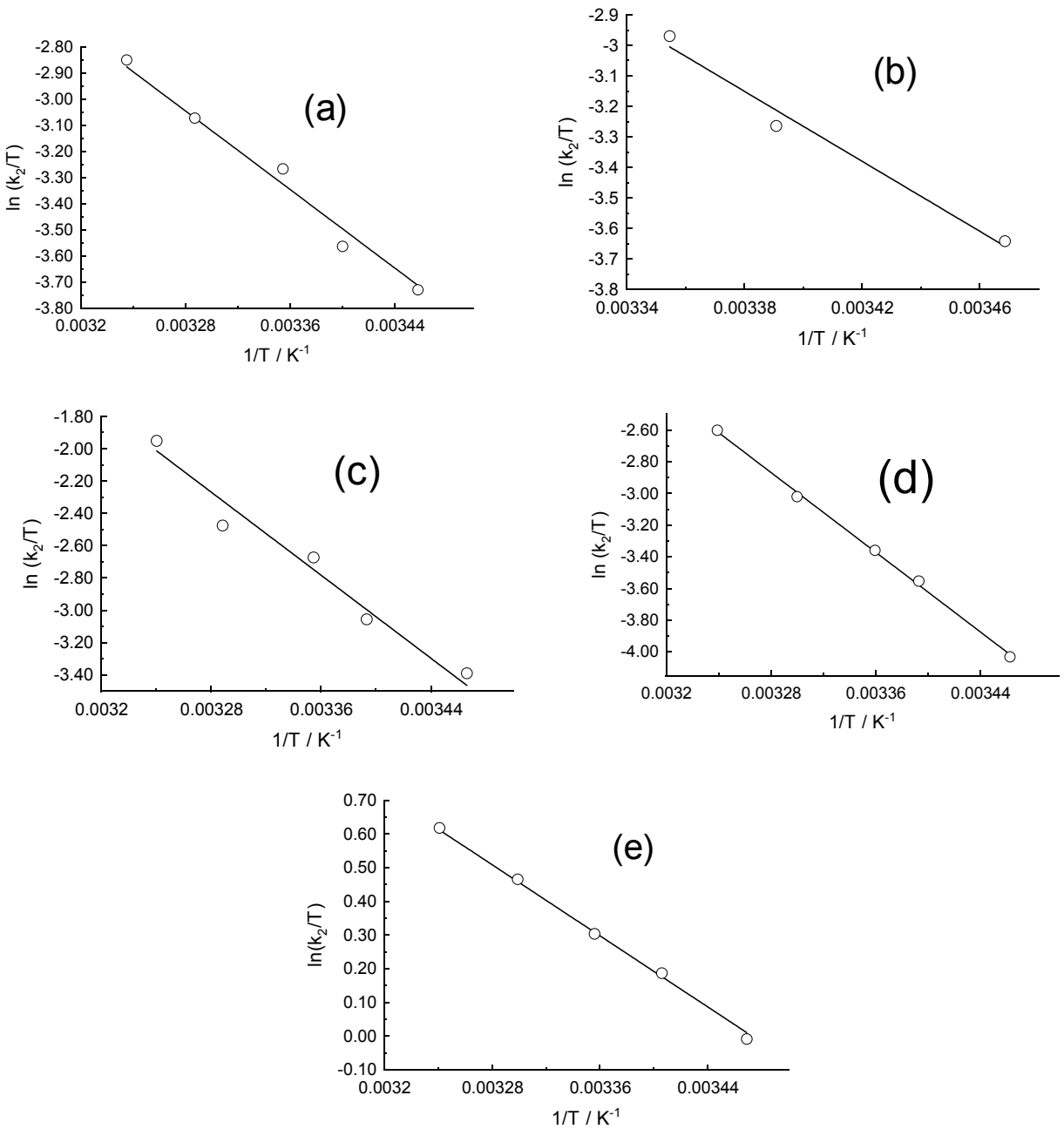

Figure 3.12. Eyring plots for the substitution reaction for the complexes (a) [Rh(drcm)(cod)] , (b) [Rh(rca)(cod)], (c) [Rh(brcm)(cod)], (d) [Rh(rcfcm)(cod)] and (e) [Rh(rctfa)(cod)] with 1,10-phenanthroline. From these plots the activation parameters ΔH^* and ΔS^* could be obtained from the intercept of the plot with the x-axis as well as the gradient of the graph.

reactions between the [Rh(β-diketonato)(cod)] complexes and 1,10-phenanthroline would be to conduct high pressure stopped flow kinetics. From the activation volumes which these studies may yield we would be able to independently confirm the associative mechanism of the reactions, but this high-pressure study falls out of the scope of this study. The proposed associative mechanism for the substitution reaction between the [Rh(β-diketonato)(cod)] complexes and 1,10-phenanthroline is shown schematically in Scheme 3.7.

Table 3.4. Activation parameters as well as second order rate constants (k_2) for the substitution reactions between the [Rh(β-diketonato)(cod)] complexes and 1,10-phenanthroline. The wavelengths given in the table are the respective wavelengths where the analyses were conducted. $\Delta G^* = \Delta H^* - T\Delta S^*$

Complex	ΔH^* (kJ mol^{-1})	ΔS^* (J K^{-1} mol^{-1})	ΔG^* (kJ mol^{-1})	k_2 (dm^3 mol^{-1} s^{-1})	λ_{exp} (nm)
[Rh(rctfa)(cod)]	22.6(4)	-130(1)	71(3)	481(7)	390
[Rh(rca)(cod)]	48(3)	-62(6)	66(3)	16.1(3)	364
[Rh(brcm)(cod)]	50(3)	-63(9)	69(3)	19.2(3)	380
[Rh(rcfcm)(cod)]	52(2)	-60(6)	69(2)	9.9(2)	380
[Rh(drcm)(cod)]	33(2)	-126(7)	61(4)	10.4(1)	388

From the schematic representation of the proposed mechanism in Scheme 3.7. it can be seen that the rate determining step may be the association of the 1,10-phenanthroline to the square planar [Rh(β-diketonato)(cod)] complex, with this association taking place on an axial rhodium position(step A). Then step B will be fast. This mechanism is, however kinetically indistinguishable of one where step A is a fast equilibrium and step B is the rate determining step with rate constant k_2.

The rate constants for the respective substitution reactions between the [Rh(β-diketonato)(cod)] complexes and 1,10-phenanthroline are dependent on the ability through which the incoming 1,10-phenanthroline ligand can associate with the square planar [Rh(β-diketonato)(cod)] complexes.

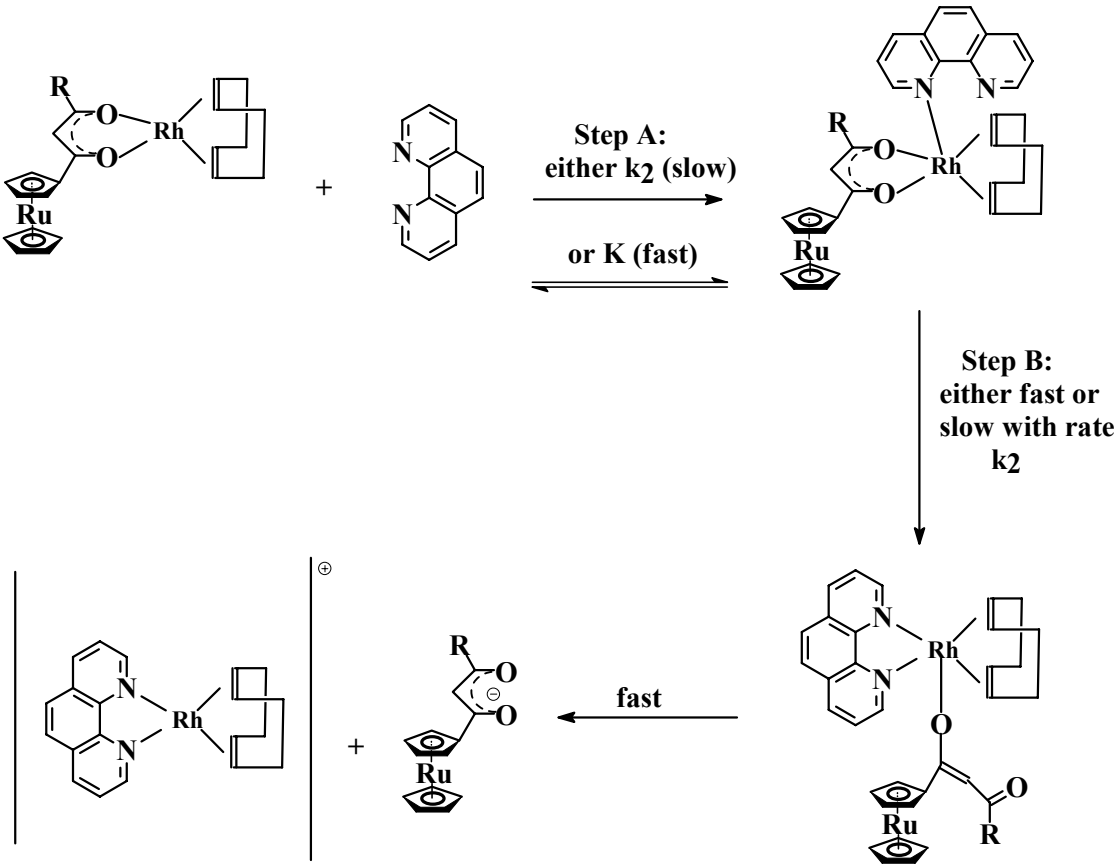

Scheme 3.7. Schematic representation of the proposed associative mechanism for the substitution reaction between the [Rh(β-diketonato)(cod)] complexes and 1,10-phenanthroline. Where R = CF_3, CH_3, C_6H_5, Rc and Fc.

The rate of β-diketanato substitution reactions from [Rh(RcCOCHCOR)(cod)] complexes by 1,10-phenanthroline are also influenced by the electron withdrawing properties of the R groups. For the substitution reaction between the complex [Rh(rctfa)(cod)] and 1,10-phenanthroline the second order rate constant is 481(7) dm^3 mol^{-1} s^{-1}. The reason attributed to this is the electron withdrawing properties of the CF_3 group (χ_R = 3.01). This electron withdrawing group weakens the bond between the Rh and the O-atoms of the [Rh(rctfa)(cod)] complex thus making it easier to break once the incoming 1,10-phenanthroline ligand has coordinated and so the reaction is able to proceed faster according to the proposed mechanism. For the other [Rh(β-diketonato)(cod)] complexes the substitution reaction rate is not as affected by the electron withdrawing properties of the R groups.

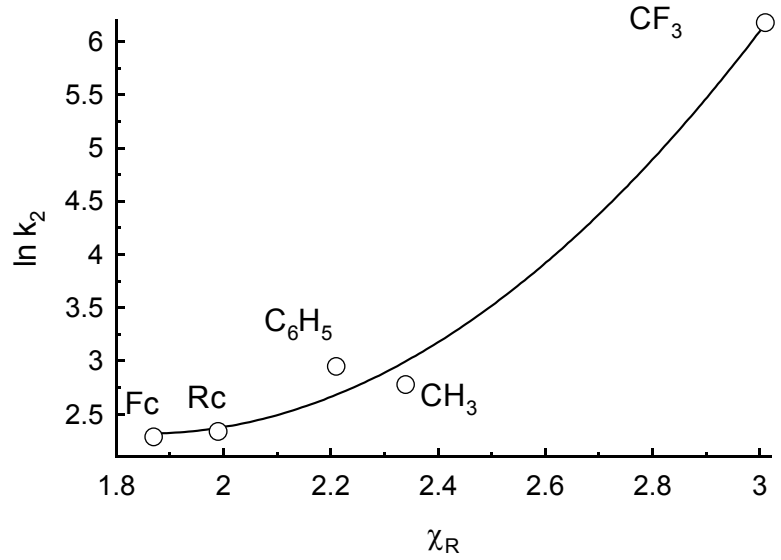

Figure 3.13. The relationship observed between group electronegativities, χ_R, and the second order rate constants for the substitution reaction of the β-diketonato moeity between [Rh(RcCOCHCOR)(cod)] and 1,10-phenanthroline.

From the above stated information the reactivity series for the substitution reaction between the [Rh(β-diketonato)(cod)] complexes and 1,10-phenanthroline is as follows:
(fastest substitution) [Rh(rctfa)(cod)] >>[Rh(rca)(cod)] > [Rh(brcm)(cod)] > [Rh(drcm)(cod)] > [Rh(rcfcm)(cod)] (slowest substitution).

3.7. CYCLIC VOLTAMMETRY

Cyclic voltammetry was conducted on all the new ruthenocene-containing β-diketones as well as their associated [Rh(RcCOCHCOR)(cod)] complexes. The effect that the R groups of each β-diketone has on the electrochemistry of the ruthenium metal in the ruthenocenyl moiety was determined. The interaction between the rhodium metal center and the ruthenium metal of the ruthenocene moiety was also investigated.

Analyses of the cyclic voltammetry data of the new ruthenocene-containing β-diketones were very complex and irreversible electrochemistry for the ruthenium metal core of the ruthenocene moiety in acetonitrile as solvent was observed. In cyclic voltammetry, reversible processes are characterised by peak potential differences of $\Delta E = E_{pa} - E_{pc} = \frac{59}{n} mV$, with n= number of electrons transferred, E_{pa} = peak anodic potential and E_{pc} = peak cathodic potential. Only peak anodic potentials were observed during ruthenium oxidation in $RcCOCH_2COR$, but no reduction peak could be detected. Figure 3.14. demonstrates this for $RcCOCH_2COCF_3$. Compared to all other R groups investigated in this study (CH_3, Rc, Fc, C_6H_5), the cyclic voltammogram of the CF_3 β-diketone was remarkably simple as it contained only one oxidation peak. The other β-diketones exhibited more than one oxidation peak, this is not what one would expect. Figure 3.14. demonstartes this for Hrca ($RcCOCH_2COCH_3$) which shows two oxidation peaks for the ruthenium core.

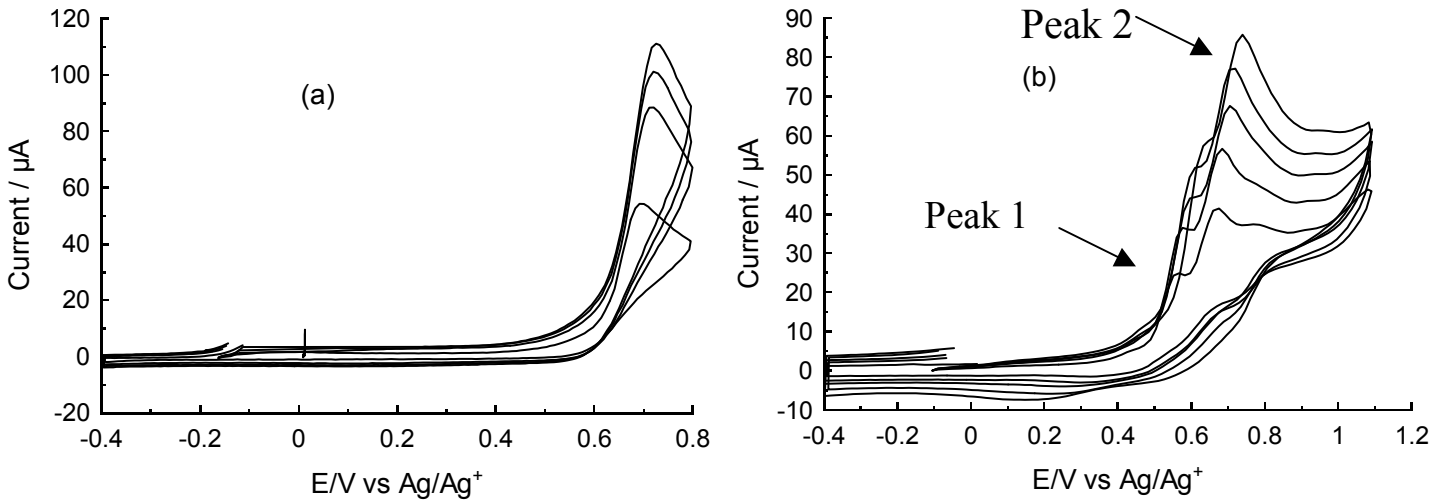

Figure 3.14. The cyclic voltammograms (a) of a 2.0 mmol dm^{-3} Hrctfa solution and (b) a 2.0 mmol dm^{-3} Hrca solution at scanrates 50 mV s^{-1}, 100 mV s^{-1}, 150 mV s^{-1}, 200 mV s^{-1} and 250 mV s^{-1}.The supporting electrolyte is 0.1 mol dm^{-3} tetrabutylammonium hexafluorophosphate (TBAHFP) in acetonitrile utilising a glassy carbon electrode.

The explanation for this complex behaviour is not certain. The multiple peaks observed for $RcCOCH_2COCH_3$ may be at least part due to adhesion of the ruthenocene-containing β-diketone to the glassy carbon working electrode surface. However the shape of cyclic voltammograms demonstrating this behavior normally exhibits a very large, sharp peak indicating large current flows. Such a peak cannot be clearly identified in the voltammogram of $RcCOCH_2COCH_3$. Peaks 1 and 2 are well defined, this is indicative of two separate species in solution. It is known from the ^1H NMR of $RcCOCH_2COCH_3$ that at equilibrium, in $CDCl_3$, this compound exists 68% in the enol form and 32% in the keto form according to the equilibrium (see Table 3.3. pg 49)

$$RcCOCH_2COCH_3 \rightleftharpoons RcCOCHC(OH)CH_3$$

It was also demonstrated in Section 3.5. that the kinetics of conversion from one form to the other is slow. The half-life of keto-enol conversion for the $RcCOCH_2COCH_3$ compound in $CDCl_3$ is $t_{\frac{1}{2}} = \frac{\ln 2}{k_{obs}} = \frac{0.693}{0.00098} = 707\ s$. This is very long on a cyclic voltammetry time scale. At a scan rate of 100 mV s^{-1}, a cyclic voltammetry experiment should be finished within 30 seconds. Thus, it is possible that peaks 1 and 2 in the CV of $RcCOCH_2COCH_3$ correspond to the enol and keto forms of this product respectively. It would also explain why $RcCOCH_2COCF_3$ apparently only shows one oxidation wave. For the CF_3 β-diketone, at equilibrium, the keto-isomer represents only 7.5% (Table 3.3.) of the compound mixture. This is low enough to greatly simplify the cyclic voltammograms of $RcCOCH_2COCF_3$ because the keto content is so low, it will not be easily observable in the voltammograms. However it may also be that multiple peaks in the cyclic voltammograms of $RcCOCH_2COCH_3$ is due to the formation of entire new species during oxidation.

The slow kinetics of keto to enol tautemerisation as possible explanation for the multiple peaks observed in the cyclic voltammograms of $RcCOCH_2COR$ gains more plausibility upon closer investigation of $RcCOCH_2COFc$. From Table 3.3. the half-life of keto-enol conversion for this β-diketone is $t_{\frac{1}{2}} = \frac{\ln 2}{k_{obs}} = \frac{0.693}{0.00107} = 647\ s$. Again, this is very long on a cyclic voltammetry scale. At a scan rate of 100 mV s^{-1}, a cyclic voltammetry experiment for this compound should also be finished within 30 seconds. This implies that the existence of a keto- and enol-isomer, provided they exist in large enough quantities, should be observable by cyclic voltammetry. From Table 3.3., $RcCOCH_2COFc$ exists as 47% in the enol form and 53% in the keto form in $CDCl_3$ according to the equilibrium.

$RcCOCH_2COFc \rightleftharpoons RcCOCHC(OH)Fc$

On the basis of the above, one would expect two reversible waves (*viz.* two oxidation and two reduction waves for the electrochemistry of the ferrocenyl group, and two oxidation waves for the electrochemistry of the ruthenocenyl group). Since the RcC(OH)CHCOFc enol-isomer is

expected to dominate very much over the RcCOCHC(OH)Fc enol-isomer, one would expect the peak potentials of the two ferrocenyl waves to be much closer to each other than the two ruthenocenyl waves. As can be seen in Figure 3.15. all these expectations were fulfilled. The peak separation of the ferrocenyl-based oxidation waves is very small: only 50 mV. Peak anodic potentials for the two ruthenocenyl waves differ by 150 mV

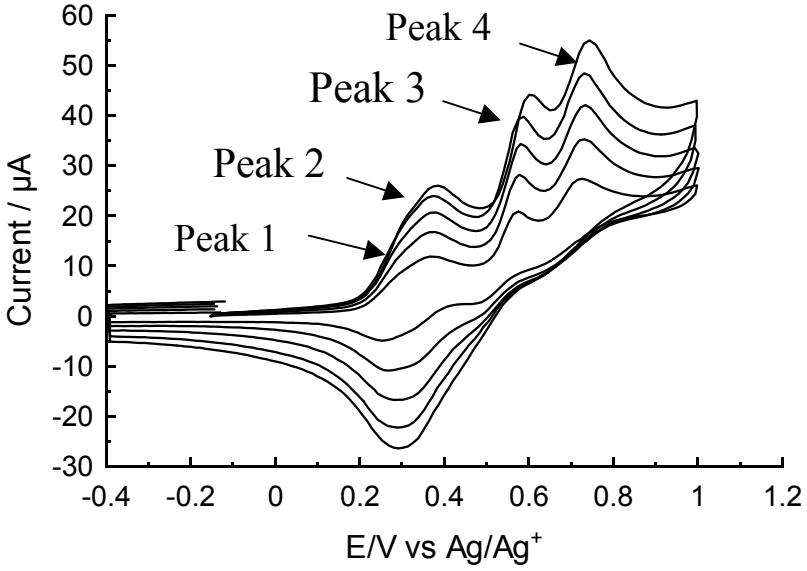

Figure 3.15. The cyclic Voltammogram of a 2,0 mmol dm^{-3} Hrcfcm solution (supporting electrolyte is 0.1 mol dm^{-3} TBAHFP) in acetonitrile on a glassy carbon electrode, scan rate 50 mV s^{-1}, 100 mV s^{-1}, 150 mV s^{-1}, 200 mV s^{-1} and 250 mV s^{-1}.

In addition, utilizing any of the scan rates employed for $RcCOCH_2COFc$, the ratio of peak currents of the two ruthenocene oxidation waves approaches 1. From the Randles-Sevcik equation, $i_p = (2.69X10^5)n^{\frac{3}{2}}AD^{\frac{1}{2}}Cv^{\frac{1}{2}}$, the current is proportional to the concentration of each species[11]. It follows that the equilibrium constant for the above equilibrium should be equal to the ratio of peak currents, provided that the ruthenocenyl oxidation wave is diffusion controlled. Table 3.3. lists this equilibrium constant as 0.9. The mutual consistency of these two values are obvious. For $RcCOCH_2COC_6H_5$ this current ratio is approximately 2.5, while K_c was reported in Table 3.3. as 5.7.

For Hdrcm $K_{c,\ kinetic}$= 2.2, while $K_{c,\ electrochemical}$ = 1.3 at 250 mV s^{-1} It should be noted though, that the K_c values in Table 3.3. are in $CDCl_3$ while the electrochemistry was performed in acetonitrile.

Figure 3.16. displays the cyclic voltammograms for all the new ruthenocene-containing β-diketones on the same axis set, while Table 3.5. contains the electrochemical data that can be obtained from it.

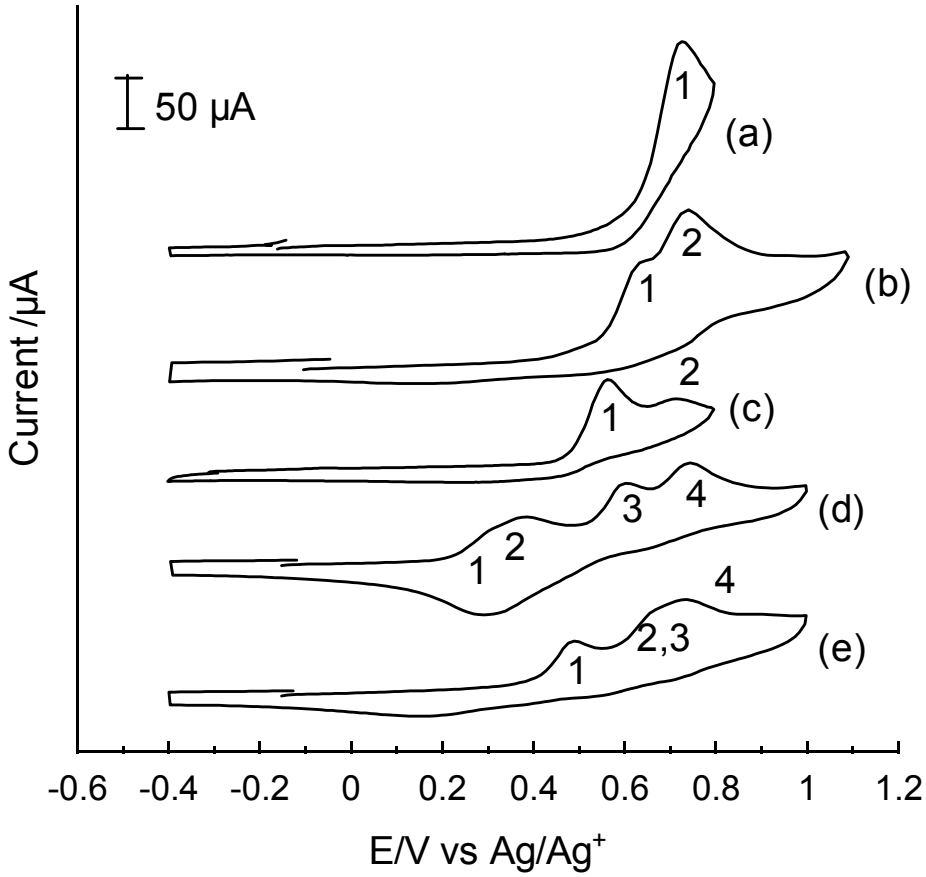

Figure 3.16. The cyclic voltammograms of 2.0 mmol dm^{-3} $RcCOCH_2COR$ (a) Hrctfa, R =CF_3, (b) Hrca, R = CH_3, (c) Hbrcm, R =C_6H_5, (d) Hrcfcm, R = Fc and (e) Hdrcm, R = Rc solutions (supporting electrolyte is 0.1 mol dm^{-3} TBAHFP) in acetonitrile utilising a glassy carbon electrode. Scanrate 250 mV/s.

A discussion on the shape of the cyclic voltammogram of $RcCOCH_2CORc$ is important. One can again make use of the keto enol equilibrium

$$Rc^1 - CO - CH = C(OH) - Rc^2 \quad \rightleftharpoons \quad Rc^3 - CO - CH_2 - CO - Rc^4 .$$

With the slow kinetics of conversion between keto and enol form, one can expect to trap two peak sets for the enol Rc group and two peak sets for the keto Rc group. The enol peak set should show two peaks, one for Rc^1 and one for Rc^2. The peak of Rc^1 and Rc^2 should have wide peak seperation because unlike in the ^1H NMR, oxidation takes place in two one electron transfer steps in the manner indicated below (the oxidation state of the Ru nucleus of each Rc group is indicated as a subscript).

$$\underset{\text{A}}{Rc^1_{II} - CO - CH = C(OH) - Rc^2_{II}} \quad \rightleftharpoons \quad \underset{\text{B}}{Rc^1_{III} - CO - CH = C(OH) - Rc^2_{II}} \quad \rightleftharpoons \quad \underset{\text{C}}{Rc^1_{III} - CO - CH = C(OH) - Rc^2_{III}}$$

It is well known that mixed valent systems like compound B exhibit oxidation at different potentials than that of A because of the different electron withdrawing properties of oxidised and reduced species. Hence peak 1 and 2 in the CV of this compound Fig3.16. e) are ascribed to the oxidation of the first and second ruthenocenyl group respectively. The peak seperation of peaks 1 and 2 is large because good communication exists between the two multivalent ruthenocenyl groups in the intermediate B *via* conjugation in the pseudoaromatic β-diketone core.

The same principle applies to the oxidation of the keto isomer

$$\underset{\text{A}}{Rc^3_{II} - CO - CH_2 - CO - Rc^4_{II}} \quad \rightleftharpoons \quad \underset{\text{B}}{Rc^3_{III} - CO - CH_2 - CO - Rc^4_{II}} \quad \rightleftharpoons \quad \underset{\text{C}}{Rc^3_{III} - CO - CH = C(OH) - Rc^4_{III}}$$

However, in this case, because the keto form exhibits less aromatic charactyer than the enol form, communication between peaks Rc^3 and Rc^4 is not as good as between Rc^1 and Rc^2 in the enol form. Hence oxidation peak seperation is not as large in the keto form. Peak 3 associated with the Rc^3 group oxidation apparently overlaps with peak 2 of Rc^2 oxidation, while the oxidation wave of the Rc^4 group is resolved as a seperate peak, labeled peak 4 in the CV of Hdrcm Figure 3.16 e).

From the experimental data obtained from the cyclic voltammograms we see that the oxidation potential for the compound $RcCOCH_2COCF_3$ and the second oxidation potential of $RcCOCH_2CORc$ are both above 0.7 V. This high oxidation potential for the $RcCOCH_2COCF_3$ β-diketone is explained by the large group electronegativity of the CF_3 group ($\chi_{CF_3} = 3.01$). Due to the electron withdrawing capabilities of this R group, there is a shift of the Ru oxidation potential to a more positive value. In contrast, the high oxidation potential for the second peak of the β-diketone $RcCOCH_2CORc$ is explained by the electron withdrawing power of the already oxidized ruthenium core of the adjacent ruthenocene moiety in the compound. The oxidized ruthenium core is capable of strongly attracting electrons thus shifting the oxidation potential for the second ruthenocene moiety to a higher potential.

A plot of peak anodic potentials versus group electonegativity should give a straight line but the peak anodic potential for the β-diketone $RcCOCH_2COFc$ does not fit the line. The ferrocene moiety of the oxidized compound affects the oxidation potential of the ruthenocene moiety and causes a higher potential for the oxidation of the ruthenium center. Figure 3.17. shows a plot of peak anodic potentials of the first oxidation peak versus group electronegativity. This graph gives a straight line and so the explanation for the keto- and enol-tautomers could possibly be a correct one.

Table 3.5. The cyclic voltammetric data obtained form the voltammograms (versus Ag/Ag^{+}) for the new ruthenocene-containing β-diketones Hrctfa R = CF_3, Hrca R = CH_3, Hrcfcm R = fc, Hbrcm R = C_6H_5 and Hdrcm R = rc. ν (scan rate), $E_{p\,i}$ (peak anodic potentials as numbered form left to right) $E^{o/}$ (formal reduction potential for the fc moeity in the β-diketone Hrcfcm). $E^{o/} = \frac{E_{pa} + E_{pc}}{2}$ **, *i* = 1, 2, 3 and 4.**

$RcCOCH_2COCF_3$				
ν / mV s^{-1}	E_{p1} / V		i_{p1} / uA	
50	0.696		51.3	
100	-		-	
150	0.716		88.1	
200	0.720		90.6	
250	0.724		112.5	
$RcCOCH_2COCH_3$				
ν / mV s^{-1}	E_{p1} / V	i_{p1} /uA	E_{p2} / V	i_{p2} /uA
50	0.560	23.2	0.671	27.0
100	0.575	31.2	0.684	33.3
150	0.600	41.1	0.705	35.4
200	0.612	46.8	0.718	37.4
250	0.634	54.7	0.739	39.5
$RcCOCH_2COC_6H_5$				
50	0.538	20.3	0.692	9.2
100	0.547	27.0	0.696	13.7
150	0.558	34.7	0.707	13.4
200	0.560	38.3	0.713	15.8
250	0.563	46.1	0.715	19.4

Table 3.5. (continued) The cyclic voltammetric data obtained form the voltammograms (versus Ag/Ag^{+}) for the new ruthenocene-containing β-diketones Hrctfa R = CF_3, Hrca R = CH_3, Hrcfcm R = fc, Hbrcm R = C_6H_5 and Hdrcm R = rc. ν (scan rate), $E_{p\,i}$ (peak anodic potentials as numbered form left to right) $E^{o/}$ (formal reduction potential for the fc moeity in the β-diketone Hrcfcm). $E^{o/} = \frac{E_{pa} + E_{pc}}{2}$ **, *i* = 1, 2, 3 and 4.**

$RcCOCH_2CORc$					
ν / mV s^{-1}	E_{p1} / V	i_{p1} /uA	Ep_2 & E_{p3} / V [a]	E_{p4} / V	i_{p4} /uA
50	0.476	9.0	0.666	0.743	20.8
100	0.480	13.2	0.676	0.747	26.4
150	0.480	18.0	0.681	0.741	33.7
200	0.484	20.9	0.676	0.735	37.4
250	0.488	24.0	0.681	0.739	44.0

$RcCOCH_2COFc$								
ν / mV s^{-1}	E_{p1} / V [a]	$E^{o/}{}_2$	i_{p2} / uA	i_{pa}/i_{pc}	E_{p3} / V	i_{p3} / uA	E_{p4} / V	i_{p4} / uA
50	0.308	0.369	10.4	1.08	0.571	20.0	0.723	25.8
100	0.318	0.370	13.7	1.10	0.580	29.6	0.731	30.4
150	0.332	0.373	17.5	0.91	0.584	34.2	0.735	31.2
200	0.329	0.377	20.3	0.90	0.588	38.2	0.735	29.7
250	0.329	0.384	35.0	1.20	0.601	44.7	0.743	34.3

a) peaks overlap to the extent that they could not be separated. Hence no peak currents are provided for these two peaks

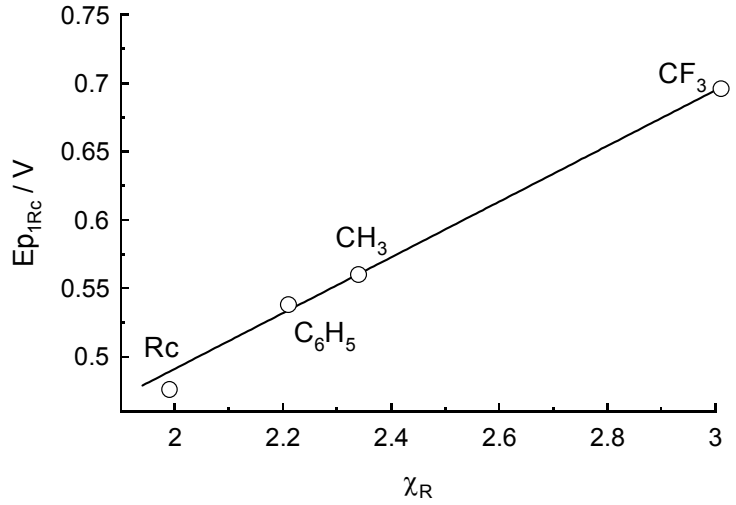

Figure 3.17. The linear relationship between group electronegativity (χ_R) and peak anodic potentials for the first oxidation peak for the ruthenocene-containing β-diketones at scan rate 50 mV s^{-1}. Hrctfa R = CF_3, Hrca R = CH_3, Hbrcm R = C_6H_5 and Hdrcm R = Rc.

In order to simplify the multiplicity of oxidation potentials for the above cyclic voltammograms, and to possibly demonstrate reversible electrochemical behaviour for the ruthenocenyl moiety, the electrochemistry of the ruthenocene-containing β-diketones was also conducted in a variety of non-coordinating solvents utilizing non-coordinating supporting electrolytes. The weaker coordinating solvents than acetonitrile considered here are α,α,α-trifluorotoluene and dichloromethane. The weaker coordinating supporting electrolyte considered for this part of the study was tetrabutylamonium tetrakis[3,5-bis(trifluoromethyl)phenyl]borate, TBATTFPB, rather than the convential tetrabutylammonium hexafluorophosphate, TBAHFP. Utilising α,α,α-trifluorotoluene as electrochemical solvent and TBATTFPB as supporting electrolyte, it was found that the cyclic voltammograms did not differentiate between more than one species (proposed as the keto- and enol-isomers in the acetonitrile study) in solution. The ruthenocene wave still did not show a reduction halfwave. It was also observed that the cyclic voltammograms suffered a great deal of background noise. Figure 3.18. demonstrates these findings for $RcCOCH_2COFc$, Hrcfcm. A further observation in analysis of the cyclic voltammogram of $RCCOCH_2COFc$ is the large ΔE_p value (ΔE_p = 0.17 V) of the ferrocenyl moiety. In acetonitrile this value was ΔE_p = 0.12 V. The larger ΔE_p value in α,α,α-

trifluorotoluene is attributable to the lower polarity of this solvent compared to acetonitrile. The higher internal resistance of this solvent should thus lead to a larger iR drop than would acetonitrile. This would account for the larger ΔE_p value that was observed in α,α,α-trifluorotoluene. The large ohmic drop in α,α,α-trifluorotoluene also explains the high noise level.

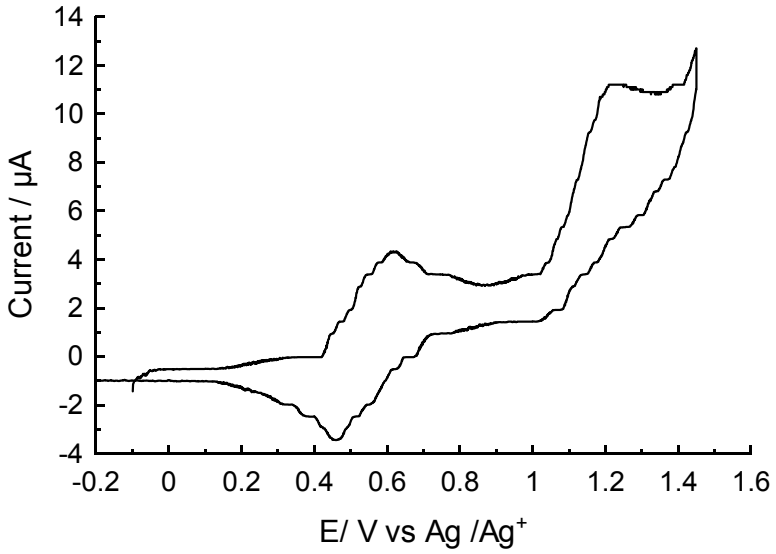

Figure 3.18. The cyclic voltammogram of a 1.0 mmol dm^{-3} Hrcfcm solution (supporting electrolyte is 0.1 mol dm^{-3} TBATTFPB) in α,α,α-trifluorotoluene on a glassy carbon electrode. Scan rate 250 mV s^{-1}

Several reasons for the absence of multiple electrochemical waves in cyclic voltammograms utilizing α,α,α-trifluorotoluene and TBATTFPB can be presented. The most plausible is that both the rate of keto to enol conversion, and *vice versa,* are fast on the time scale for cyclic voltammetry in this solvent. Alternatively the β-diketones may only exist in one isomeric form in this solvent and hence the keto and enol peak coalesce into one observed peak. However, at this stage of our knowledge on ruthenocene electrochemistry, it is not possible to rule out the possibility that the source of the multiple waves in the acetonitrile electrochemical study described above is not the keto to enol equilibrium at all. It may be due to the different species that form in acetonitrile solutions that do not form in α,α,α-trifluorotoluene.

This possibility is underlined by the chemical study that was performed by Taube in 1980. Taube proved the existence of $[Os^{III}(C_5H_5)_2]_2^{2+}$, $[Os^{IV}(C_5H_4)_2]_2^{2+}$, and $[Os^{IV}(C_5H_5)_2(CH_3CN)]^{2+}$ in acetonitrile solutions. Similar compounds have not yet been isolated for the ruthenocene case. Studies in this laboratory, as a result of the research program followed in this M.Sc. study, are currently underway to address this question.

The electrochemical behaviour of the new β-diketones of this study in dichloromethane as solvent paralleled that observed for α,α,α-trifluorotoluene. See Figure 3.19. The ΔE_p value for the ferrocenyl group in $RcCOCH_2COFc$, however, did become slightly smaller. It was measured as $\Delta E_p = 0.14$ V.

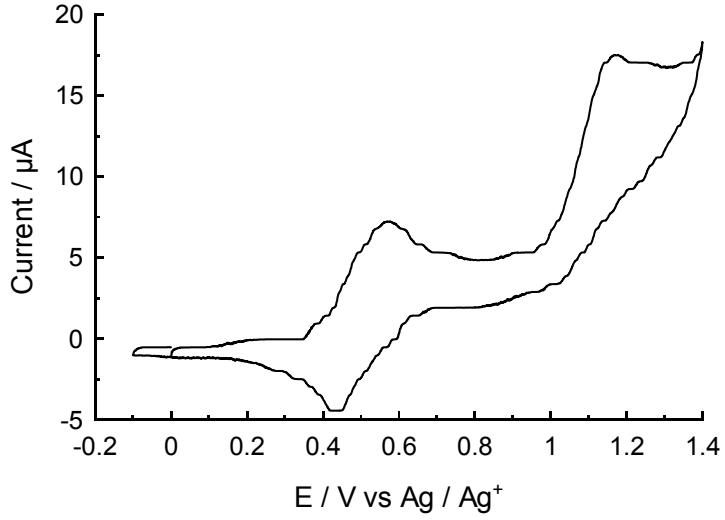

Figure 3.19. The cyclic voltammogram of a 1.0 mmol dm^{-3} Hrcfcm solution (supporting electrolyte is 0.1 mol dm^{-3} TBATTFPB) in dichloromethane on a glassy carbon electrode. Scan rate 250 mV s^{-1}.

Analyses of the cyclic voltammograms of the [Rh(β-diketonato)(cod)] complexes showed irreversible electrochemistry for the ruthenium metal core in the ruthenocenyl moiety, as well as irreversible electrochemistry for the rhodium(I) centre. Only peak anodic potentials for these complexes are reported, as there were no reduction peaks observed for the ruthenium and

rhodium metal centers. Paralleling the behaviour of the free β-diketones, multiple ruthenium and rhodium oxidation waves were observed. Figure 3.20. demonstrates this for the complex [Rh(RcCOCHCOCH$_3$)(cod)].

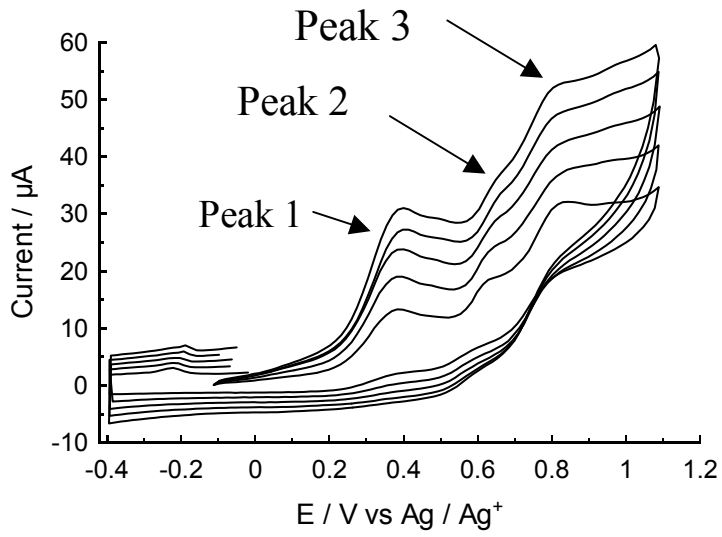

Figure 3.20. The cyclic voltammogram of a 2.0 mmol dm^{-3} [Rh(RcCOCHCOCH$_3$)(cod)] solution (supporting electrolyte is 0.1 mol dm^{-3} TBAHFP) in CH$_3$CN on a glassy carbon electrode. Scan rates 50 mV s^{-1}, 100 mV s^{-1}, 150 mV s^{-1}, 200 mV s^{-1} and 250 mV s^{-1}.

For the complex [Rh(RcCOCHCOFc)(cod)] reversible electrochemistry was obtained for the ferrocene fragment of this molecule and this is shown in Figure 3.21. The extreme complexity in terms of the multiple oxidation waves are clearly observable. This time, however, keto to enol tautomerism cannot explain the multiple peaks associated with the redox active metal centers. It is clear that an extensive research program is required to follow up on this initial exploratory electrochemical study of this research program before the electrochemistry of ruthenocene containing β-diketones and their rhodium complexes of the type [Rh(RcCOCHCOR)(cod)] will be fully understood.

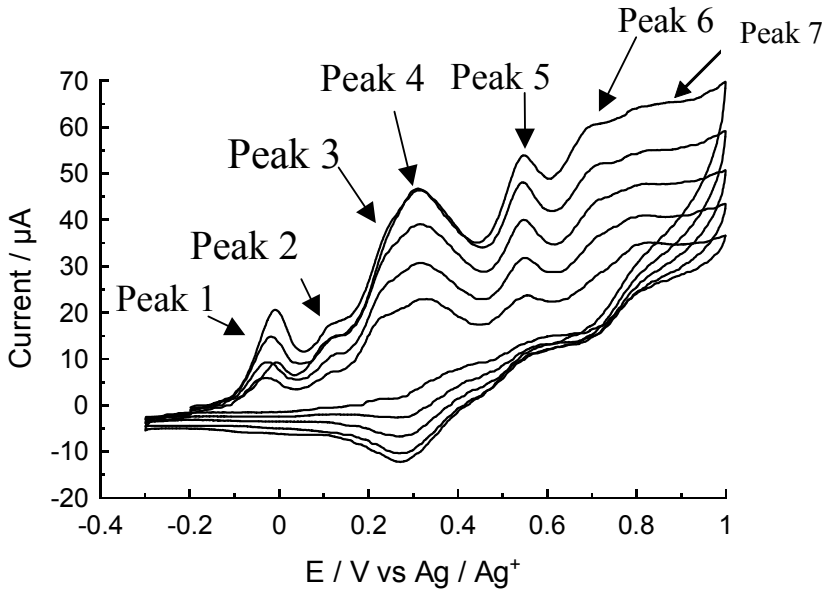

Figure 3.21. The cyclic voltammogram of a 2.0 mmol dm^{-3} [Rh(RcCOCHCOFc)(cod)] solution (supporting electrolyte is 0.1 mol dm^{-3} TBAHFP) in CH_3CN on a glassy carbon electrode. Scan rates 50 mV/s, 100 mV/s, 150 mV/s, 200 mV/s and 250 mV/s.

Figure 3.22. displays the cyclic voltammograms for all the new [Rh(β-diketonato)(cod)] complexes on the same axis set, while Table 3.6. contains the electrochemical data for the [Rh(β-diketonato)(cod)] complexes obtained from these cyclic voltammograms.

The multiple oxidation signals observed for each of the β-diketone complexes make any interpretation as to what they mean at this stage of our knowledge of [Rh(β-diketonato)(cod)] electrochemistry a futile exercise. The most that can be deduced at this stage, is that the oxidation of the rhodium center apparently takes place prior to the oxidation of the ruthenium center, and that the oxidation potentials of both these metal centers drift to more positive values as the group electronegativity of the R group on [Rh(RCCOCHCOR)(cod)] increases. Thus the oxidation potentials of the complex with R = CF_3 are the largest, whereas the first observed oxidation potentials of the complexes with R = Fc or Ph are the smallest.

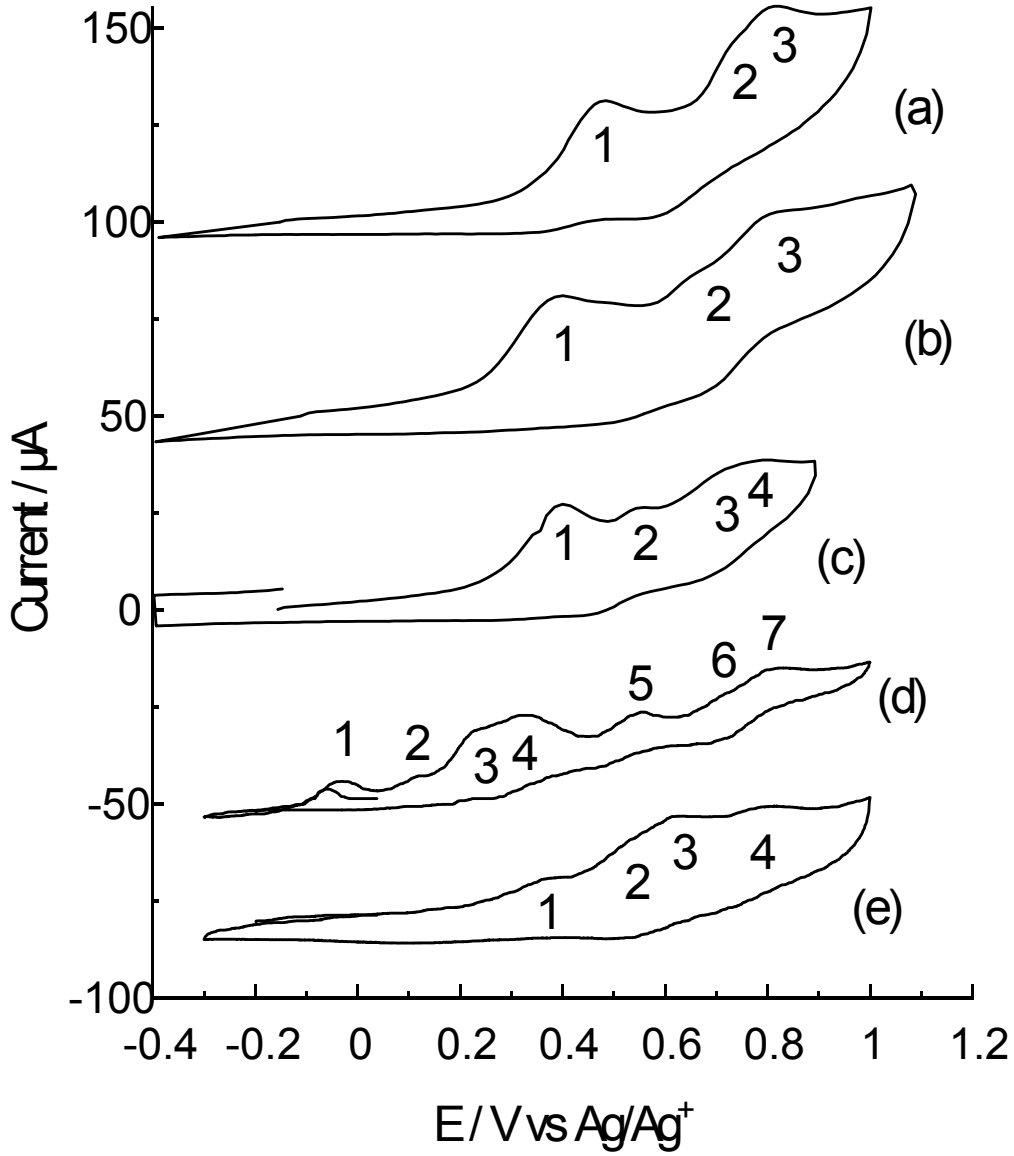

Figure 3.22. The cyclic voltammograms of 2.0 mmol dm^{-3} (a) [Rh(RcCOCHCOCF_3)(cod)], (b) [Rh(RcCOCHCOCH_3)(cod)], (c) [Rh(RcCOCHCOC_6H_5)(cod)], (d) [Rh(RcCOCHCOFc)(cod)] and (e) [Rh(RcCOCHCORc)(cod)] solutions (supporting electrolyte is 0.1 mol dm^{-3} TBAHFP) in acetonitrile on a glassy carbon electrode. Scan rates 250 mV s^{-1}.

Table 3.6. The cyclic Voltammetric data obtained from the voltammograms (versus Ag/Ag^{+}) for the [Rh(β-diketonato)(cod)] complexes [Rh(rctfa)(cod)], [Rh(brcm)(cod)], [Rh(rca)(cod)], [Rh(rcfcm)(cod)] and [Rh(drcm)(cod)]. ν = scan rate, E_{pi} = peak anodic potentials as numbered from left to right with $E_{p1} = E_{Rh}$, i = 1-7.

[Rh(RcCOCHCOCF$_3$)(cod)]						
ν / mV s^{-1}	E_{p1} / V	i_{p1} / μA	E_{p2} / V	E_{p3} / V [a]	i_{p3} / μA [a]	
50	0.450	11.4	0.725	0.815	25.7	
100	0.456	16.4	0.712	0.847	30.3	
150	0.460	18.6	0.737	0.827	37.9	
200	0.468	22.2	0.741	0.827	44.5	
250	0.476	25.7	0.737	0.815	51.8	
[Rh(RcCOCHCOCH$_3$)(cod)]						
ν / mV s^{-1}	E_{p1} / V	i_{p1} / μA	E_{p2} / V	i_{p2} / μA	E_{p3} / V	i_{p3} / μA
50	0.384	10.0	0.637	16.2	0.832	22.6
100	0.386	15.6	0.650	19.5	0.832	25.0
150	0.387	16.9	0.647	25.4	0.845	25.7
200	0.405	21.1	0.665	25.0	0.826	25.7
250	0.394	23.8	0.664	31.5	0.820	24.2
[Rh(RcCOCHCOC$_6$H$_5$)(cod)]						
ν / mV s^{-1}	E_{p1} / V	i_{p1} / μA	E_{p2} / V	i_{p2} / μA	E_{p4} / V [b]	i_{p4} / μA
50	0.381	8.9	0.536	11.1	0.778	22.8
100	0.388	14.4	0.542	12.2	0.794	28.9
150	0.391	16.6	0.541	17.4	0.802	31.6
200	0.396	21.4	0.547	19.9	0.800	35.0
250	0.395	23.9	0.545	22.1	0.797	40.5

a)Estimated values only due to poor peak resolutiom

b) Data in this column is peak 4. A shoulder to the left of E_{p4} is observed. The resolution of this peak E_{p3} , is to poor to give accurately measured currents or potentials.

Table 3.6. continued The cyclic Voltammetric data obtained from the voltammograms (versus Ag/Ag^{+}) for the [Rh(β-diketonato)(cod)] complexes [Rh(rctfa)(cod)], [Rh(brcm)(cod)], [Rh(rca)(cod)], [Rh(rcfcm)(cod)] and [Rh(drcm)(cod)]. ν = scan rate, E_{pi} = peak anodic potentials as numbered from left to right with $E_{p1} = E_{Rh}$, *i* = 1-7.

[Rh(RcCOCHCOFc)(cod)]									
ν / mV s^{-1}	E_{p1} / V	i_{p1} / μA	E_{p2} / V	E_{p3} / V [a]	E_{p4} / V [a]	E_{p5} / V	i_{p5} / μA [a]	E_{p6} / V [a]	E_{p7} / V [a]
50	0.007	7.7	0.116	0.231	0.316	0.554	14.0	-	0.811
100	-0.030	4.3	0.118	0.255	0.316	0.548	17.2	-	0.803
150	-0.028	7.7	0.118	0.249	0.312	0.548	36.5	0.721	0.811
200	-0.018	12.9	0.118	0.259	0.312	0.543	31.3	0.719	0.818
250	-0.011	18.9	0.118	0.259	0.312	0.545	43.0	0.706	0.795

[Rh(RcCOCHCORc)(cod)]			
ν / mV s^{-1}	E_{p1} / V	E_{p3} / V a	E_{p4} / V [a]
50	0.360	-	-
100	0.360	-	0.806
150	0.365	-	0.810
200	0.364	-	0.812
250	0.365	0.628	0.812

a) Estimated values only due to poor peak resolution

The cause of multiple oxidation waves as well as the search for the ultimate product(s) during oxidation for the complexes of this study is at present a topic of further research in this laboratory. It is expected that in the near future of this follow-up study program, much more of

this important and very interesting ruthenocene-based electrochemical system will be understood.

4. EXPERIMENTAL

4.1. CHEMICALS

$RhCl_3$ (Strem), ruthenocene (Strem), aluminium trichloride (Aldrich) and other solid reagents (Merck) were used without further purification. Lithium diisopropyl amide, 1-iodo-3,5-bis(trifluoromethyl)benzene (Aldrich), dimethoxyethane (Aldrich), 2-chlorobenzoylchloride (Aldrich), acetic anhydride (Merck) and cycloocta-1,5-diene (Aldrich) were used without further purification, other liquid reagents and solvents were distilled prior to use; water was double distilled. Tetrahydrofuran (THF) was dried by refluxing under a nitrogen atmosphere over sodium wire and distilled directly before use. Methanol was dried by refluxing under a nitrogen atmosphere over molecular sieve beads (0,5nm porosity) and distilled directly before use.

4.2. TECHNIQUE AND APPARATUS

4.2.1. GENERAL

Column chromatography was performed on Kieselgel 60 (Merck, grain size 0.063-0.2 mm, eluent ether-hexane = 1:1 by volume (for the compounds acetylruthenocene, Hbrcm, Hdrcm, [Rh(rctfa)(cod)], [Rh(brcm)(cod)], [Rh(rcfcm)(cod)], [Rh(drcm)(cod)]) or ether-hexane = 4:1 by volume (for compound Hrctfa).

Nuclear magnetic resonance spectra (NMR) were obtained using a Bruker 300 MHz AM-300 instrument. Chemical shifts are reported as δ-values (ppm) relative to trimethylsilane (δ=0,00 ppm).

Infrared-spectra (wavenumber / cm^{-1}) were obtained with use of a Hitachi spectrophotometer Model 270-50 with a dataprocessor. The IR spectra for solids were obtained in a potassium bromide matrix, spectra for liquids were obtained from thin films between NaCl discs.

UV-spectrophotometric measurements were made with a computer controlled Cary 50 UV-Vis spectrophotometer. Solvents were methanol unless otherwise indicated.

pH readings were obtained using an Orion model SA 720, equipped with a glass electrode. The pH meter was calibrated using buffers at pHh 4.00 and 9.18 and these were made up according to IUPAC standards as described in the literature[1]. The temperature was controlled using a water bath to within 25.0 °C ± 0,1°C.

Elemental analysis was conducted by the Canadian Microanalytical Service Ltd.

4.2.2. $pK_a^{/}$ - DETERMINATIONS

The analyte was dissolved in a solvent system of water:acetonitrile (9:1). In all cases the ionic strength was maintained at 0.1 mol dm^{-3} with $NaClO_4 \cdot H_2O$. UV-spectra of the protonated (0.2 mmol dm^{-3} β-diketone at pH = 2) and the unprotonated forms (0.2 mmol dm^{-3} β-diketone at pH = 12) of the β-diketones were obtained from these dissolved analyte systems. From this data an analytical wavelength was chosen at which the $pK_a^{/}$ could be determined (Hrca, 319 nm; Hrctfa, 315 nm; Hbrcm, 365 nm). The analytical wavelengths for the compounds Hrcfcm and Hdrcm could not be determined according to this method as their $pK_a^{/}$ values are above 13. The analytical wavelength was chosen where the change in absorbance between the protonated and unprotonated forms is greatest. The titration's of the solutions were done with 0.1mol dm^{-3} and 1mol dm^{-3} NaOH or with 0.1 mol dm^{-3} and 1 mol dm^{-3} $HClO_4$ depending whether an acidic or a

basic titration was performed. An effort was made to ensure that the increase in volume during the titration was no more than 5%. The $pK_a^{/}$ values where obtained by insertion of the absorption/pH data obtained into the Equation 3.1. The equation fitting was conducted using the least squares fitting program MINSQ[2].

4.2.3. ISOMERIZATION KINETICS STUDY

Monitoring of the conversion of keto- to enol-isomer

An acetonitrile/ether mixture (ca 1:1 by volume) (50mg β-diketone in 10ml) of Hrca or Hrctfa were prepared for the respective β-diketones. An aqueous solution of 0.1 mol dm^{-3} NaOH solution was prepared, and the β-diketone in the organic layer was extracted into the aqueous layer to convert the β-diketone to the keto-isomer. The organic layer was then discarded and 2.5ml of $CDCl_3$ was added to the aqueous layer. Acidification with HCl allowed β-diketone extraction into the $CDCl_3$ layer; the aqueous layer was discarded and the $CDCl_3$ layer was washed with water. From this organic layer the NMR analysis was performed.

At different times the % keto-isomer was determined and the observed first order rate constant, k_{obs}, was obtained utilizing Equation 3.2. and Equation 3.4. as well as the fitting program MINSQ[2]. The individual rate constants k_1 and k_{-1} were obtained by simultaneously solving Equations 3.3. and $k = k_1 + k_{-1}$.

Monitoring of the conversion of enol- to keto-isomer

The solvent $CDCl_3$ was dried and made acid free by running it through a small column of basic alumina just prior to use. NMR spectra of the compounds Hrca, Hbrcm, Hrcfcm

and Hdrcm were obtained from $CDCl_3$ solutions with β-diketone concentrations between 5.5 mg and 9.6 mg per g $CDCl_3$. In the solid state, after enough time has elapsed, the equilibrium is driven completely to the enol-isomer[3]. Therefore, upon dissolving aged samples of the β-diketones in $CDCl_3$, the formation of keto-isomers until the solution equilibrium position was reached could be monitored. For the Hrctfa the observed rate constant could only be followed by monitoring the conversion of keto- to enol-isomer, as the % of keto-isomer in the equilibrium position is 7.62%. For Hrca the isomerization could be followed from both the keto- and enol-isomer sides of the equilibrium.

4.2.4 SUBSTITUTION KINETICS

Due to the fact that the substitution kinetics proceeded very quickly, a computer-controlled Applied PHOTOPHYSICS SX.18MV Stopped Flow Instrument collected kinetic data. The rate constants were determined using the associated Applied Photophysics software. The temperature was controlled using a water bath to within 0.1°C.

All substitution reactions were performed in freshly distilled methanol under pseudo first order conditions, where the 1,10-phenantroline concentrations were in a 10 to 600 times excess compared to the rhodium complex concentration (1×10^{-5} $mol.dm^{-3}$). The reactions were also conducted at five different temperatures between 15°C and 36°C with an appropriate excess concentration of the 1,10-phenantroline.

4.2.5 CYCLIC VOLTAMMETRY

Cyclic voltammetry was conducted using a computer-controlled BAS model C-27 voltammograph. The temperature was controlled using a water bath at 25.0 °C ± 0.1°C.

Cyclic voltammetry was conducted on 1-2 mM solutions in

a) dried distilled acetonitrile with 0.1M *n*-tetrabutylammonium hexafluorophosphate
b) dried distilled acetonitrile with 0.1M *n*-tetrabutylammonium tetrakis[3,5-bis(trifluoromethyl)phenyl]borate
c) dried distilled dichloromethane with 0.1M *n*-tetrabutylammonium tetrakis[3,5-bis(trifluoromethyl)phenyl]borate
d) dried distilled α,α,α-trifluorotoulene with 0.1M *n*-tetrabutylammonium tetrakis[3,5-bis(trifluoromethyl)phenyl]borate

The three-electrode cell that was used, consisted of a glassy carbon working electrode, a Pt-counter electrode and an Ag/Ag^+ (0,01 mol dm^{-3} $AgNO_3$) reference electrode. The reference electrode consisted of a silver wire inserted into a solution of 0,01 mol dm^{-3} $AgNO_3$ and 0,1 mol dm^{-3} *n*-tetrabutylammonium hexafluorophosphate in acetonitrile, in a luggin capillary with a vycor tip. For the experiments not done in acetonitrile it was necessary to employ the use of a salt bridge. The salt bridge employed consisted of the Ag/Ag^+ reference electrode inserted into a luggin capillary with a vycor tip consisting of a solution of 0,1 mol dm^{-3} *n*-tetrabutylammonium hexafluorophosphate in acetonitrile.

4.3. SYNTHESIS

4.3.1. SYNTHESIS OF METALLOCENE METHYL ESTERS

4.3.1.1. SYNTHESIS OF METHYL FERROCENOATE

(i) SYNTHESIS OF 2-CHLOROBENZOYLFERROCENE

Ferrocene (37.2 g; 0.2 mol) and 2-chlorobenzoylchloride (25.4 ml; 35 g; 0.2 mol) was dissolved in DCM (250 ml). The solution was stirred and placed in an ice bath. $AlCl_3$ (28 g; 0.2 mol;) was added in small portions over 2 hours in order to keep the temperature under 5ºC. After addition, the reaction was kept cool for 5 minutes and then stirred at room temperature for 4 hours. The resulting mixture was cooled and water (200 ml) was carefully added and the resulting mixture stirred for 30 minutes. The layers were separated and the H_2O layer was extracted with DCM (2 X 50 ml). DCM layers where combined, washed with H_2O (100 ml), then with 10% NaOH (2 X 100 ml) and again with H_2O (100 ml). The organic layer was separated and dried over $MgSO_4$. This solution was then filtered and evaporated under reduced pressure to obtain 2-chlorobenzoylferrocene. Yield: 53,45 g (82,33 %) m.p. 72-73°C ;δ_H (300MHz; $CDCl_3$) 4.25 (5H; s; C_5H_5), 4.58 (2H; t; C_5H_4), 4.72 (2H; t; C_5H_4), 7.3-7.5 (4H; m; C_6H_4Cl).

(ii) SYNTHESIS OF FERROCENECARBOXYLIC ACID

A 1l three necked flask was charged with dimethoxyethane (200 ml) and potassium *t*-butoxide (100 g; 0.89 mol) under nitrogen and H_2O (4.4 ml; 0.24 mol) was added with stirring. 2-chlorobenzoylferrocene (53.45 g; 0.16 mol) was added to the resulting mixture and the reaction mixture was refluxed and stirred for an hour. The reaction mixture was then cooled and poured into H_2O (1 l). The resulting aqueous solution was washed with ether (6 X 150 ml), and these ether portions were back extracted with 10% NaOH (4 X 50 ml). The aqueous phases where combined and acidified with concentrated HCl. The precipitate that formed was collected by filtration and air-dried. The product was dissolved in $CHCl_3$ and washed with H_2O (3 X 100 ml), dried over $MgSO_4$, filtered and the $CHCl_3$ evaporated under reduced pressure to obtain ferrocenecarboxylic acid. Yield: 26.98 g (71,21%) d.p. 171ºC;δ_H (300MHz; $CDCl_3$) 4.28(5H; s; C_5H_5), 4.49 (2H; t; C_5H_4), 4.88 (2H; t; C_5H_4).

(iii) SYNTHESIS OF METHYL FERROCENOATE

Ferrocenecarboxylic acid (13.68 g; 0.06 mol) was refluxed in methanol (600 ml) in the presence of concentrated H_2SO_4 (0.5 ml) under a N_2 atmosphere for 48 hours. The resulting solution was poured over ice (500 g) and extracted with ether (3 X 350 ml). The combined ether extractions were washed with H_2O (4 X 200 ml) 0.5 mol dm^{-3} NaOH (3 X 100 ml) and again with H_2O (3 X 200 ml). The resulting solution was then dried over $MgSO_4$, filtered and the organic layer was evaporated to obtain methylferrocenoate. Yield: 12.44 g (85.63 %) m.p. 69ºC;δ_H (300MHz; $CDCl_3$) 4.22 (5H; s; C_5H_5), 4.41 (2H; t; C_5H_4), 4.82 (2H; t; C_5H_4), 3.82 (3H; s; OCH_3); IR(KBr cm^{-1}) 1704 (C=O).

4.3.1.2. SYNTHESIS OF METHYL RUTHENOCENOATE

(i) SYNTHESIS OF 2-CHLOROBENZOYLRUTHENOCENE

Ruthenocene (5.49 g; 0.024 mol) and 2-chlorobenzoylchloride (4.15 g; 3.00 ml; 0,024 mol) was dissolved in DCM (250 ml). The solution was stirred and placed in an ice bath. $AlCl_3$ (4.74 g; 0.036 mol) was added in small portions over 2 hours in order to keep the temperature at 5ºC. After addition, the reaction was kept cool for 5 minutes and then stirred at room temperature for 4 hours. The resulting mixture was cooled, and water (200 ml) was carefully added and the resulting mixture stirred for 30 minutes. The layers were separated and the H_2O layer was extracted with DCM (2 X 50 ml). DCM layers were combined, washed with H_2O (100 ml), then with 10% NaOH (2 X 100 ml) and again with H_2O (100 ml). The organic layer was separated and dried over $MgSO_4$. This solution was then filtered and evaporated under reduced pressure to obtain 2-chlorobenzoylruthenocene. Yield: 5.91 g (67.41 %) m.p. 88-90°C ;δ_H (300MHz; $CDCl_3$) 4,64 (5H; s; C_5H_5), 4,84 (2H; t; C_5H_4), 5,03 (2H; t; C_5H_4), 7,3-7,5 (4H; m; C_6H_4Cl).

(ii) SYNTHESIS OF RUTHENOCENOIC ACID

A 500 ml three necked flask was charged with dimethoxyethane (50 ml) and potassium *t*-butoxide (30.54 g) under nitrogen and H_2O (1.5ml) was added with stirring. 2-

chlorobenzoylruthenocene (2.51 g; 6.79 mmol) was added to the resulting mixture and this mixture was refluxed and stirred overnight. The reaction mixture was then cooled and poured into H_2O (200 ml). The resulting aqueous solution was washed with ether (6 X 50 ml), and these ether portions were back extracted with 10% NaOH (2 X 100 ml). The aqueous phases were combined and acidified with concentrated HCl. The precipitate that formed was collected by filtration, washed with H_2O and then air-dried. The product was dissolved in $CHCl_3$ and washed with H_2O (3 X 100 ml), dried over $MgSO_4$, filtered and the $CHCl_3$ evaporated under reduced pressure to obtain ruthenocenoic acid. Yield: 0.84 g (45.22 %) m.p. 167-168ºC;δ_H (300MHz; $CDCl_3$) 4,65(5H; s; C_5H_5), 4,77 (2H; t; C_5H_4), 5,19 (2H; t; C_5H_4).

(iii) SYNTHESIS OF METHYL RUTHENOCENOATE

Ruthenocenecarboxylic acid (0.84 g; 2.44 mmol) was refluxed in methanol (600 ml) in the presence of concentrated H_2SO_4 (0.5 ml) under a N_2 atmosphere for 48 hours. The resulting solution was poured over ice (500 g) and extracted with ether (3 X 350 ml). The combined extractions were washed with H_2O (4 X 200 ml) 0.5 mol dm^{-3} NaOH (3 X 100 ml) and again with H_2O (3X 200 ml). The resulting solution was then dried over $MgSO_4$, filtered and the organic layer was evaporated under reduced pressure to obtain methylruthenocenoate. Yield: 0.85 g (95.00 %) m.p. 89-91ºC;δ_H (300MHz; $CDCl_3$) 4,62 (5H; s; C_5H_5), 4,72 (2H; t; C_5H_4), 5,15 (2H; t; C_5H_4), 3.75 (3H; s; OCH_3); IR(KBr cm^{-1}) 1707 (C=O).

4.3.2. SYNTHESIS OF ACETYL RUTHENOCENE (Scheme 3.1.)

Ruthenocene (1.10 g; 4.76 mmol) and aluminium trichloride (4.42 g; 10.67 mmol; 2.2 eq) in DCM (100 ml) was brought to reflux. Acetic anhydride (0.39 ml; 5.06 mmol; 1eq) in DCM (25 ml) was added dropwise to the reaction mixture. The reaction mixture was allowed to reflux for a further hour after addition of the acetic anhydride. Water (100 ml)

was added and the resulting mixture was allowed to reflux for a further 20 minutes. The layers were separated and the organic layer was washed with H_2O (3 X 100 ml). The organic layer was dried over anhydrous sodium sulfate. The DCM was evaporated under reduced pressure. The resulting solid was dissolved in diethyl ether, and the acetylruthenocene was separated from the reagents by column chromatography (R_f =0.47). Yield: 0.80 g (61.33 %);m.p. 108-110°C; δ_H (300 MHz, $CDCl_3$) 5.11 (2H; t; C_5H_4), 4.8 (2H; t; C_5H_4), 4.62 (5H; s; C_5H_5) and 2.32 (3H; s; CH_3).

4.3.3. SYNTHESIS OF β-DIKETONES

4.3.3.1. SYNTHESIS OF

1-RUTHENOCENYL-4,4,4-TRIFLUOBUTAN-1,3-DIONE (Hrctfa) (Scheme 3.1.)

The system was degassed and filled with a nitrogen atmosphere that was maintained through the entire duration of the experiment. Acetylruthenocene (0.80 g; 2.92 mmol) was dissolved in dry THF (20 ml) and lithium diisopropylamide (1.45 ml of a 2.0 mol dm^{-3} solution; 2.9 mmol) was added. The reaction mixture was stirred for 20 minutes. Ethyltrifluoroacetate (0.35 ml; 2.92 mmol) was added and the reaction mixture was stirred overnight. Hexane (20 ml) was added as well as ether (40 ml). Hydrochloric acid (20 ml, 1 mol dm^{-3}) was added and the reaction mixture was stirred for 20 minutes. The layers were separated and the organic layer of the reaction mixture was washed with water (4 X 100 ml) to remove the THF, then dried over sodium sulfate and filtered. Hrctfa was separated from the reagents by column chromatography (R_f = 0.91). Yield: 0.90 g (83 %); m.p. 102-104°C (Found: C, 45.51; H, 3.00 $C_{14}F_3H_{11}O_2Ru$ requires C, 45.51; H, 3.00); δ_H (300 MHz, $CDCl_3$) %enol (55.6 %), 6.03 (1H; s; COC<u>H</u>COH), 5.20

(2H; t; C_5H_4), 4.63 (5H; s; C_5H_5) %keto (44.4 %), 3.00 (2H;s;$COCH_2CO$), 5.12 (2H; t; C_5H_4) and 4.70 (5H;s;C_5H_5).

4.3.3.2. SYNTHESIS OF

1-RUTHENOCENYL-3-PHENYLPROPAN-1,3-DIONE (Hbrcm) (Scheme 3.1.)

The system was degassed and filled with a nitrogen atmosphere that was maintained through the entire duration of the experiment. Acetylruthenocene (0.86 g; 3.14 mmol) was dissolved in dry THF (20 ml) and lithium diisopropylamide (1.6 ml of a 2.0 mol dm^{-3} solution; 3.14 mmol) was added and the reaction mixture was stirred for 20 minutes. Methyl benzoate (0.4 ml; 3.14 mmol) was added and the reaction mixture was stirred overnight. Hexane (20 ml) was added as well as ether (40 ml). Hydrochloric acid (20 ml, 1mol dm^{-3}) was added and the reaction mixture was stirred for 20 minutes. The layers were separated and the organic layer of the reaction mixture was washed with water (4X100 ml) to remove the THF and then dried over sodium sulfate and filtered. Hbrcm was separated from the reagents by column chromatography (R_f = 0.66). Yield: 489 mg (41.3 %) ;m.p. 110°C; (Found: C, 60.38; H, 4.38 $C_{19}H_{16}O_2Ru$ requires C, 60.45; H, 4.27); δ_H (300MHz; $CDCl_3$) only an enol isomer was detected, 4.59 (5H; s; C_5H_5), 4.80 (2H; t; C_5H_4), 5.20 (2H; t; C_5H_4), 6.28 (1H; s; COCHCOH), 7.46 (3H; C_6H_5) and 7.85 (2H; C_6H_5).

4.3.3.3. SYNTHESIS OF

1-RUTHENOCENYL-3-METHYLPROPAN-1,3-DIONE (Hrca) (Scheme 3.1.)

The system was degassed and filled with a nitrogen atmosphere that was maintained through the entire duration of the experiment. Acetylruthenocene (0.70 g; 2.56 mmol) was dissolved in dry THF (20 ml) and lithium diisopropylamide (3.3 ml of an 2.0 mol dm^{-3} solution; 6.60 mmol) was added and the reaction mixture stirred for 20 minutes. Ethyl acetate (0.3 ml; 3.07 mmol; 1.2 eq) was added and the reaction mixture stirred overnight. Ether was added in excess to precipitate the lithium salt out of the reaction mixture, this solution was filtered and the precipitate washed with ether. The precipitate was hydrolyzed with hydrochloric acid (1mol dm^{-3}). The product was then extracted from the aqueous layer by ether, and the layers were separated. The organic layer was washed with water (4X100 ml) and dried over sodium sulfate and filtered. Hrca was obtained by evaporating the ether under reduced pressure. Yield 216 mg (26.8 %); m.p. 111°C; (Found: C, 53.93; H, 4.85 $C_{14}H_{14}O_2Ru$ requires C, 53.30; H, 4.47); δ_H (300MHz; $CDCl_3$) %enol (50.5 %), 2.31 (3H; d; CH_3), 5.11 (2H; t; C_5H_4), 4.59 (5H; s; C_5H_5), 5.64 (1H; d; COCHCOH) %keto (49.5 %), 2.06 (3H; d; CH_3), 5.14 (2H; t; C_5H_4) and 4.61 (5H; s; C_5H_5).

4.3.3.4. SYNTHESIS OF 1-RUTHENOCENYL-3-FERROCENYLPROPAN-1,3-DIONE (Hrcfcm) (Scheme 3.1.)

The system was degassed and filled with a nitrogen atmosphere that was maintained through the entire duration of the experiment. Acetylruthenocene (503 mg; 1.84 mmol) was dissolved in dry THF (3 ml) and Lithium diisopropylamide (1 ml of a 2.0 mol dm^{-3} solution; 1.84 mmol) was added and the reaction mixture was stirred for 20 minutes. Methyl ferrocenoate (451 mg; 1.84 mmol) was dissolved in dry THF (5 ml). The resulting solution was added to the reaction mixture with cooling and the reaction mixture was stirred overnight. Ether was added in excess to precipitate the lithium salt

out of the reaction mixture, this solution was filtered and the precipitate washed with ether. The precipitate was hydrolyzed with hydrochloric acid (1mol dm^{-3}). The product was extracted from the aqueous layer by ether, and the layers separated. The organic layer was washed with water (4 X 100 ml) and dried over sodium sulfate and filtered. Hrcfcm was obtained by evaporating the ether under reduced pressure. Yield: 305 mg (34.13 %); m.p.178°; (Found: C, 56.80; H, 4.16 $C_{23}FeH_{20}O_2Ru$ requires C, 56.77; H, 4.14); δ_H (300MHz; $CDCl_3$) %enol to Fc side (48.43 %), 5.9 (1H; s; COCHCOH), 5.19 (2H; t; C_5H_4 Rc), 4.60 (5H; s; C_5H_5 Rc), 4.51 (2H; t; C_5H_4 Fc), 4.20 (5H; s; C_5H_5 Fc), %enol to Rc side (13.95 %), 5.14 (2H; t; C_5H_4 Rc), 4.72 (2H; t; C_5H_4 Fc), 4.56 (5H; s; C_5H_5 Rc), 3.99 (5H; s; C_5H_5 Fc), %keto (37.62%), 5.24 (2H; t; C_5H_4 Rc), 5.10 (2H; t; C_5H_4 Fc), 4.61 (5H; s; C_5H_5 Rc) 4.23 (5H; s; C_5H_5 Fc) and 2.28 (2H; s; $COCH_2CO$).

4.3.3.5. SYNTHESIS OF

1,3-DIRUTHENOCENYLPROPAN-1,3-DIONE (Hdrcm) (Scheme 3.1.)

The system was degassed and filled with a nitrogen atmosphere that was maintained through the entire duration of the experiment. Acetyl ruthenocene (94 mg; 0.35 mmol) was dissolved in dry THF (3 ml) and lithium diisopropylamide (0.17 ml of a 2.0 mol dm^{-3} solution; 0.35 mmol) was added and the reaction mixture was stirred for 20 minutes. Methyl ruthenocenoate (100 mg; 0.35 mmol) was added in the solid form by way of Schlenck apparatus with cooling, the resulting solution was stirred overnight. Ether was added in excess to precipitate the lithium salt out of the solution, the solution was filtered and the precipitate washed with ether. The precipitate was hydrolyzed with hydrochloric acid (1mol dm^{-3}). The product was extracted from the aqueous layer by ether and the layers separated. The organic layer was washed with water (4 X 100 ml) and dried over sodium sulfate. Hdrcm was separated form the reagents by column chromatography (R_f =

0,66). Yield: 51 mg (28.03 %); m.p. 182°C; (Found: C, 53.29; H, 4.08 $C_{23}H_{20}O_2Ru_2$ requires C, 51.96; H, 3.79); δ_H (300MHz; $CDCl_3$) %enol (39.43 %), 5,83 (1H; s; COCHCOH), 5,17 (2H; t; C_5H_4), 4,78 (2H; t; C_5H_4), %keto (60.57 %), 3,88 (2H; s; $COCH_2CO$), 5,23 (2H; t; C_5H_4), 4,83 (2H; t; C_5H_4).

4.3.4. SYNTHESIS OF RHODIUM COMPLEXES

4.3.4.1. SYNTHESIS OF

DI-μ-CHLORO-BIS[(1,2,5,6-η)1,5-CYCLOOCTADIENE]RHODIUM (Scheme 3.2.)

$RhCl_3 \cdot 3H_2O$ (1.02 g: 4.89 mmol) was dissolved in 20 drops of H_2O at room temperature after which ethanol (24 ml) was added with stirring. 1,5-cyclooctadiene (7 ml) was slowly added to the mixture and the resulting mixture was refluxed at 78°C for 2½ hours. The mixture was cooled in an ice bath, the precipitate of di-μ-chloro-bis[(1,2,5,6-η)1,5-cyclooctadiene]rhodium was filtered and washed with cold methanol and dried in the dark. Yield: 744 mg (61.74 %); d.p. 243°C δ_H (300MHz, $CDCl_3$), 1.78(4H,m,half of $4CH_2$), 2.5(4H,m,half of $4CH_2$), 4.25 (4H,m,4CH).

4.3.4.2. SYNTHESIS OF THE [Rh(rctfa)(cod)] COMPLEX (Scheme 3.2.)

$[Rh_2Cl_2(cod)_2]$ (71 mg; 0.14 mmol) was dissolved in dimethylformamide (6 ml) and Hrctfa (101 mg; 0.27 mmol) was added. After 30 minutes of stirring the product was precipitated by the slow addition of ice water. The product was filtered off and dissolved

in ether. The organic layer was washed with water (3X100 ml) and dried over sodium sulfate. The organic layer was filtered. [Rh(rctfa)(cod)] was separated from the reagents by column chromatography (R_f = 0.97). Yield: 72 mg 45.47 %; m.p. 153°C; (Found: C, 46.51; H, 4.10 $C_{22}F_3H_{22}O_2RhRu$ requires C, 45.59; H, 3.83); δ_H (300MHz; $CDCl_3$) 5.84 (1H; s; COCHCO), 5.00 (2H; t; C_5H_4), 4.71 (2H; t; C_5H_4), 4.54 (5H; s; C_5H_5), 4.11 (4H; m; olefinic protons of C_8H_{12}), 2.46 (4H; m; ½ aliphatic protons of C_8H_{12}) and 1.83 (4H; m; ½ aliphatic protons of C_8H_{12}).

4.3.4.3. SYNTHESIS OF THE [Rh(rca)(cod)] COMPLEX (Scheme 3.2.)

$[Rh_2Cl_2(cod)_2]$ (117 mg; 0.2379mmol) was dissolved in dimethylformamide (6 ml) and Hrca (147 mg; 0.47 mmol) was added. After 90 minutes of stirring the product was precipitated by the slow addition of ice water. The product was filtered off and air-dried. Yield: 120 mg (49.18 %): m.p. 133-135°C; (Found: C, 50.36; H, 5.47. $C_{22}H_{25}O_2RhRu$ requires C, 50.28; H, 4.79); δ_H (300MHz; $CDCl_3$) 5.56 (1H; d; COCHCO), 4.98 (2H; t; C_5H_4), 4.65 (2H; t; C_5H_4), 4.55 (5H; s; C_5H_5), 4.25 (4H; m; olefinic protons of C_8H_{12}), 2.50 (4H; m; ½ aliphatic protons of C_8H_{12}) and 1.97 (4H; m; ½ aliphatic protons of C_8H_{12}).

4.3.4.4. SYNTHESIS OF THE [Rh(brcm)(cod)] COMPLEX (Scheme 3.2.)

$[Rh_2Cl_2(cod)_2]$ (45 mg; 0.09 mmol) was dissolved in dimethylformamide (6 ml) and Hbrcm (67 mg; 0.18mmol) was added. After 30 minutes of stirring the product was precipitated by the slow addition of ice water. The product was filtered off and dissolved in ether. The organic layer was washed with water (3X100 ml) and dried over sodium sulfate. The organic layer was filtered. [Rh(brcm)(cod)] was separated from the reagents by column chromatography (R_f = 0.93). Yield: 45 mg (42.88 %); m.p. 160°C; (Found: C,

53.58; H, 5.45 $C_{27}H_{27}O_2RhRu$ requires C, 55.17; H, 4.63); δ_H (300MHz; $CDCl_3$) 7.75 (2H; m; C_6H_5), 7.40 (3H; m; C_6H_5), 6.23 (1H; s; COCHCO), 4.57 (5H; s; C_5H_5), 4.69 (2H; t; C_5H_4), 5.07 (2H; t; C_5H_4), 4.17 (4H; m; olefinic protons of C_8H_{12}), 2.54 (4H; m; aliphatic protons of C_8H_{12}) and 1.89 (4H; m; aliphatic protons of C_8H_{12}).

4.3.4.5. SYNTHESIS OF THE [Rh(rcfcm)(cod)] COMPLEX (Scheme 3.2.)

$[Rh_2Cl_2(cod)_2]$ (41 mg; 0.08 mmol) was dissolved in dimethylformamide (6 ml) and Hrcfcm (80 mg; 0.16 mmol) was added. After 5 minutes of stirring the product was precipitated by the slow addition of ice water. The product was filtered off and dissolved in ether. The organic layer was washed with water (3X100 ml) and dried over sodium sulfate. The organic layer was filtered. [Rh(rcfcm)(cod)] was separated from the reagents by column chromatography (R_f = 0.94). Yield: 21 mg (18.27 %); m.p. 161°C; (Found: C, 54.74; H, 4.92. $C_{31}FeH_{31}O_2RhRu$ requires C, 53.43; H, 4.49); δ_H (300MHz; $CDCl_3$) 5.88 (1H; s; COCHCO), 5.05 (2H; t; C_5H_4 Rc), 4.69 (2H; t; C_5H_4 Rc), 4.66 (2H; t; C_5H_4 Fc), 4.56 (5H; s; C_5H_5 Rc), 4.34 (2H; t; C_5H_4 Fc), 4.14 (5H; s; C_5H_5 Fc), 4.09 (4H; m; olefinic protons of C_8H_{12}), 2.54 (4H; m; aliphatic protons of C_8H_{12}) and 1.87 (4H; m; aliphatic protons of C_8H_{12}).

4.3.4.6. SYNTHESIS OF THE [Rh(drcm)(cod)] COMPLEX (Scheme 3.2.)

$[Rh_2Cl_2(cod)_2]$ (23 mg; 0,05 mmol) was dissolved in dimethylformamide (6 ml) and Hdrcm (50 mg; 0,01 mmol) was added. After 30 minutes of stirring the product was precipitated by the slow addition of ice water. The product was filtered off and dissolved

in ether. The organic layer was washed with water (3X100 ml) and dried over sodium sulfate. The organic layer was filtered. [Rh(drcm)(cod)] was separated from the products by column chromatography (R_f = 0.83). Yield: 36 mg (51,26 %); d.p. 204°C; (Found: C, 49.66; H, 5.69. $C_{31}H_{31}O_2RhRu_2$ requires C, 50.26; H, 4.27); δ_H (300MHz; $CDCl_3$) 5.82 (1H; s; COCHCO), 5.00 (4H; t; 2 C_5H_4), 4.67 (4H; t; 2 C_5H_4), 4.56 (10H; s; 2 C_5H_5), 4.06 (4H; m; olefinic protons of C_8H_{12}), 2.50 (4H; m; aliphatic protons of C_8H_{12}) and 1.88 (4H; m; aliphatic protons of C_8H_{12}).

4.3.5. SYNTHESIS OF ELECTROLYTES

4.3.5.1. SYNTHESIS OF SODIUM TETRAKIS

[3,5-BIS(TRIFLUOROMETHYL) PHENYL] BORATE TRIHIDRATE

An ethereal solution of 3,5-bis(trifluoromethyl)phenyl-magnesium iodide was prepared by stirring a mixture of 1-iodo-3,5-bis(trifluoromethyl)benzene (4.78 g; 14.06 mmol), Mg turnings (0.42 g; 17.10 mmol) and anhydrous ether (13 ml) for 1 hour. An ethereal solution of born trifluoride (365 mg; 2.52 mmol) was added dropwise over 40 minutes into the reaction mixture, and the resulting mixture was allowed to reflux for 12 hours under dry conditions. The reaction mixture was poured into an aqueous sodium carbonate solution (24 g in 100 ml H_2O) with vigorous stirring. The precipitated $MgCO_3$ was filtered off and the aqueous phase separated. This aqueous layer was extracted with ether (4 X 50 ml). All the ether extracts were combined. The product was obtained by eluting from a Kieselgel column, using hexane, then DCM, then methanol. The DCM and methanol fractions were combined and evaporated to obtain sodiumtetrakis[3,5-bis(trifluoromethyl)phenyl]borate. Yield: 2.70 g (81,80 %) m.p. 272°C δ_H (300MHz;

$CDCl_3$) 7,67 (4H; s; 4 $C_6H_3(CF_3)_2$), 7,78 (8H; t;4 $C_6H_3(CF_3)_2$); IR(KBr cm^{-1}) 3430; 1614; 1362; 1284; 1120-1140.

4.3.5.2. SYNTHESIS OF TETRABUTYLAMMONIUM TETRAKIS [3,5-BIS(TRIFLUOROMETHYL)PHENYL]BORATE

Hot aqueous tetrabutylammonium bromide (1.65 g; 5.11 mmol) was added to a hot aqueous solution of sodiumtetrakis[3,5-bis(trifluoromethyl)phenyl]borate (4.80 g; 5.11 mmol), and the resulting precipitate was filtered off. The precipitate was eluted with hexane, benzene, ether and methanol from a Kieselgel column. The ether and methanol fractions were combined and evaporated to obtain tetrabutylammonium tetrakis[3,5-bis(trifluoromethyl)phenyl]borate. Yield: 4.57 g (80.87 %); m.p. 84°C; δ_H (300MHz; $CDCl_3$) 7,55 (4H; s; 4 $C_6H_4(CF_3)_2$); 7,71 (8H; t; 4 $C_6H_4(CF_3)_2$); 0,98 (12H; t; $4C_3$-CH_3); 1,36 (8H; m; C_2-CH_2-C); 1,51 (8H; m; C-CH_2-C-C); 3,0 (8H; m; CH_2-C_3); IR(KBr cm^{-1}) 3420; 1617; 1359; 1275.

5. SUMMARY AND FUTURE PERSPECTIVES

5.1. SUMMARY

The Claisen condensation of an appropriate ester with acetyl ruthenocene under the influence of lithium diisopropylamide yielded the five new ruthenocenyl containing β-diketones 1-ruthenocenyl-4,4,4,-trifluorobutane-1,3-dione (Hrctfa), 1-ruthenocenyl-3-phenylpropane-1,3-dione (Hbrcm), 1-ruthenocenylbutane-1,3-dione (Hrca), 1-ruthenocenyl-3-ferrocenylpropane-1,3-dione (Hrcfcm) and 1,3-diruthenocenylpropane-1,3-dione (Hdrcm). The Rh-complexes [Rh(rctfa)(cod)], [Rh(brcm)(cod)], [Rh(rca)(cod)], [Rh(rcfcm)(cod)] and [Rh(drcm)(cod)] were prepared form the reaction between $[Rh_2Cl_2(cod)_2]$ and the ruthenocene-containing β-diketones .

The $pK_a^{/}$ values for the compounds Hrctfa (7.36(3)), Hbrcm (11.31(4)) and Hrca (10.22(1)) were determined in water containing 10% acetonitrile. Those of Hrcfcm and Hdrcm are larger than 13.

Substitution kinetics of the β-diketonato ligand from the complexes [Rh(rctfa)(cod)], [Rh(brcm)(cod)], [Rh(rca)(cod)], [Rh(rcfcm)(cod)] and [Rh(drcm)(cod)] by 1,10-phenantroline was studied with stopped flow UV spectroscopy. The electronic influence of the various β-diketonato side groups on the substitution rate results in an increase in the substitution rate according to the series (values in brackets are second order substitution rate constants in units mol^{-1} dm^3 s^{-1}) $CF_3(481) >> C_6H_5(21.7) > CH_3(16.1) > Rc(10.4) > Fc(9.9)$. The relatively large negative entropy values are indicative of an associative mechanism.

The isomerization kinetics of the β-diketones Hrctfa, Hrca, Hbrcm, Hrcfcm and Hdrcm was studied by NMR spectroscopy. It was shown that the rate of isomerization is effected by the electronic influence of the various β-diketone side groups, the isomerization rate was shown to increase according to the series $Rc > Fc > CH_3 >> C_6H_5 > CF_3$.

Cyclic voltammetry was conducted on the β-diketones Hrctfa, Hrca, Hbrcm, Hrcfcm and Hdrcm as well as their associated [Rh(β-diketonato)(cod)] complexes. Irreversible electrochemistry was obtained for all the ruthenium metal centers and only the oxidation potentials were observed,

multiple oxidation peaks were discovered in acetonitrile. The various R groups have an effect on the oxidation potentials of the ruthenium core with the more electronegative R groups moving the oxidation potential to a higher potential. The rhodium centers are oxidised at lower potentials than the ruthenium centers. Use of non-coordinating solvents as well as non-coordinating supporting electrolytes, simplified the multiplicity of the oxidation peaks, but did not induce electrochemical reversibility.

The group electronegativity for the ruthenocenyl group was determined according to the Gordy scale by using a plot of known group electronegativities versus carbonyl stretching frequencies for known methyl esters. The determined value was $\chi_{rc} = 1.94$

5.2. FUTURE PERSPECTIVES

Future studies in this field could concern synthesizing a wider range of β-diketones to determine if there are relations between the different R groups electronegativities and the different physical properties (*viz*: $pK_a^{/}$, E_{pa}, $k_{isomerization}$ etc.) of the compounds. Data from the present study is not enough to draw clear conclusions in this regard.

High pressure stopped flow kinetics should be conducted to independently confirm whether the mechanism for the substitution reaction between the [Rh(β-diketonato)(cod)] complexes and 1,10-phenantroline is associative mechanism in nature.

Further electrochemical analysis must be done to determine the formal reduction potentials of the Rc moiety in the various β-diketone compounds, as well for the complexes [Rh(β-diketonato)(cod)]. Especially studies at low temperature and in non-coordinating solvents utilizing non-coordinating supporting electrolytes may be benificial. Isolation of oxidized products will also greatly enhance the present understanding of electrochemical behavior of ruthenocene derivatives.

Conductometric analysis should be done on the compounds Hrcfcm and Hdrcm to determine their respective $pK_a^{/}$ values.

The present study also laid the foundations for expanding metallocene chemistry to include other metallocenes such as osmocene, cobaltocene and nickelocene.

APPENDIX A

NMR DATA

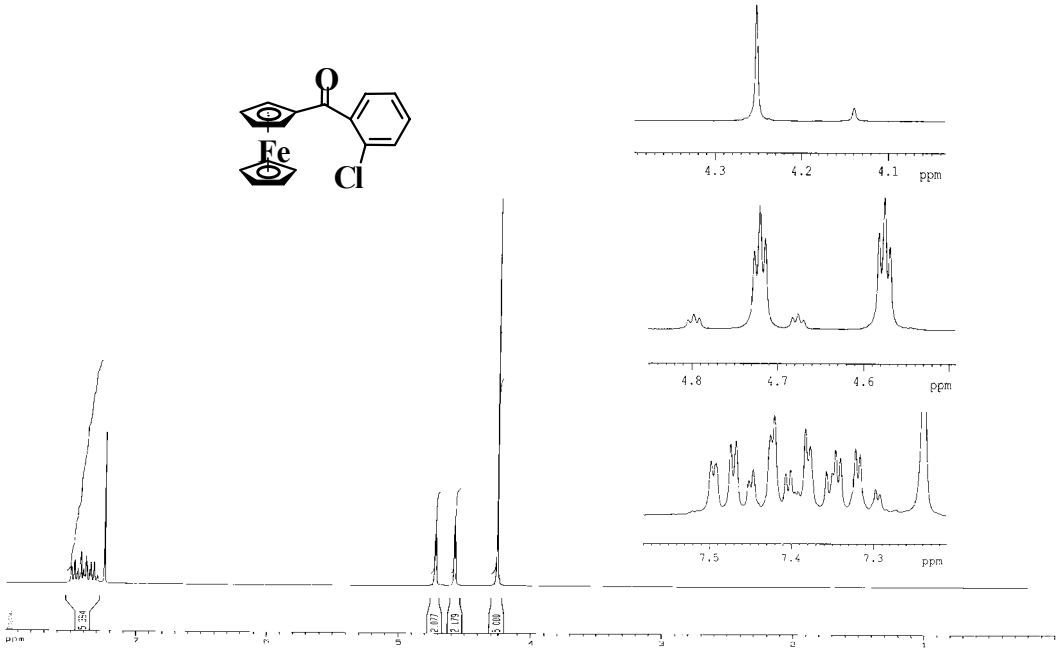

Spectrum A.1. ^{1}H NMR-spectrum of $FcCOC_6H_4Cl$

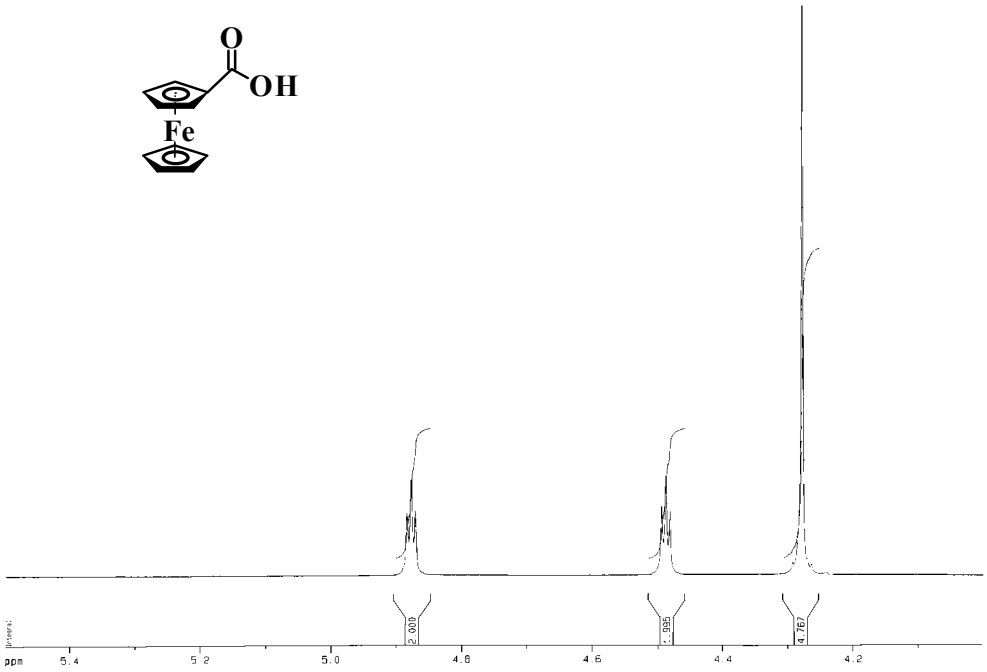

Spectrum A.2. ^{1}H NMR-spectrum of FcCOOH

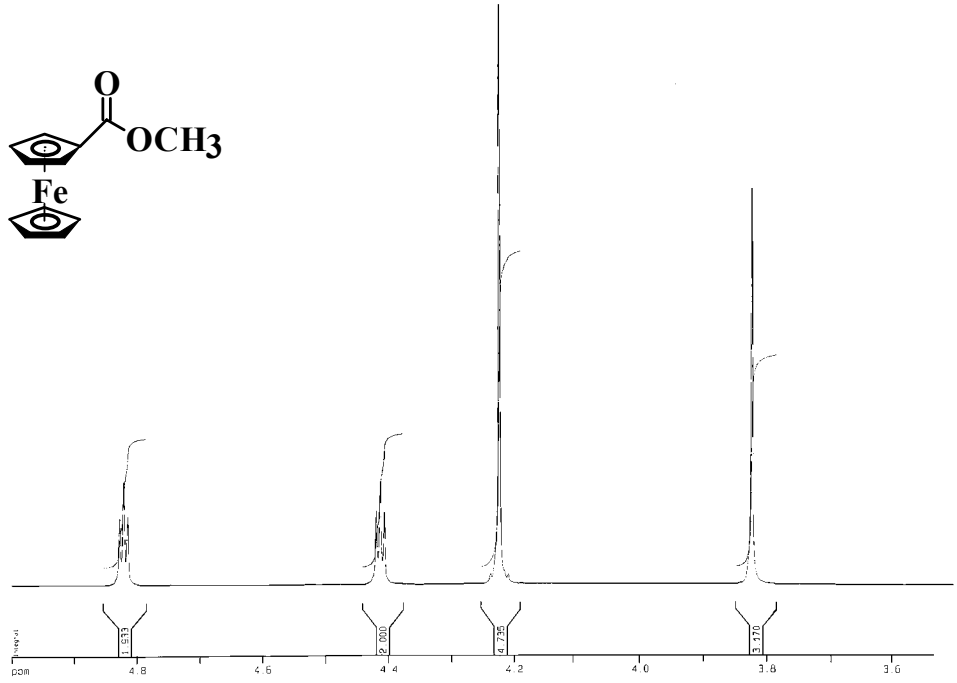

Spectrum A.3. ^{1}H NMR-Spectrum of $FcCOOCH_3$

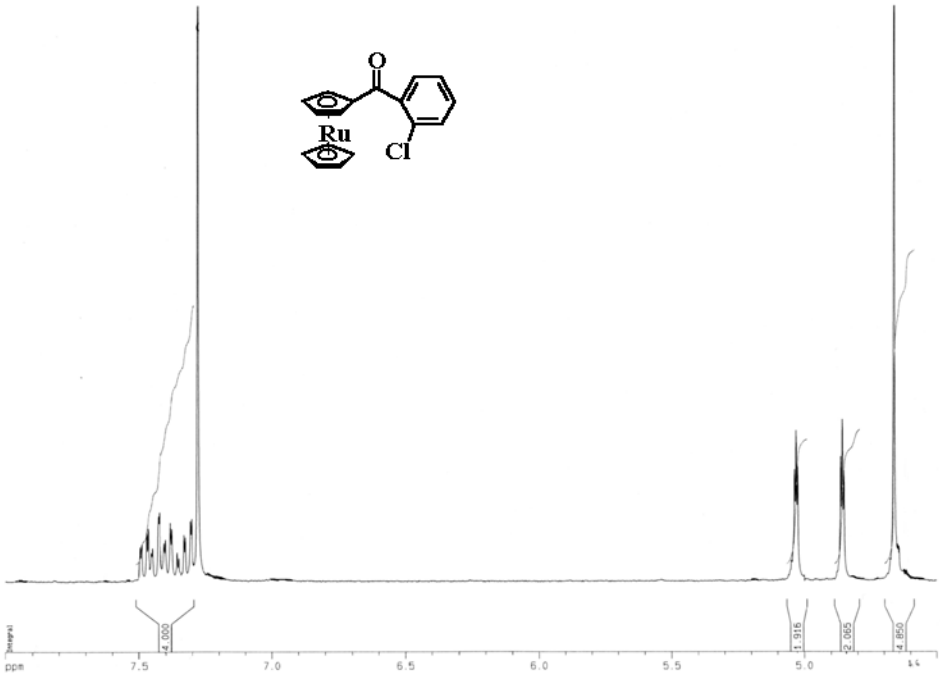

Spectrum A.4. ^{1}H NMR-Spectrum of $RcCOC_6H_4Cl$

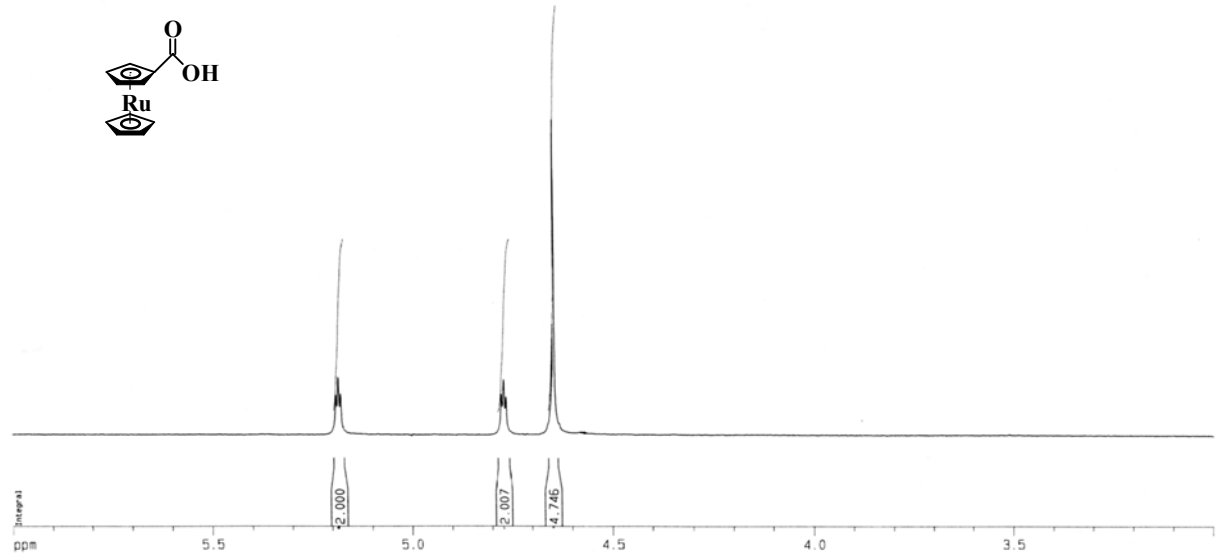

Spectrum A.5. ^{1}H NMR-Spectrum of RcCOOH

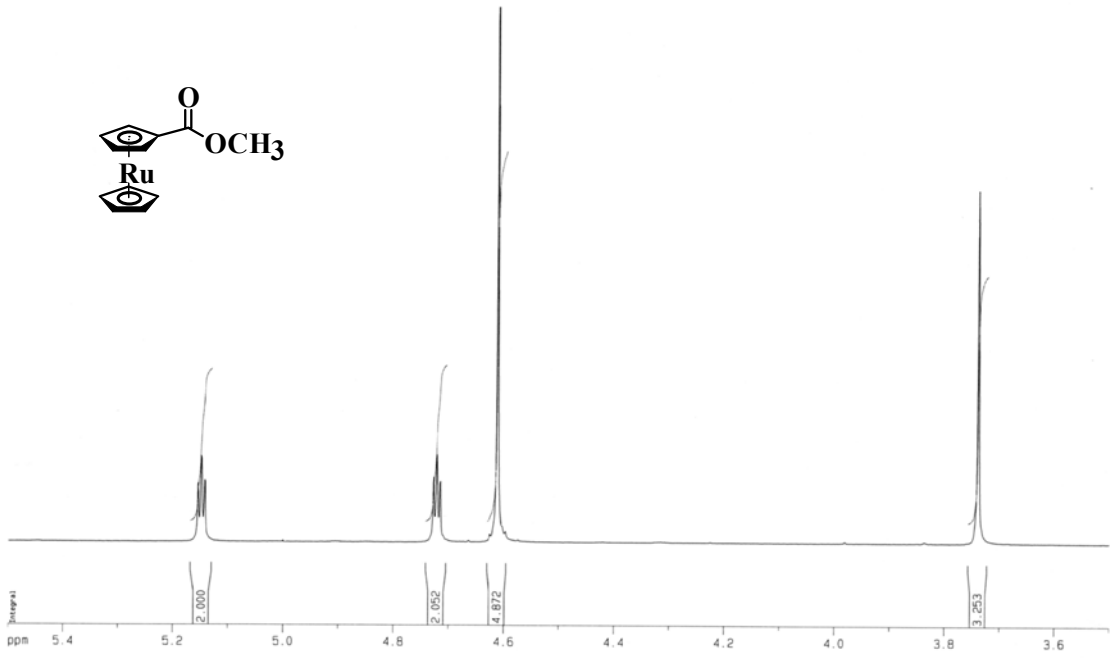

Spectrum A.6. ^{1}H NMR-Spectrum of RcCOOCH$_3$

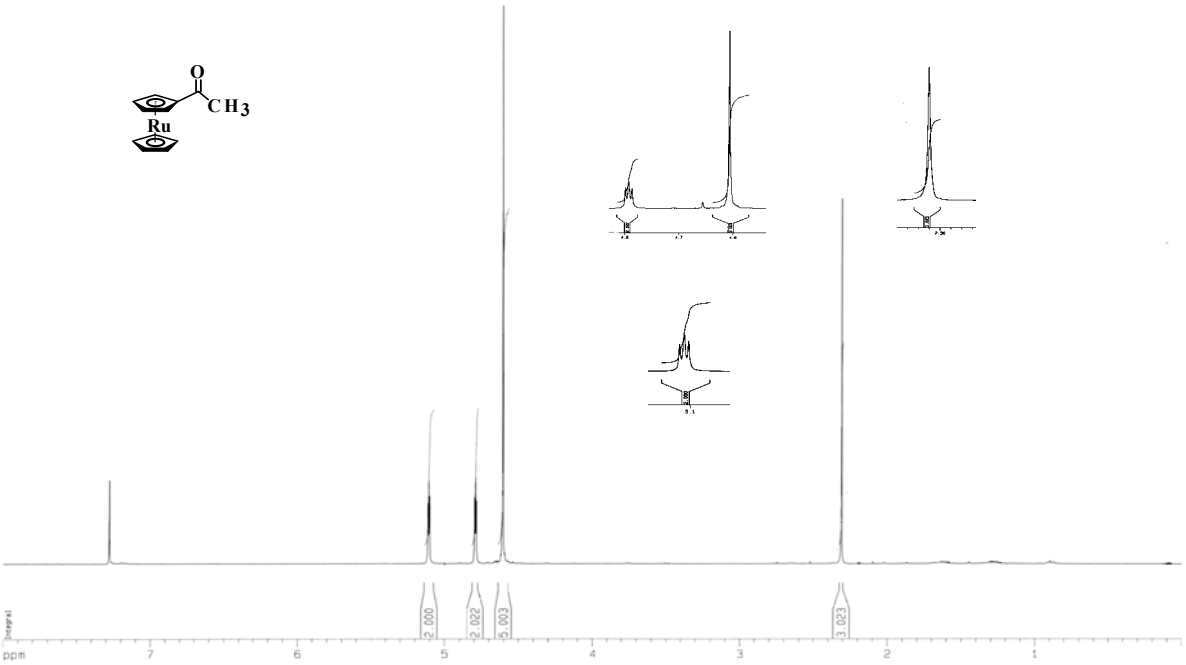

Spectrum A.7. ^{1}H NMR-Spectrum of $RcCOCH_3$

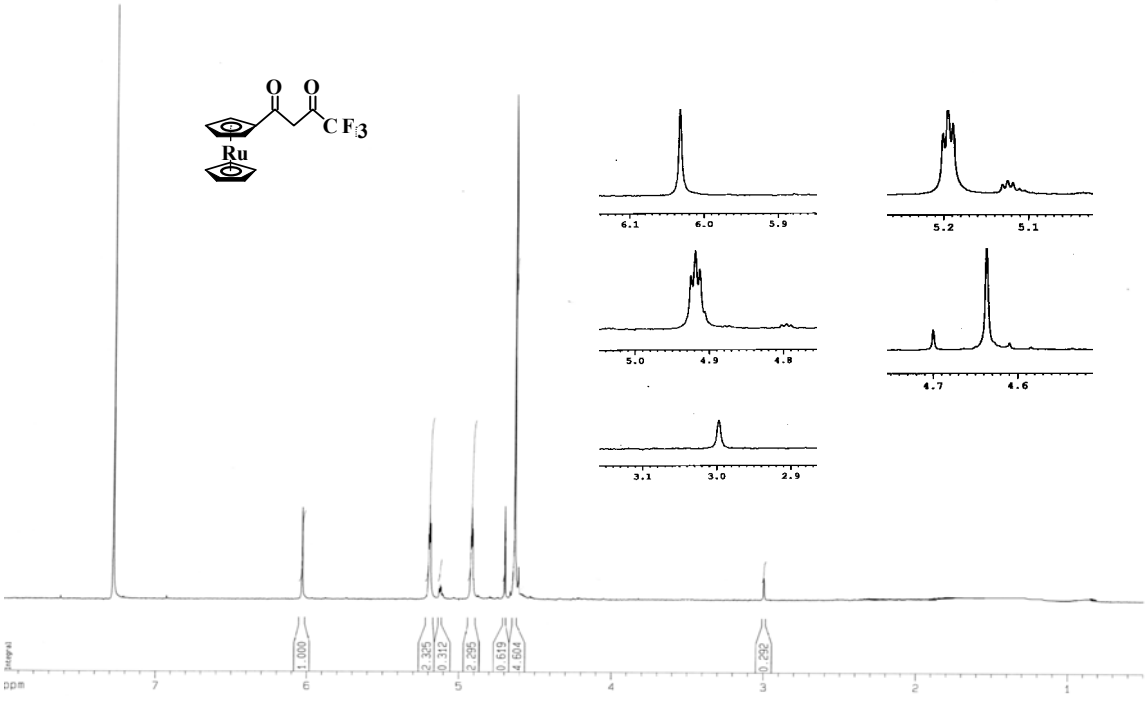

Spectrum A.8. ^{1}H NMR-Spectrum of $RcCOCH_2COCF_3$

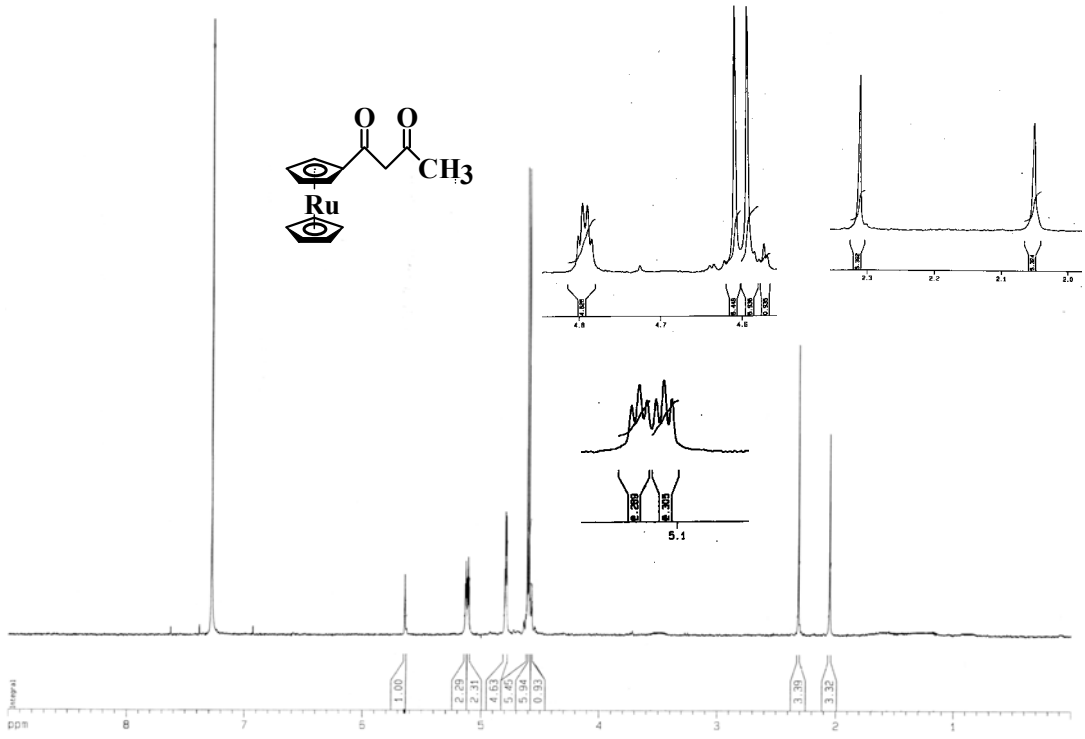

Spectrum A.9. ^{1}H NMR-Spectrum of $RcCOCH_2COCH_3$

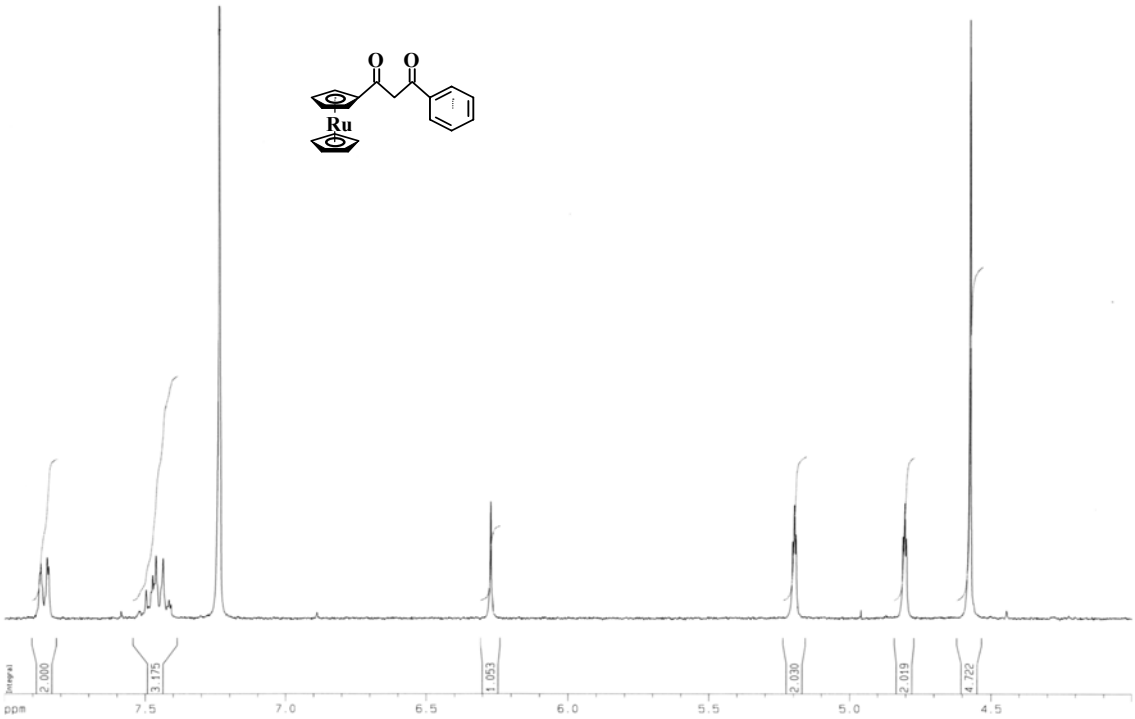

Spectrum A.10. ^{1}H NMR-Spectrum of $RcCOCH_2COC_6H_5$

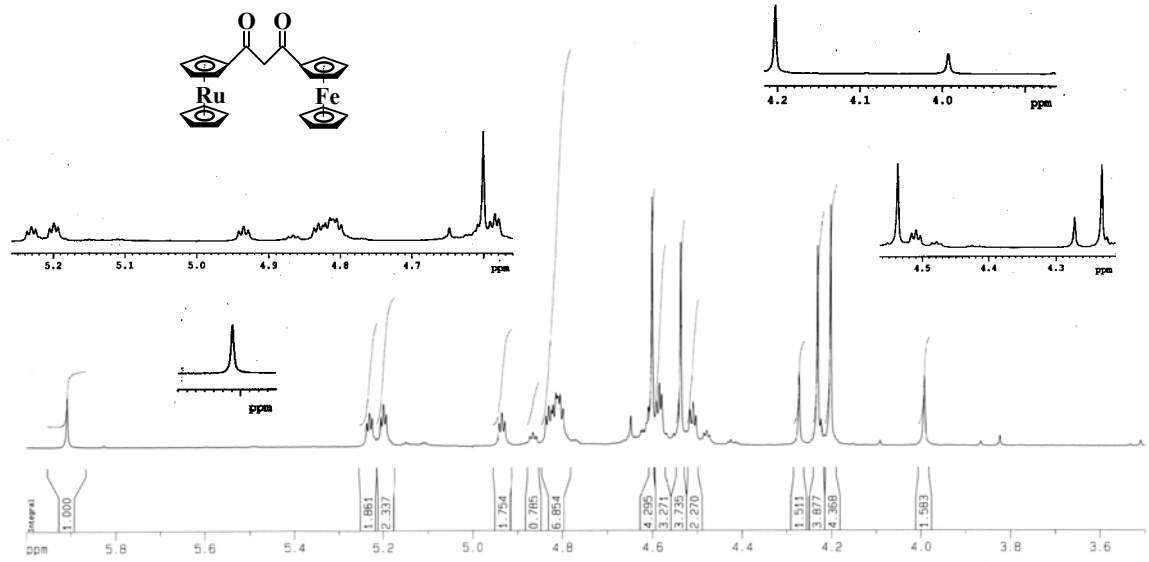

Spectrum A.11. ^{1}H NMR-Spectrum of RcCOCH$_2$COFc

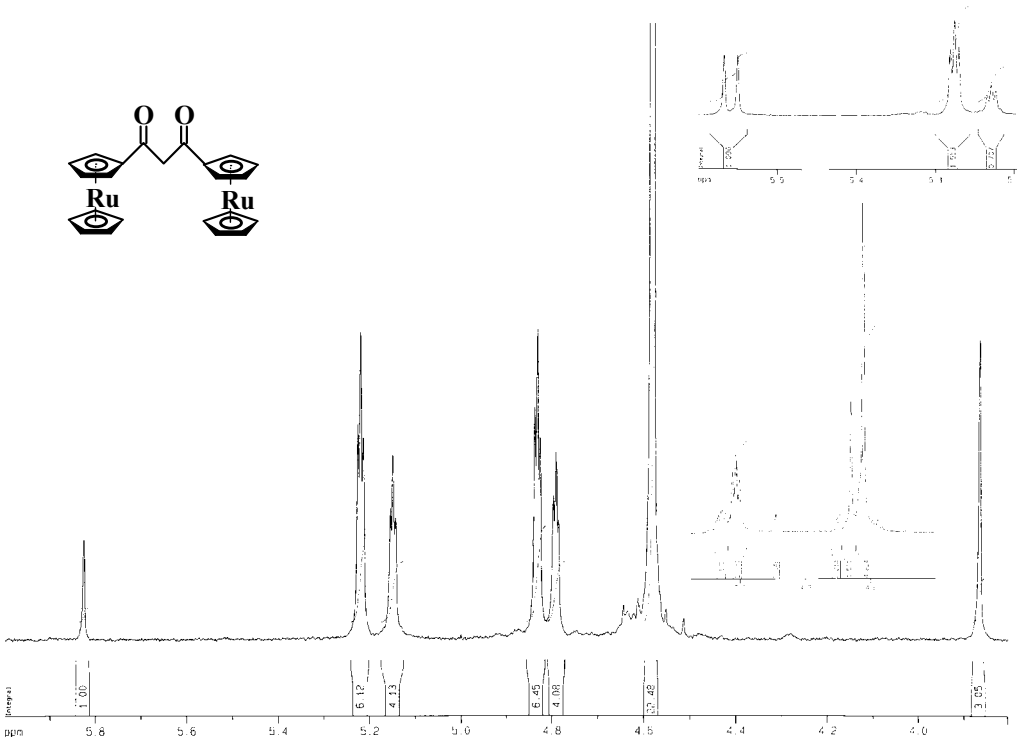

Spectrum A.12. ^{1}H NMR-Spectrum of RcCOCH$_2$CORc

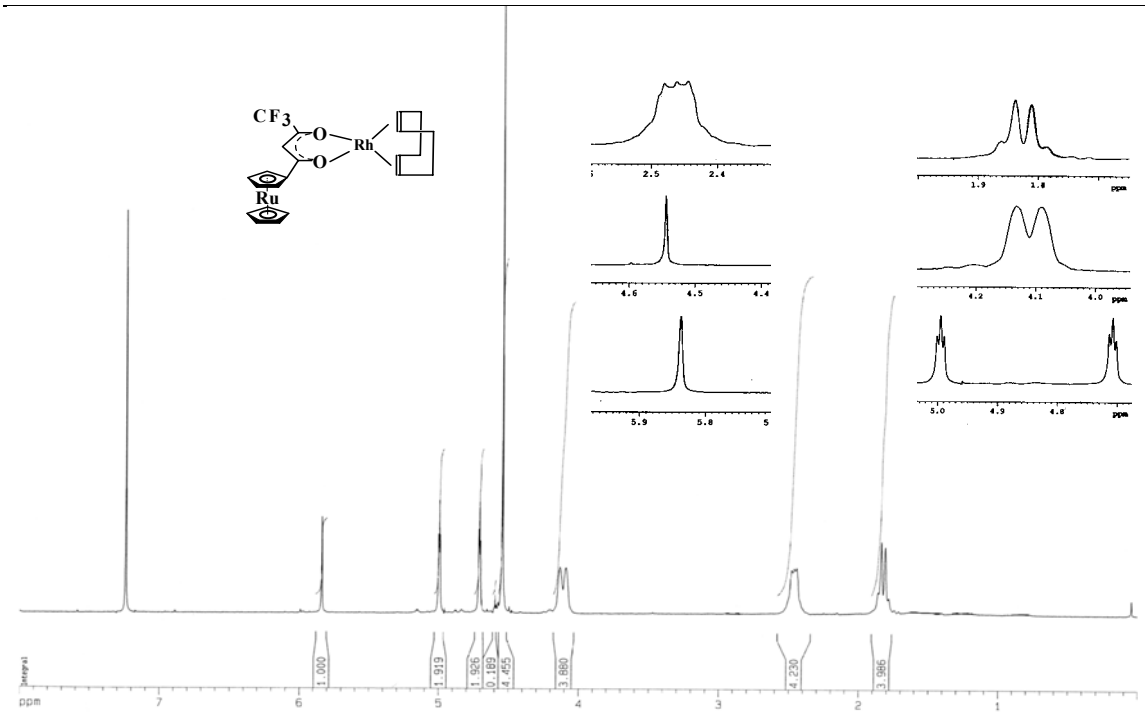

Spectrum A.13. ^{1}H NMR-Spectrum of [Rh(RcCOCHCOCF$_3$)(COD)]

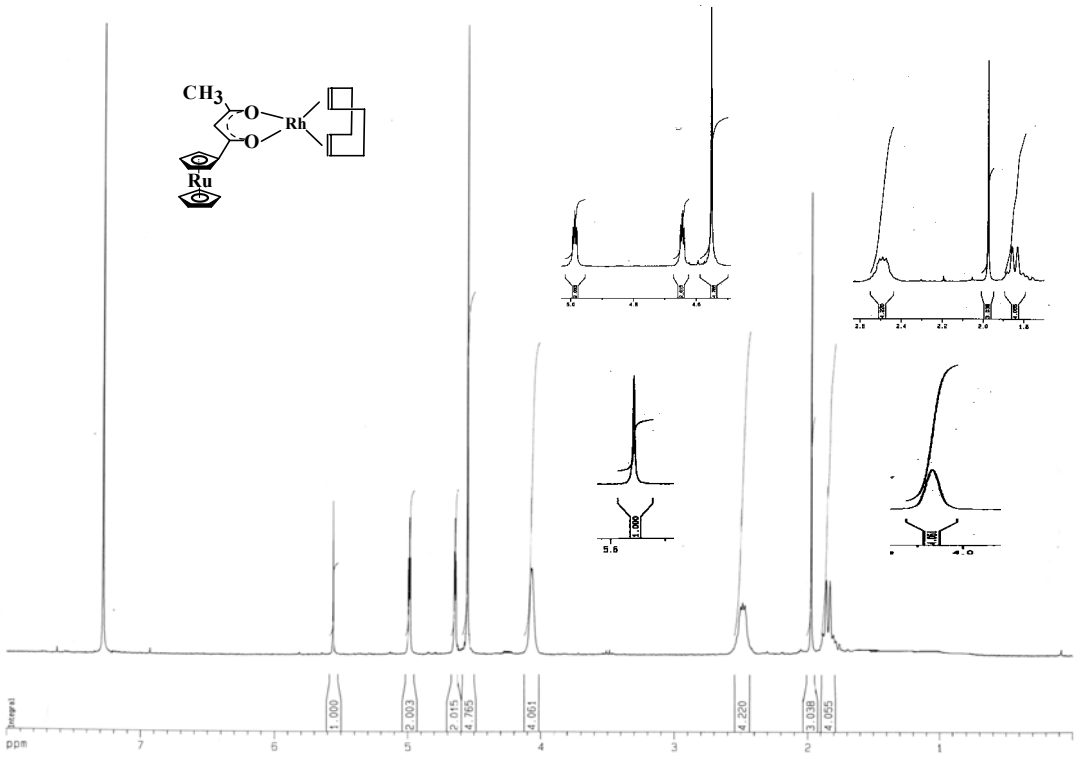

Spectrum A.14. ^{1}H NMR-Spectrum of [Rh(RcCOCHCOCH$_3$)(COD)]

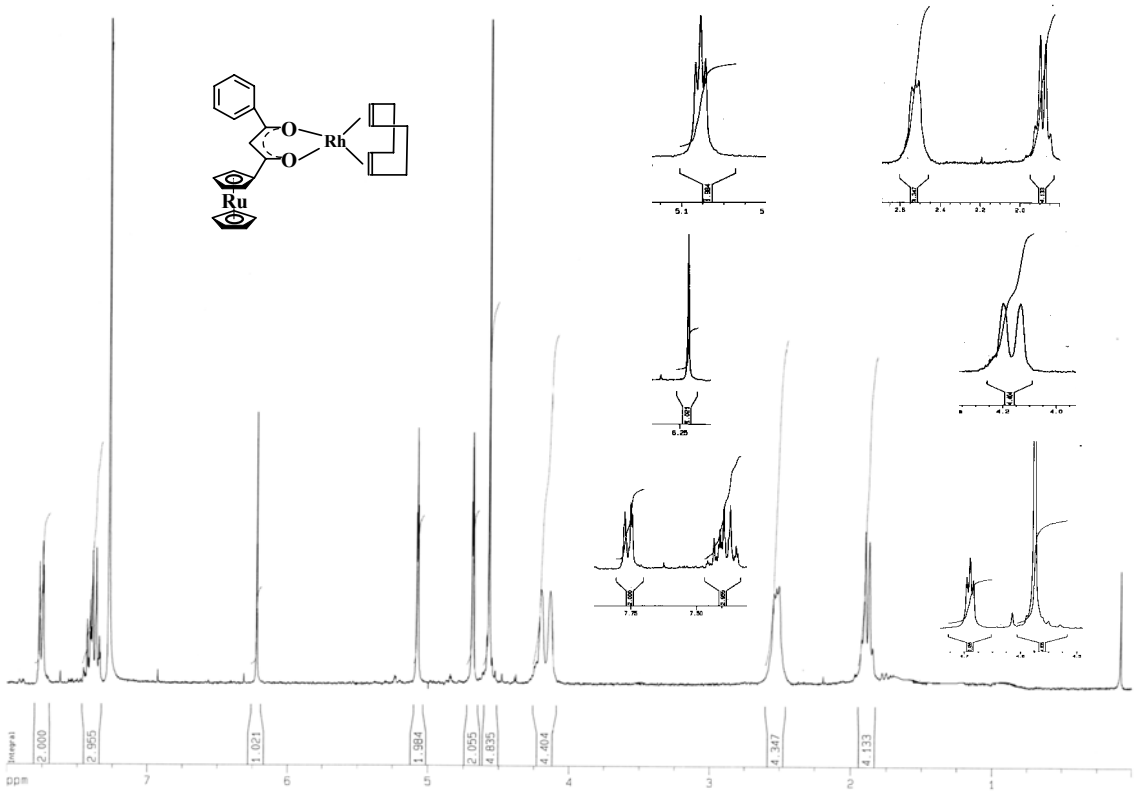

Spectrum A.15. ^{1}H NMR-Spectrum of [Rh(RcCOCHCOC$_6$H$_5$)(COD)]

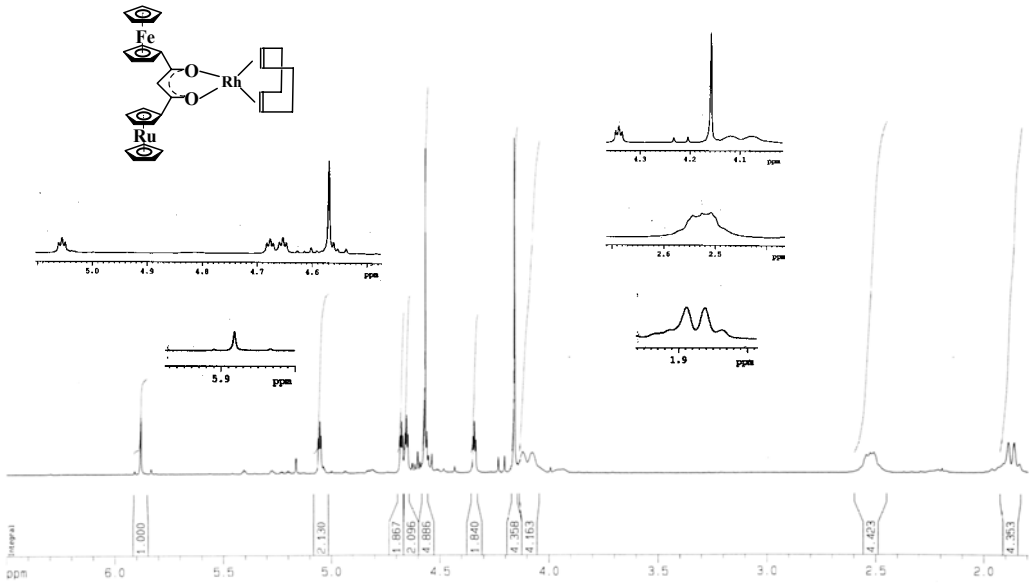

Spectrum A.16. ^{1}H NMR-Spectrum of [Rh(RcCOCHCOFc)(COD)]

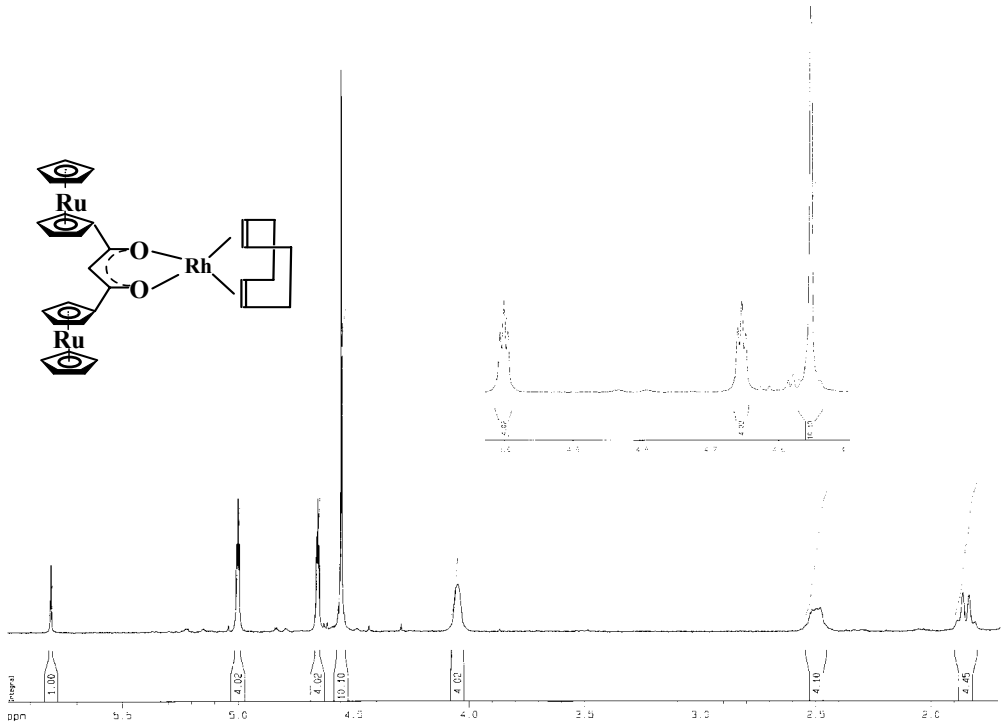

Spectrum A.17. ^{1}H NMR-Spectrum of [Rh(RcCOCHCORc)(COD)]

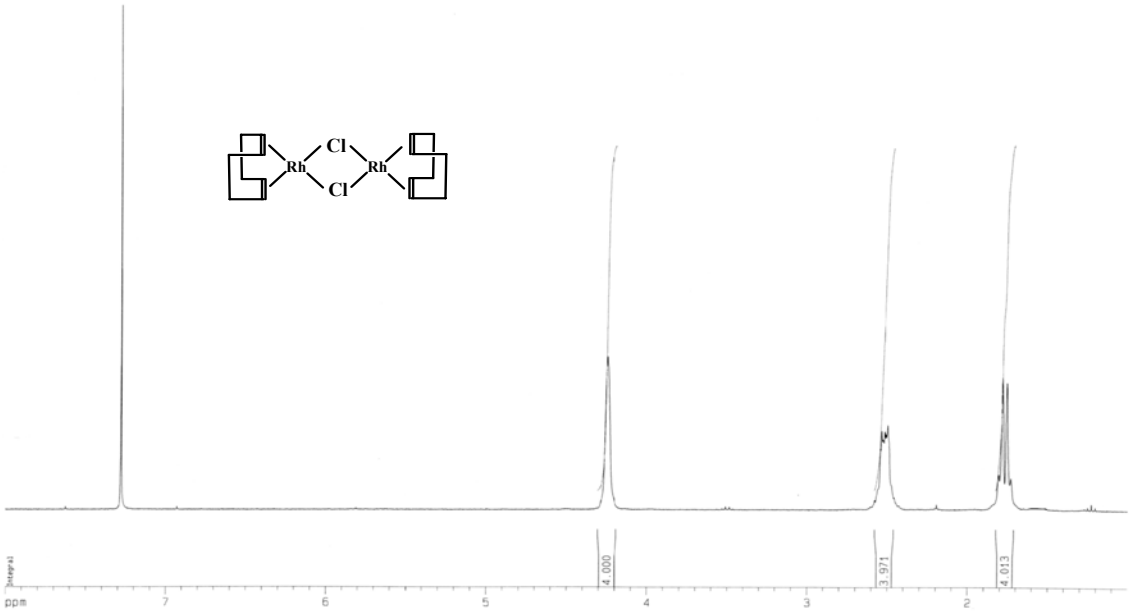

Spectrum A.18. ^{1}H NMR-Spectrum of $Rh_2Cl_2(COD)_2$

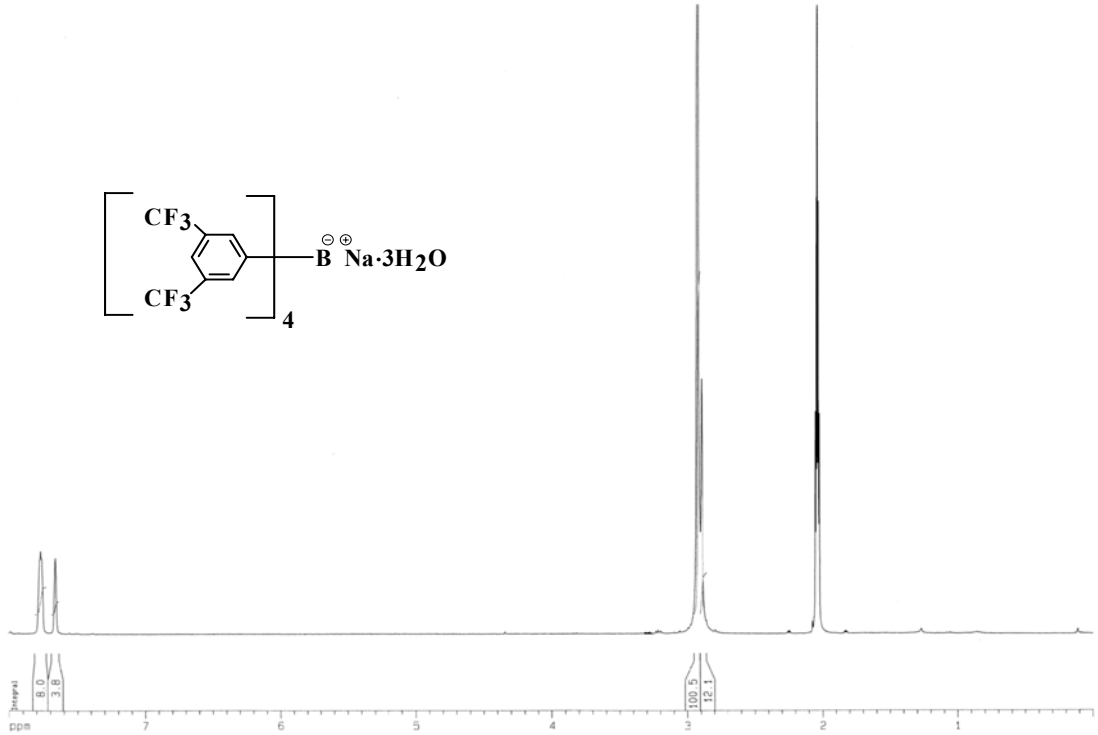

Spectrum A.19. ^{1}H NMR-Spectrum of Tetrakis[3,5-Bis(Trifluoromethyl)Phenyl]Borate

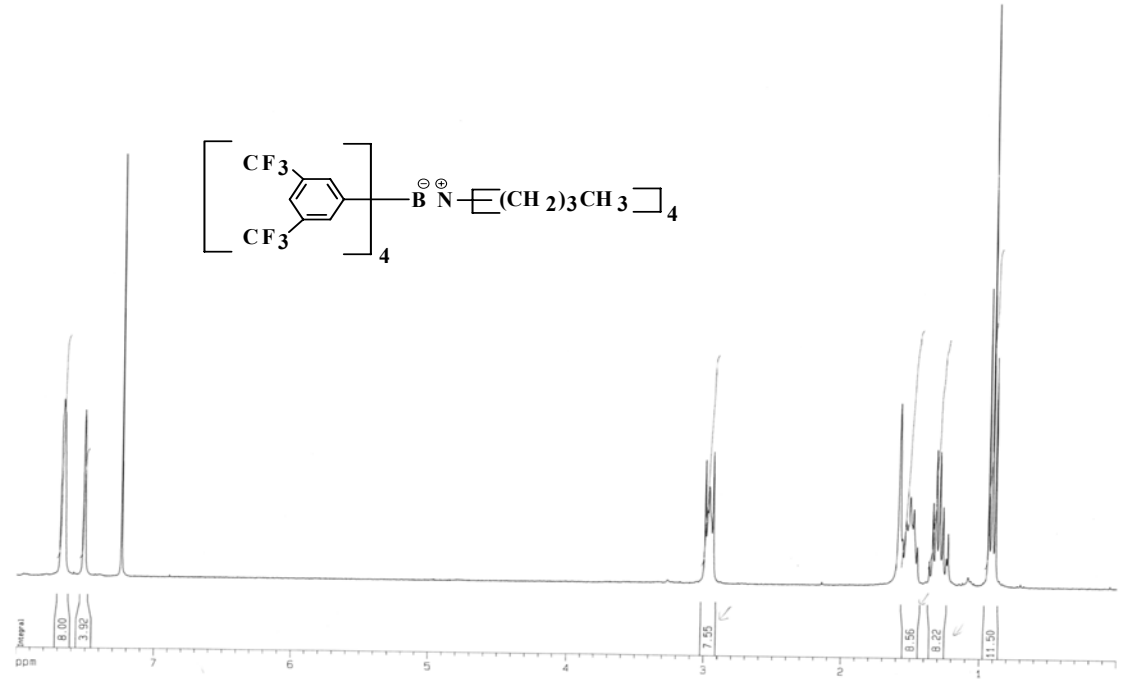

Spectrum A.20. ^{1}H NMR-Spectrum of Tetrabutylammonium Tetrakis [3,5-Bis(Trifluoromethyl)Phenyl]Borate

APPENDIX B

BIBLIOGRAPHY

CHAPTER 1

1. J. Stary , *The Solvent Extraction of Metal Chelates*, Macmilllan, 1964, pp 51-55
2. Y. Marcus and A.S. Keates, *Ion Exchange and Solvent Extraction of Metal Complexes*, Wiley-Interscience, 1969, pp 499-521
3. I. Bennet, N.J.P. Broom, R. Cassels, J.S. Elder, N.D. Masson and P.J. O'Hanlon, *Bioorg.Med.Chem.Lett*, **9**, 1999, 1847
4. D. Forster and T.W. Dekleva, *J.Chem.Educ*, **63**, 1986, 204
5. P.M. Matilis, A. Haynes,G.J. Sunley and M.J. Howard, *J.Chem.Soc.,Dalton Trans*, 1996, 2187
6. W.R. Cullen, S.J. Rettig and E.B. Wickenheiser, *J.Mol.Catal*., **66**, 1991, 251
7. F.A. Cotton, G. Wilkinson and P.L. Gaus, *Basic Inorganic Chemistry, 3rd edition*, John Wiley & Sons, 1995, pp 718-719
8. T.G. Vosloo, W.C. du Plessis and J.C. Swarts, *Inorg. Chim. Acta*, **331**, 2002, 188

CHAPTER 2

1. *Comprehensive Organometallic Chemistry Vol 4*, ed. G. Wilkinson, F.G. Stone and E. Abel, Pergamon Press, 1982, pp 759-773
2. M.D. Rausch, E.O. Fischer and H. Gurbert, *J.Am.Chem.Soc*., 1960, **82**, 76
3. D.E. Bublitz, W.E. McEwan and J. Kleinberg; *J.Am.Chem.Soc*., 1962, **84**, 1845
4. O. Hofer and K. Schloegel, *J.Organomet.Chem*,, 1968, **13**, 443
5. G. Schmitt and S. Özman, *J.Org.Chem*., 1976, **41**, 3331
6. A.J. Pearson, *Metallo-organic Chemistry*, John Wiley & Sons, 1985, pp 310-322
7. *Organic Synthesis*, **56**, John Wiley & Sons, 1977, pp 28-31
8. P.J. Graham, R.V. Lindsey, G.W. Parshall, M.L. Peterson and G.M. Whitman, *J.Am.Chem.Soc*., 1957, **79**, 3416
9. A.J. Pearson, *Metallo-organic Chemistry*, John Wiley & Sons, 1985, pp 335-341
10. *Comprehensive Organometalic Chemistry Vol 4*, ed. G. Wilkinson, F.G. Stone and E. Abel, Pergamon Press, 1982, pp 771-773
11. M. Suzuki, A. Watanabe and R. Noyori, *J.Am.Chem.Soc*., 1980, **102**, 2095

12. J. March, *Advanced Organic Chemistry, 4th Edition*, John Wiley & Sons Inc., New York, 1992, pp 1072-1074
13. M. Roth, P. Dubs, E. Götschi and A. Eschenmoser; *Helv.Chim.Acta*, 1971, **54**, 710
14. S. Umetani, Y. Kawase, Q.T.H. Le and M. Matusi*, J.Chem.Soc., Dalton Trans*., 2000, 2787
15. R.M. Cravero, M. Gonzalez-Sierra and A.C. Oliveri, *J.Chem.Soc., Perkins Trans 2*, 1993, 1067
16. P.J. Chapman, G. Meerman, I.C. Gunlus, R. Srinivasan and K.L. Rinehart Jr., *J.Am.Chem.Soc*., 1966, **88**, 618
17. G. Grogan, J. Gfaf, A. Jones, S. Parsons, N.J. Turner and S.L. Flitsch, *Angew.. Chem., Int. Ed.Engl.*, 2001, **40**, 1111
18. C.R. Hauser and J.K. Lindsay, *J.Org.Chem*., 1957, **22**, 482
19. V. Weinmayr, *Naturwissenchaften*, 1958, **45**, 311
20. W.R. Cullen, S.J. Rettig and E.B. Wickenheiser, *J.Mol.Catal*., 1991, **66**, 251
21. W.C. du Plessis, T.G. Vosloo & J.C. Swarts, *J.Chem.Soc., Dalton Trans.,* 1998, 2507
22. C.E. Cain, T.A. Mashburn,Jr & C.R. Hauser; *J.Org.Chem.,* 1961, **26**, 1030
23. C.R. Hauser and C.E. Cain; *J.Org.Chem.,* 1958, **23**, 1142
24. H. Nishidi, N. Takada, M. Yoshimura, T. Sonoda & H. Kobayashi, *Bull.Chem.Soc.Jpn*, 1984, **57**, 2600
25. K.V. Baker, J.M. Brown, N. Hughes, A.J. Skarnulis and A. Sexton, *J.Org.Chem*., 1991, **56**, 698
26. L. Boymond, M. Rottlander, G. Cahiez and P. Knochel, *Angew.Chem.,Int.Ed.Engl*., 1998, **37**, 1071
27. E.C. Ashby and R. Reed, *J.Org.Chem*., 1966, **31**, 971
28. M.J. Gallagher, S. Harvey, C.L. Raston and R.E. Sue, *J.Chem.Soc.,Chem.Commun*., 1988
29. J. March, *Advanced Organic Chemistry, 4th Edition*, John Wiley & Sons, Inc., New York, 1992, pp 622-625
30. A. Boudin, G. Cerveau, C. Chuit, R.J.P. Corriu and C. Reye, *Tetrahedron*, 1989, **45**, 171
31. H. Nishidia, N. Takada, M. Yoshimura, T. Sonada and H. Kobayashi, *Bull. Chem. Soc. Jpn*, 1984, **57**, 2600
32. M. Rozencweig, D.D. von Hoff, M. Slavik and F.M. Muggia, *Ann. Int.Med.*, 1977, **86**, 803
33. R.F. Ozols, *Semin. Oncol*., 1989, **16**, 22
34. S. Adachi, T. Ogasawara, E. Wakimoto, Y. Tsuji, T. Takemura, K. Koyama, Y. Takayasu, J. Inoue and N. Nakao, *Cancer (N.Y.),* 2001, **91**, 74

35. J.M. Ward, M.E. Grabin, E. Berlin and D.M. Yoong, *Cancer Res*., 1977, **37**, 1238

36. J.H. Burchenal, K. Kalaher, T. O'Toole and J. Chisholm, *Cancer Res*., 1977, **37**, 3455

37. N.K. Kim, T. Kim, S. Shin, J.A. Lee, Y. Cho, K.H. Kim, D. Kim, D.S. Heo and Y. Bang, *Cancer (N.Y.)*, 2001, **91**, 1549

38. J.C. Swarts and C.J. van Rensburg, *Ferrocene compounds for cancer treatment*, patent no: PCT/IBO1/02258 Dated 29 Jan 2003

39. L. Messori, P. Orioli, D. Vullo, E. Alessio and E. Lengo, *Eur.J.Biochem*., 2000, **267**, 1206

40. T. Tsuruo, H. Iida, S. Tsukagoshi and Y. Sakuari, *Biochem.Pharm.,* 1981, **30**, 213

41. V. Conter and W.T. Beck, *Bioch.Pharm.*, 1983, **32**, 723

42. R. Herken and M. Wenzel, *Eur.J.Nucl.Med*., 1985, **10**, 56

43. J. Shani, T. Livshitz and M. Wenzel, *Int.J.Nucl.Med.Bio*., 1985, **12**, 13

44. J.C. Swarts, D.M. Swarts, D.D. Maree, E.W. Neuse, C. La Madeleine and J.E. Van Lier, *Anticancer Res*., 2000, **20**, 1-5

45. R.A. Sánchez-Delgado, M. Navarro, H. Pérez and J.A. Urbina, *J. Med.Chem*., 1996, **39**, 1095

46. E. Dadachova, *J.Labelled Comp. Radiopharm*., 1999, **42**, 287

47. K. Chibale, J.R. Moss, M. Blackie, D. van Schalkwyk and P.J. Smith, *Tetrahedron Lett*., 2000, **41**, 6231

48. C. Biot, G. Glorian, L.A. Maciejewski, J.S. Brocard, O. Domarle, G. Blampain, P. Millet, A.J. Georges, H. Absello, D. Dive and J. Lebibi, *J.Med.Chem*., 1997, **40**, 3715

49. P. Beagley, M.A.L. Blackie, K. Chibale, C. Clarkson, J.R. Moss and P.J. Smith, *J.Chem.Soc.,Dalton Trans*., 2002, 4426

50. G.A. Mabbott, *J.Chem.Educ*., 1983, **60**, 697

51. P.T. Kissinger and W.R. Heineman, *J.Chem.Educ*., 1983, **60**, 702

52. D.H. Evans, K.M. O'Conneil; R.A. Peterson and M.J. Kelly, *J.Chem. Educ*., 1983, **60**, 290

53. J.J. Van Benschoten, J.Y. Lewis and W.R. Heineman, *J.Chem.Educ*., 1983, **60**, 772

54. M. Tsionsky, A.J. Bard and M.V. Mirkin, *J.Am.Chem.Soc*., 1997, **119**, 10785

55.Y. Wu, T. Komatsu and E. Tsuchida, *Inorg.Chim.Acta*, 2001, **322**, 120

56. D.R. van Staveren, E. Bothe, T. Weyhermüller and N. Mtezler-Nolte, *Chem.Commun. (Cambridge)*, 2001, 131

57. R. Cosmo, C. Kautz, K. Meerholz, J. Heinze and K. Müllen, *Angew.Chem.,Int.Ed.Engl*., 1989, **28**, 604

58. T. Kuwana, D.E. Bublitz and G. Hoh, *J.Am.Chem.Soc*., 1960, **82**, 5811

59. M.G. Hill, W.M. Lamanna and K.R. Mann, *Inorg.Chem*., 1991, **30**, 4687
60. R.J. Gale and R. Job, *Inorg.Chem*., 1981, **20**, 42
61. C. Jacob, A.Y. Safronov, S. Wilson, H.A.O. Hill and T.F. Booth, *J.Electroanal.Chem*., 1997, **427**, 161
62. M. Sati, G. Maruyama and A. Tanemura, *J.Organomet.Chem*., 2002, **655**, 23
63. C. Ohrenberg and W.E. Geiger, *Inorg.Chem*., 2000, **39**, 2948
64. R.J. Le Suer and W.E. Geiger, *Angew.Chem.,Int.Ed.Engl.*, 2000, **39**, 248
65. L. Pospišil, B.T. King and J. Michl, *Electrochim.Acta*, 1998, **44**, 103
66. W.J. Moore, *Physical Chemistry, 4th Edition*, Longman Group Limited, 1972, pp 333-334
67. R.M. Cravero, M. González-Sierra and A.C. Olivieri, *J.Chem.Soc., Perkin Trans. 2*, 1993, 1067
68. W. Blokzijl, J.B.F.N. Engberts and M.J. Blandamer, *J.Chem.Soc., Perkin Trans. 2*, 1994, 455
69. E. Iglesias and V. Ojea-Cao, *J.Org.Chem*., 1999, **64**, 3954
70. W.C. du Plessis, W.L. Davis, S.J.Cronje and J.C. Swarts, *Inorg.Chim.Acta*, 2001, **314**, 97
71. G.E. Rodgers, *Introduction to Coordination, Solid State, and Descriptive Inorganic Chemistry*, McGraw-Hill , 1994, pp 94-116
72. F.A. Cotton, G. Wilkinson and P.L. Gaus, *Basic Inorganic Chemistry 3rd Edition*, John Wiley & Sons, Inc., 1995, pp 200-204
73. R.G. Wilkins, *The Study of Kinetics and Mechanism of Reactions of Transition Metal Complexes*, Allyn & Bacon Inc., 1974, pp 223-235
74. G.M. Barrow, *Physical Chemistry 6th Edition*, McGraw-Hill Companies Inc., 1996, pp 730-732
75. R.G. Mortimer, *Physical Chemistry*, The Benjamin/Cummings Publishing Company Inc., 1993, pp 910-913
76. B. Stevens, *Chemical Kinetics*, Chapman & Hall, 1965, pp 37-43
77. J.G. Leipoldt, S.S. Basson, J.J.J. Schlebuch and E.C. Grobler, *Inorg.Chim.Acta*, 1982, **62**, 113
78. J.H. Potgieter, *J.Organomet.Chem*., 1989, **366**, 369
79. J.G. Leipoldt, G.J. Lamprecht and E.C. Steynberg, *J.Organomet.Chem*., 1990, **397**, 239
80. J.G. Leipoldt and E.C. Grobler, *Transition Met.Chem. (Weinheim, Ger)*, 1986, **11**, 110
81. J.G. Leipoldt, E.C. Steynberg and R. van Eldik, *Inorg.Chem*., 1987, **26**, 3068
82. J.G. Leipoldt, G.J. Lamprecht and E.C. Steynberg; *J.Organomet.Chem*., 1991, **402**, 259
83. T.G. Vosloo, W.C. duPlessis and J.C. Swarts; *Inorg.Chim.Acta*, 2002, **331**, 188

84. D.D. Ebbing, *General Chemistry 5th edition*, 1996, Houghton Mifflin Company, pp 666-673
85. A. Albert and E.P. Sejeant, *The Determination of Ionization Constants 3rd edition*, 1984, Chapman and Hall, pp 70-101
86. L. Helm, MINSQ, Non-Linear parameter estimation and model development, least squares parameter optimisation V3.12, MicroMath Scientific Software, Salt Lake City, UT, 1990
87. W.C. duPlessis, J.C. Erasmus, G.J. Lamprecht, J. Conradie, T.S. Cameron, M.A.S. Aquino and J.C. Swarts, *Can.J.Chem*., 1999, **77**, 378
88. S. Aygen and R. van Eldik, *Chem.Ber*., 1989, **122**, 315
89. M. Ellinger, H. Duschner and K. Starke, *J.Inorg.Nucl. Chem*., 1978, **40**, 1063
90. A. Albert and E.P. Sejeant, *The Determination of Ionization Constants 3rd edition*, 1984, Chapman and Hall, pp 110-119
91. R.M. Fuos and C.A. Kraus, *J.Am.ChemSoc*., 1933, **55**, 476
92. P. Ballinger and F.A. Long, *J.Am.ChemSoc*, 1960, **82**, 795
93. P. Ballinger and F.A. Long, J.Am.Chem.Soc., 1959, **81**, 1050
94. F.A. Cotton, G. Wilikinson and P.L. Gaus, *Basic Inorganic Chemistry 3rd Edition*, John Wiley & Sons,Inc., 1995, pp 63-67
95. P.R. Wells, *Progress in Physical Organic Chemistry*, 1968, **6**, pp 111-145
96. R.E. Kagarise, *J.Am.Chem.Soc*., 1955, **77**, 1377
97. N. Inamoto and S. Masuda, *Chem. Lett*., 1982, 1003

CHAPTER 3

1. M.D. Rausch, E.O. Fischer and H. Gurbert, *J.Am.Chem.Soc*., 1960, **82**, 76
2. J. Chatt and L.M. Venanzi, *J.Chem.Soc*., 1957, 4735
3. R.E. Kagarise, *J.Am.Chem.Soc.*, 1955, 1377
4. W.C. du Plessis, T.G. Vosloo and J.C. Swarts, *J.Chem.Soc., Dalton Trans.,* 1998, 2507
5. R.G. Wilkins, *The study of kinetics and mechanism of reactions of transition metal complexes*, Allyn and Bacon, Boston, 1974, 44-45
6. B.S. Furniss, A.J. Hannaford, P.W.G. Smith and A.R. Tatchell, *Vogel's textbook of practical organic chemistry*, Longman, Harlow, 5th edn., 1989, 622
7. A. Albert and E.P. Sejeant, *The Determination of Ionization Constants*, Chapmann and Hall, London, 3rd edn., 1984, 8

8. J.L. Burdett and M.T. Rogers, *J.Am.Chem.Soc*., 1964, **86**, 2105
9. W.C. du Plessis, W.L. Davis, S.J. Cronje and J.C. Swarts, *Inorg. Chim. Acta*, 2001, **314**, 97
10. T.G. Vosloo, W.C. du Plessis and J.C. Swarts, *Inorg. Chim. Acta*, 2002, **331**, 188
11. P.T. Kissinger and W.R. Heineman, *J.Chem.Ed.*, 1983, **60**, 702

CHAPTER 4

1. G.H. Jefferey, J. Bassett, J. Mendham and R.C. Denney, *Vogel's Textbook of Quantitative Chemical Analysis, 5th Edition*, Longman Scientific & Technical, 1991, pp 830-832
2. L. Helm, MINSQ, Non-Linear parameter estimation and model development, least squares parameter optimisation V3.12, MicroMath Scientific Software, Salt Lake City, UT, 1990
3. W.C. du Plessis, W.L. Davis, S.J. Cronje and J.C. Swarts; *Inorg.Chim.Acta*, 2001, **314**, 97

ABSTRACT

New ruthenocene-containing β-diketones 1-Ruthenocenyl-4,4,4,-trifluorobutan-1,3-dione [Hrctfa, $pKa^{/}$ = 7.31(3)], 1-ruthenocenylbutan-1,3-dione [Hrca, $pKa^{/}$ = 10.22(4)] 1-ruthenocenyl-3-phenylpropan-1,3-dione [(Hbrcm, $pKa^{/}$ = 11.31(4)], 1-ruthenocenyl-3-ferrocenylpropan-1,3-dione [(Hrcfcm; $pKa^{/}$ >13)], and 1,3-diruthenocenylpropane-1,3-dione [(Hdrcm, $pKa^{/}$ >13)], were prepared by the Claisen Condensation of acetylruthenocene and the appropriate ester under the influence of lithium diisopropylamide.

The group electronegativity of the ruthenocenyl group (Rc) was determined from the linear relationship between the methyl ester (RCOOMe) infrared carbonyl stretching frequencies and the group electronegativities of known R groups, R = CF_3, CH_3, C_5H_5, H, Fc.

The [Rh(β-diketonato)(cod)] complexes [Rh(rctfa)(cod)], [Rh(rca)(cod)], [Rh(brcm)(cod)], [Rh(rcfcm)(cod)] and [Rh(drcm)(cod)] were obtained by treating the appropriate β-diketones (Hrctfa, Hrca, Hbrcm, Hrcfcm and Hdrcm) with $[Rh_2(cod)_2Cl_2]$.

Kinetics results for the conversion of the β-diketones (Hrctfa, Hrca, Hbrcm, Hrcfcm and Hdrcm) from the enol to the keto form and *vice versa* are reported.

Kinetics results for the substitution of β-diketonato ligand from the [Rh(β-diketonato)(cod)] complexes ([Rh(rctfa)(cod)], [Rh(rca)(cod)], [Rh(brcm)(cod)], [Rh(rcfcm)(cod)] and [Rh(drcm)(cod)]) with 1,10-phenantroline in methanol are also presented. Large negative activation entropy values obtained, suggested an associative substitution mechanism. All substitution reactions had no observable mechanistic solvent pathway contribution.

Oxidation potentials (E_{pa} *vs* Ag/Ag^+) for the ruthenium core in the free β-diketones (Hrctfa, Hrca, Hbrcm, Hrcfcm and Hdrcm), as well as in the [Rh(β-diketonato)(cod)] complexes ([Rh(rctfa)(cod)], [Rh(rca)(cod)], [Rh(brcm)(cod)], [Rh(rcfcm)(cod)] and [Rh(drcm)(cod)]) are reported. The peak anodic potentials (E_{pa} *vs* Ag/Ag^+) for oxidation of the rhodium(I) center were determined.

Keywords: Ruthenocene, β-diketones, rhodium, group electronegativties, cyclic voltammetry, substitution kinetics, isomerization kinetics

OPSOMMING

Nuwe rutenoseen-bevattende β-diketone, 1-rutenoseniel-4,4,4-trifluorobutaan-1,3-dioon [Hrctfa, $pK_a^{/}$ = 7.31(3)], 1-rutenosenielbutaan-1,3-dioon [Hrca, $pK_a^{/}$ = 10.22(4)], 1-rutenoseniel-3-fenielpropaan-1,3-dioon [Hbrcm, $pK_a^{/}$ = 11.31(3)], 1-rutenoseniel-3-ferrosenielpropaan-1,3-dioon [Hrcfcm, $pK_a^{/}$ > 13] en 1,3-dirutenosenielpropaan-1,3-dioon [Hdrcm, $pK_a^{/}$ > 13] is berei deur die Claisen kondensasie van asetielrutenoseen en die toepaslike ester onder die invloed van litiumdiisopropielamied.

Die groepelektronegatiwiteit van die rutenoseniel groep (Rc) was bepaal vanaf die lineêre verband tussen die metiel ester (RCOOMe) infrarooi karbonielstrekkingsfrekwensie en die groep elektronegatiwiteit van bekende R groepe, R = CF_3, CH_3, C_6H_5, H, Fc.

Die [Rh(β-diketonato)(cod)]-komplekse [Rh(rctfa)(cod)], [Rh(rca)(cod)], [Rh(brcm)(cod)], [Rh(rcfcm)(cod)] en [Rh(drcm)(cod)] is berei vanaf die reaksie tussen die toepaslike β-diketone (Hrctfa, Hrca, Hbrcm, Hrcfcm en Hdrcm) en $[Rh_2(cod)_2Cl_2]$.

Kinetiese resultate vir die omskakeling van die β-diketone (Hrctfa, Hrca, Hbrcm, Hrcfcm en Hdrcm) van die enol- na die keto-isomeer en omgekeerd word gerapporteer.

Kinetiese resultate vir die substitusie van die β-diketonato ligand van die [Rh(β-diketonato)(cod)]-komplekse [Rh(rctfa)(cod)], [Rh(rca)(cod)], [Rh(brcm)(cod)], [Rh(rcfcm)(cod)] en [Rh(drcm)(cod)]) met 1,10-fenantrolien in metanol word ook aangebied. Die groot negatiewe entropie waardes wat verkry is, dui op ‘n assosiatiewe substitusie meganisme. Alle substitusie reaksies vind met die afwesigheid van ‘n oplosmiddelroete plaas.

Oksidasiepotensiale (E_p waardes *vs.* Ag/Ag^+) van die rutenium kern in die vry β-diketone (Hrctfa, Hrca, Hbrcm, Hrcfcm en Hdrcm), en in die [Rh(β-diketanato)(cod)] komplekse, [Rh(rctfa)(cod)], [Rh(rca)(cod)], [Rh(brcm)(cod)], [Rh(rcfcm)(cod)] en [Rh(drcm)(cod)]) is bepaal. Die piek oksidasiepotensiale (E_p waardes *vs.* Ag/Ag^+) vir die oksidasie van die rodium(I) kern is bepaal.